MEASURING MELANOPSIN FUNCTION IN HUMANS TO UNDERSTAND PHOTOPHOBIA IN MIGRAINE

Harrison McAdams

A DISSERTATION

in

Neuroscience

Presented to the Faculties of the University of Pennsylvania

in

Partial Fulfillment of the Requirements for the

Degree of Doctor of Philosophy

2020

Supervisor of Dissertation	Graduate Group Chairperson
_____	_____
Geoffrey Aguirre, MD, PhD	Joshua Gold, PhD
Associate Professor of Neurology	Professor of Neuroscience

Dissertation Committee:

Ted Satterthwaite, MD, Assistant Professor of Psychiatry (Committee Chair)

Jessica Morgan, PhD, Assistant Professor of Ophthalmology

John Detre, MD, Professor of Neurology

Anna Matynia, PhD, Associate Researcher Ophthalmologist

ABSTRACT

MEASURING MELANOPSIN FUNCTION IN HUMANS TO UNDERSTAND PHOTOPHOBIA IN MIGRAINE

Harrison McAdams

Geoffrey Aguirre

Bright light can be uncomfortable, and sometimes even painful, to look at. Bright light, however, hurts more in numerous clinical contexts, including in people who suffer from migraine headache. This pathology is referred to as photophobia or light sensitivity. Migraineurs tend to not only be light sensitive during headaches, but between headaches as well. Prior work has tentatively linked photophobia to the melanopsin and intrinsically photosensitive retinal ganglion cell (ipRGC) system.

In the first chapter, this work describes how we can effectively probe the ipRGC system in healthy human subjects. We highlight the utility of silent substitution to selectively stimulate melanopsin to thereby isolate the ipRGCs from the rest of the retina. We then demonstrate that pupillometry is a stable measure of the response to this selective stimulation, and shows temporal properties consistent with the prolonged signal transduction associated with melanopsin.

In the second chapter, we then extend these insights to the study of photophobia in migraine, comparing light-related responses in people with migraine to headache free controls. Through this project, we show that migraineurs find

melanopsin-isolating stimuli more uncomfortable than headache free controls, providing some of the strongest evidence to date that variation in ipRGC function relates to clinical pathology in humans. We also show that migraineurs find cone-isolating stimuli more uncomfortable, suggesting that both melanopsin and cone signals contribute to photophobia. Finally, we show that pupil constriction is not similarly enhanced in migraine. By demonstrating this dissociation in light-mediated responses, we reveal a selective amplification of ipRGC signals, in a manner consistent with a post-retinal localization of photophobia.

TABLE OF CONTENTS

LIST OF ILLUSTRATIONS

Figure 3.S1 – Pupil response amplitudes by stimulus and group

LIST OF TABLES

Chapter 1 - Introduction

The ipRGC System, the Retina, and Physiology

Much of visual science has been concerned with phototransduction originating in rods and cones. These signals are routed through the retinal ganglion cells, which form the optic nerve, and project to the thalamus and other brainstem targets. Relatively recently, however, a novel opsin called melanopsin was discovered in the frog[1]. Subsequent investigation showed that melanopsin was also found and functioned within a subset (~1-3%) of retinal ganglion cells, including in humans[2–6]. The presence of melanopsin within these cells renders them intrinsically photosensitive. That is, if all synaptic input to these cells was blocked, light would elicit spiking activity within one of these intrinsically photosensitive retinal ganglion cells (ipRGCs) through phototransduction by melanopsin. These ipRGCs also receive synpatic input from rods and cones[7–10], so any activity within an ipRGC could result from intrisic signaling from melanopsin or extrinsic signaling from rods and cones.

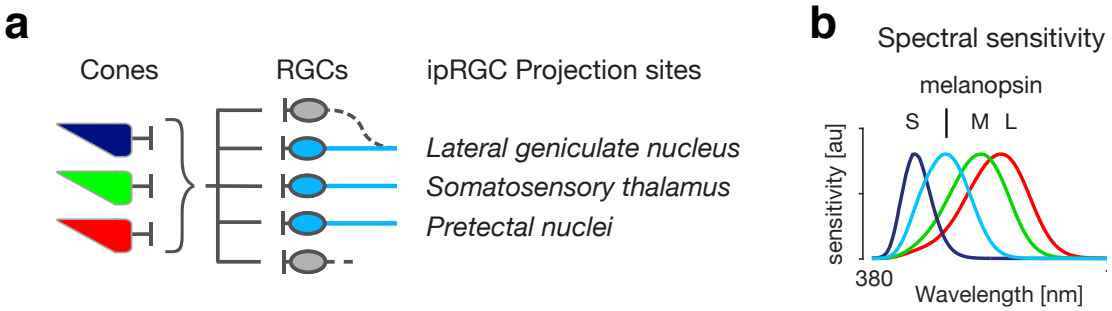

Figure 1. ipRGC system overview. a. Signals from cones are routed through retinal ganglion cells to various post-retinal locations, including to thalamus and brainstem targets (note not all targets are shown). A subset of those retinal ganglion cells are intrinsically photosensitive (shown in blue) due to the presence of melanopsin. b. The spectral sensitivity functions of melanopsin, as well as the three classes of cones (L-, M-, and S-wavelength sensitive cones).

Spectral sensitivity functions describe the relative sensitivity or likelihood of photon capture for a given photopigment as a function of wavelength. The peak spectral sensitivity for melanopsin is around 480 nm (in the “blue” light range)[11], situating it in between the peaks of the short-wavelength sensitive and medium-wavelength sensitive cones. The melanopsin spectral sensitivity function also overlaps extensively with that of rods. The dendritic arbor of ipRGCs is generally quite large[12]. As melanopsin is also expressed and functional in dendrites[11], this feature enables ipRGCs to have rather large receptive fields allowing for substantial integration across space[12]. The signaling cascade associated with phototransduction by melanopsin is evolutionarily distinct from that of the rods and cones[1]. While rods and cones represent ciliary photoreceptors, their phototransduction ultimately results in hyperpolarization upon photon capture mediated by the G-protein transducin[13]. In contrast, rhabdomeric photoreceptors like melanopsin use a different G protein, Gq/11, and result in ipRGC depolarization upon photon capture[13,14]. One consequence of these signaling differences is that the duration of the signaling cascade associated with melanopsin is remarkably prolonged, about 20 times that of rods and 100 times that of cones[15].

Although initially assumed to be a homogeneous population of light level sensors, more sensitive cellular and molecular techniques have revealed a striking diversity amongst ipRGCs. The field now recognizes at least 5 distinct subtypes of ipRGCs[21]. They can be differentiated on the basis of morphology, including soma size and location and size of their dendritic fields. The various

subtypes also show different functional properties, including sensitivity of the intrinsic photoresponse as well as form of receptive fields or synaptic inputs. As future work continues to characterize ipRGC function, it is important to recognize the ipRGCs do not all behave uniformly.

The Melanopsin Response Persists

The ipRGCs receive synaptic input from cones[7–10]. Consequently, activity within the ipRGC can result from intrinsic excitation transduced by melanopsin, or extrinsic excitation originating from cones. Although both photoreceptor classes are capable of driving excitation within the ipRGC, their temporal properties differ. Extrinsic signaling originating in cones shows adaptation within ipRGCs; spiking activity decays under constant conditions[10]. In contrast, the melanopsin response is marked by prolonged firing with minimal to no adaptation[10]. In fact, certain ipRGCs have been recorded from that show melanopsin activation can result in continued firing capable of lasting for hours[22]. This relative response persistence can be functionally significant, as it enables melanopsin to signal irradiance, the type of slow changes in ambient brightness that occur over the course of a day.

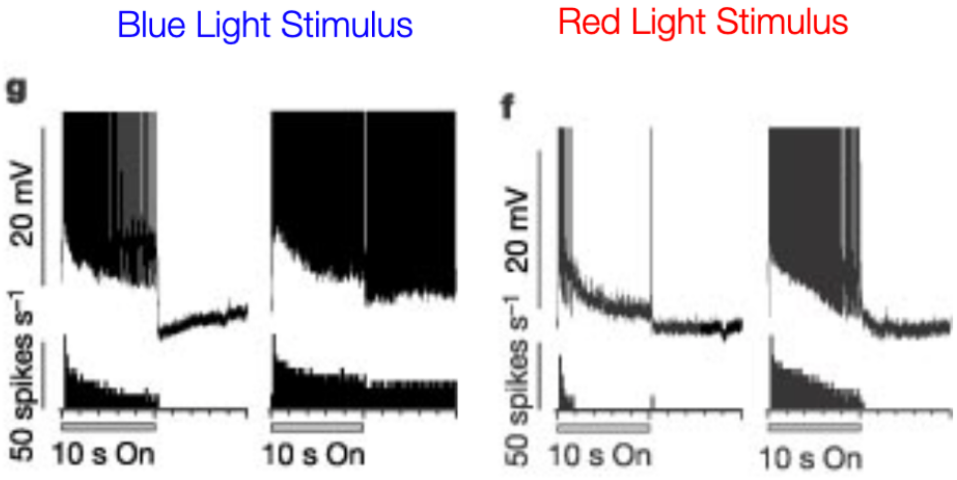

Figure 2. A demonstration of the relative persistence of the melanopsin response. Single unit recordings from ipRGCs within an isolated primate retina in response to blue light that targets melanopsin (and the cones) to red light, which targets mainly the cones. For each stimulus wavelength, two stimulus intensities are presented, with the brighter condition shown on the right within each inset. The blue light stimulus shows a sustained response for the entire light step while the red light response shows adaptation in response to the less intense stimulus. The more intense stimulus evokes sustained activity at both wavelengths, but the blue light response is notable for its persistence even following stimulus offset. Figure adapted from Dacey 2005[10].

ipRGCs and the Reflexive Functions of Vision

ipRGCs are generally thought to use this irradiance-related signal to mediate the "reflexive functions of vision." The term is intended to differentiate from "image forming" or spatial representational functions more commonly associated with vision. Functions mediated by ipRGCs have also been referred to as "non-image forming," but as the precise role of ipRGCs and melanopsin in conscious vision remains unclear, this label seems less useful. The most well-described reflexive visual functions linked to ipRGCs are control of pupil size and entrainment of the circadian rhythm.

Control of pupil size, which encompasses regulating both the size of the pupil in response to a steady light stimulus and how the pupil changes size over time in response to a change in light stimulus (i.e. the pupillary light reflex), is performed by ipRGCs via projections to the olivary pretectal nucleus in the brainstem[23–25]. The current literature suggests that ipRGCs may be the sole retinal input for control of pupil size, as ablation of ipRGCs dramatically attenuates the ability of the pupil to constrict to light in mice[26,27]. Cone, rod, and melanopsin signaling contributes to changes in pupil size, with the influence of cones dominating early and the relative contribution of melanopsin increasing over time[28]. Both the M1 and M2 classes of ipRGC are thought to contribute to the pupillary light reflex, through projections to the olivary pretectal nucleus shell and core, respectively[29].

Entrainment of the circadian rhythm is accomplished by projections of ipRGCs to the hypothalamus, including the suprachiasmatic nucleus (SCN)[11]. In actuality, entrainment of the circadian rhythm is multifaceted, and can be subdivided into related functions including melatonin suppression and circadian phase shifting, amongst others. Both of these related functions highlight the significance of the temporal differences in melanopsin and cone signaling, as cone signaling can be less effective[28,30] (although still present[31,32]). Again, both M1 and M2 classes of ipRGCs project to the SCN, but these M1 ipRGCs appear molecularly distinct from those that mediate pupil constriction[33].

Although the complete contribution of melanopsin to conscious vision remains unclear, multiple lines of evidence implicate melanopsin in the

perception of brightness. Spitschan et al showed that targeted melanopsin stimulation evokes a conscious visual percept, which subjects described as "uncomfortable brightness"[34], while Brown and colleagues indicated that subjects rated spectra with increased melanopic content as brighter[35]. Several groups have also attempted to quantify the way in which cone and melanopsin signals combine to produce the perception of brightness[36,37]. The details in these approaches differ, but all agree that increased melanopsin signaling makes light appear brighter. Although the ipRGC pathways involved in conscious brightness perception are uncertain, they presumably involve cortex, and melanopsin signals reach the cortex including human visual cortex[34].

Other manifestations of the role of melanopsin in the perception of brightness relate back to the reflexive functions of vision, in that they are behaviors associated with innate responses to bright light. For example, ipRGCs are thought to mediate light-induced lacrimation, a protective reflex[38]. In addition, work in mice has shown a role for melanopsin signaling in light avoidant behavior. From a developmental perspective, ipRGCs may be capable of driving light avoidance in mice at a developmental stage prior to when rod and cone signaling begin[39]. This ipRGC-dependent light aversion appears to carry into adulthood, as ablation of ipRGCs reduces the amount of time mice avoid a bright light[40]. Finally, there is evidence to suggest that ipRGCs mediate the experience of discomfort induced by bright light. Signals related to head pain carried by the trigeminal system were found to be modulated by light signals carried by ipRGCs in a rodent model through an interaction at the level of the somatosensory

thalamus[41]. The exact relationship between the perceptual experiences of light-induced discomfort, light avoidance, and the perception of brightness more generally is unresolved, as is full demonstration of their anatomical substrates.

ipRGC Systems in Pathology

Taken as a whole, it is interesting to note that these reflexive functions of vision all go awry in a number of disease contexts. For example, failures of circadian rhythm entrainment can manifest as sleep disturbances, which are found in a number of clinical entities. Similar observations have led to the speculation that perhaps pathology affecting these ipRGC systems may cause these symptoms[42]. Consequently, there is much interest in looking at ways to quantify ipRGC function in human subjects and asking if dysfunction is present in certain clinical conditions. This project is focused on photophobia, which can be interpreted as the normal process of brightness perception or light-induced discomfort exacerbated and made pathological. Photophobia, also known as light sensitivity, is found in a number of clinical contexts, including dry eye and traumatic brain injury. One of the most common causes is migraine headache[43].

Techniques to Probe Melanopsin Function

One of the main challenges in studying any purported ipRGC-mediated function is the need to isolate the melanopsin-specific response from that of the rods or cones. That is, researchers need a way to selectively stimulate melanopsin. The key difficulty is the extent to which the spectral sensitivities of

the various photopigments overlap. Shining a non-specific white light stimulus, for example, will activate melanopsin, all three classes of cones, and even the rods under specific circumstances. We can measure a response to this white light stimulus, but it is unclear how to delineate the contributions from each of these photoreceptors to the observed response. Although animal models, particularly in the rodent, offer a rich toolset to probe these systems, this review will focus on techniques available to investigation of humans.

One of the most common techniques is to compare the response to narrow-band stimulation of shorter-wavelength or blue light to longer-wavelength or red light. The motivation for the approach is as follows. Blue light is close to the peak spectral sensitivity of melanopsin, so any response elicited will have a relatively large contribution from melanopsin. This blue light stimulus will stimulate the cones (and potentially the rods), however, as well. The red light stimulus, in contrast, places minimal excitation on melanopsin but still excites the cones. The idea is one can compare the blue and red light responses, and since cone activity is reasonably matched between the two conditions, apparent differences in these responses we might relate to melanopsin.

This technique has been used most extensively to characterize the pupil response. Yet the increased temporal resolution offered by pupillometry offers additional benefits, as researchers can take advantage of the relatively persistent nature of the melanopsin response to better differentiate it from that of cones. In one of the earliest explorations of this approach, Gamlin and colleagues looked at the pupillary light reflex to narrow-band pulses of red and blue light stimuli[24].

They showed that the form of these responses over time differ extensively between the two chromatic conditions, as the blue response is remarkable for sustained pupil constriction extending past stimulus offset, and this persistent constriction is not apparent in the red response. This finding is entirely consistent with the known temporal properties of the melanopsin and cone responses, as the melanopsin response tends to persist while the cone response adapts. To validate this intuition, Gamlin and colleagues created an action spectrum for pupil constriction in non-human primates at a timepoint following stimulus offset, and showed it closely resembled the spectral sensitivity function of melanopsin. These results offer a second principle by which researchers can extract more of a melanopsin-specific response: examine pupil constriction later in time after stimulus offset to accentuate the different temporal properties of melanopsin and the cones. This approach has become known as the post-illumination pupil response or PIPR and has become quite popular for its relative ease of deployment. The work has also been effectively extend to human subjects, with work in humans showing its relative melanopsin-ness[44] and reliability[45]. Many groups have used the PIPR to look for variation of melanopsin function in

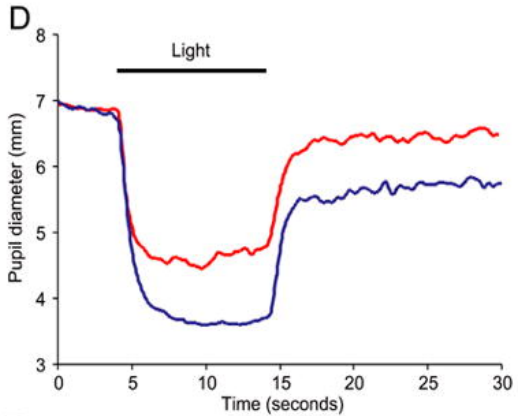

Figure 3. A demonstration of the PIPR, from Gamlin et al[24], showing pupil size over time in response to a light pulse. Note the enhanced sustained constriction, including following stimulus offset, in the blue light response.

pathology, including in multiple sclerosis, Parkinson's disease[46], idiopathic intracranial hypertension[47], traumatic brain injury[48], glaucoma[49,50], diabetes[51], retinitis pigmentosa[52], Leber's hereditary optic neuropathy[53], Smith-Magenis syndrome[54], and depression[55].

Although a useful technique, the PIPR or red-blue narrow-band approach more generally is not without its limitations. Most procedures involve presenting the stimulus against a dark background, which will introduce a significant rod component mainly to the blue light response. In addition, there is evidence that cones can also contribute to a sustained pupil response[23,56]. Although the PIPR reflects perhaps overwhelmingly the contribution of melanopsin, it is not truly melanopsin-specific, which challenges any claims that, for example, differences between clinical populations in the PIPR can be attributable solely to melanopsin.

Silent substitution provides an effective alternative that can better elicit a melanopsin-specific response[57]. Silent substitution involves the creation of metamers, which are two spectra of light that produce differing levels of excitations for some photoreceptor classes, but equal excitation for the others. Switching between these metamers then produces a response which can be attributed theoretically exclusively to the photoreceptor classes whose excitations vary, as the change is essentially "silent" to the non-modulated photoreceptor classes. This technique can be used to target any photoreceptor class or combination of photoreceptor classes, including to create melanopsin-targeted or cone-targeted stimulation.

In addition to requiring more sophisticated equipment to employ relative to the PIPR, other challenges must be addressed to ensure the stimuli have their intended effects. Cones lying in the penumbral shadow of the retinal vasculature have effectively altered spectral sensitivities and can respond to nominally cone-silenced stimuli; slow modulations can help prevent this effect[58]. Macular pigment similarly alters the spectral sensitivity within the macula, which can be avoided by stimulating away from this central region. Even with these considerations, practical reality dictates that the stimuli will never be as "silent" as desired. A good practice, then, is to carefully measure all stimuli and calculate any contrast inadvertently placed on nominally silenced photoreceptors.

Photophobia in Migraine

Migraine is one of the most common neurologic conditions, affecting approximately 18% of women and 6% of men[59]. Besides headache, patients with migraine report discomfort from light or photophobia as their most burdensome symptom[60]. Photophobia continues to be bothersome for migraineurs between headaches, as patients have a lower threshold for pain from light as compared with headache-free controls[61].

Considerable work has been done in elucidating the circuity underlying photophobia. At the most basic level, all proposed circuity has a sensory arm responsible for transducing the light-related signal. This light-related signal then modulates the perception of pain or discomfort carried by a distinct somatosensory pathway. Work in both animal models and humans heavily

implicates ipRGCs as one of the main conduits for the sensation of light in photophobia. In a mouse model, postnatal ablation of ipRGCs reduces light-aversive behavior[40]. In humans, some patients with blindness resulting from rod and cone degeneration continue to experience exacerbation of head pain by light, suggesting the remaining ipRGCs are sufficient to give rise to photophobia[41]. Lastly, Stringham and colleagues created an action spectrum for light sensitivity in humans, which showed a peak at shorter wavelengths consistent with a melanopsin-mediated response[62]. The literature is also fairly conclusive in its ability to localize the somatosensory arm of photophobia to the trigeminal system. The trigeminal system is generally involved with the perception of pain and discomfort of the head, and sensitization of this system is thought to be a causal factor in migraine headache[63]. Besides headache, the trigeminal system has also been directly implicated photophobia[64]. For example, exogenous manipulation of the trigeminal system effectively exacerbates light sensitivity in people with migraine interictally[65]. In summary, the model put forth by most of the literature is that the head pain-related signals are carried by the trigeminal system, and these signals are exacerbated by light via input from ipRGCs.

This basic mechanism still leaves unresolved the question as to the site of this interaction between the ipRGC and trigeminal systems. The literature proposes three main locations for where this interaction may occur. Okamoto and colleagues used Fos staining in a rat to reveal neurons within the caudal trigeminal brainstem activated by bright light[66,67]. Subsequent experiments

suggest this activity is mediated by light-induced ocular vasodilation and activation of ocular trigeminal afferents. These experiments, however, did not elucidate the photoreceptor basis of the observed trigeminal activity. Work from Noseda and colleagues, again in a rat model, propose a distinct mechanism that shifts focus to the thalamus[41]. They identified ascending dura-sensitive thalamic neurons whose activity was increased by a light stimulus, and show through tracing of projections of retinal ganglion cells that ipRGCs directly abut and synapse onto these dura- and light-sensitive neurons within the somatosensory thalamus. Finally, work from Matynia and colleagues offers a third mechanism notable for its entirely distinct sensory arm[68]. They showed that the photopigment melanopsin is functionally expressed on trigeminal afferents innervating the eye. Even in the absence of a functioning optic nerve, sensitized mice remain light avoidant in a manner dependent on melanopsin expression. It is also important to point out that this mechanism seems most relevant in sensitized animals, in that no behavioral light aversion was seen in animals that lacked functioning optic nerves but were not chemically sensitized. How these distinct mechanisms work together and extend to light sensitivity in humans remains unclear.

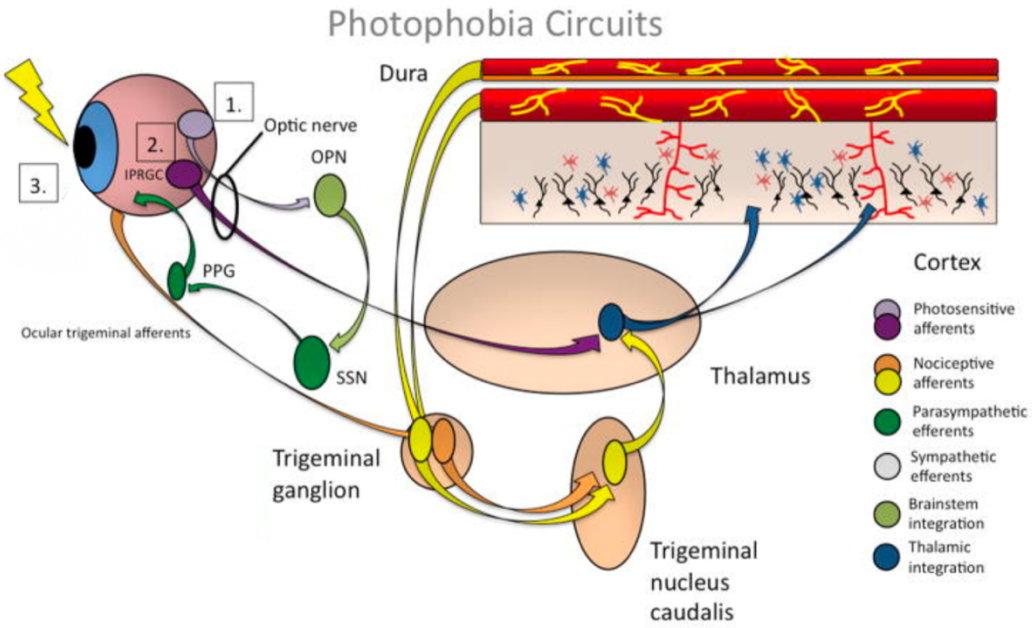

Figure 4. Photophobia circuits. 1. (Okamoto mechanism[66,67]) Ganglion cells project light-related signaling to the olivary pretectal nucleus (OPN; light green). OPN projections activate superior salivatory nucleus (SSN; dark green), which via pterygopalatine ganglion, causes ocular vasodilation and activation of ocular trigeminal afferents (orange) which are heavily expressed on blood vessels. These afferents, with cell bodies in the trigeminal ganglion, project to trigeminal nucleus caudalis, thalamus and cortex. 2. (Noseda mechanism[41]) Intrinsically photosensitive retinal ganglion cells (IPRGCs) project directly to thalamic neurons (blue) that also receive intracranial nociceptive afferent signal (yellow neurons in trigeminal ganglion and trigeminal nucleus caudalis). Thalamic neurons fire in response to light and pain stimuli. Their output projects diffusely to sensory and association cortex. 3. (Matynia mechanism[68]) Trigeminal nerve afferents innervating the eye (including the cornea, iris, and choroid) contain melanopsin, respond to light, and are thought to contribute to light avoidant behavior in sensitized mice in a manner independent of the optic nerve. Figure and legend adapted from Digre 2013[43].

Assuming these circuits contribute to the perception of bright light as uncomfortable, it remains unknown where or how this circuity goes awry in pathology, including migraine. One simple yet unresolved framing of this question is whether photophobia results from sensitization of the sensory apparatus itself at the level of the retina (i.e. the ipRGCs themselves are in some way

hyperexcitable), or whether photophobia is a consequence of post-retinal or downstream processing. Burstein and colleagues have suggested that photophobia may originate in the retina, as differences in discomfort elicited by monochromatic stimuli are also found at the level of the retina in terms of the magnitude of ERG recordings[69]. This study, however, failed to fix the size of the pupil across the different stimuli. As different wavelengths of light will produce varying degrees of pupil constriction, this discrepancy leaves open the possibility that increased discomfort to certain wavelengths of light results from more light entering through a larger pupil. In a departure from this prior work, this same group has also pointed towards a role instead for rods in driving migraine-type photophobia,[70] but a similar failure to fix pupil size complicates that interpretation.

In contrast, other lines of evidence are consistent with a post-retinal localization for the pathophysiology underlying photophobia in migraine. Numerous lines of evidence point to cortical abnormalities in migraine, particularly the notion that the cortex in migraine is hyperexcitable. This hyperexcitability is apparent both in terms of the phenomenon of cortical spreading depression and enhanced responses to sensory stimulation[71]. Further, pharmacologic work points to a post-retinal process, as exogenous administration of calcitonin gene-related peptide (CGRP) into the brain of transgenic mice is sufficient to exacerbate light avoidant behavior[72]. These authors go on to speculate that the likely site of action is the trigeminal nucleus caudalis, consistent with the mechanism put forth by Okamoto.

Finally, the photoreceptor basis of photophobia is unresolved, even assuming the ipRGCs are the main pathway involved. Rodent models have suggested roles for both melanopsin and cone signaling[40]. Blind patients with migraine, presumably only able to signal light with melanopsin, can be light sensitive, emphasizing the role of melanopsin in these patients[41]. Whether melanopsin is still relevant in normally sighted individuals, and indeed whether cones also contribute, are unknown.

Towards Neural Correlates of Light Sensitivity

In order to effectively translate mechanistic insight to human patients, we need ways to probe these systems in human subjects. Without the ability to directly measure photophobia-related signals in migraine, we must examine other, more accessible light-related responses and determine how they relate to the pathophysiology in question. Besides a clinical tool to aid in diagnosis, this approach can empower further basic science insight into photophobia, including its photoreceptor basis or localization.

Much work has attempted to elucidate neural correlates of interictal light sensitivity in migraine. One of the most consistent findings is cortical hyperresponsiveness in migraine, in which various cortical measure shows an increased response magnitude in migraine. As one example, researchers have shown an increase in response in the magnitude of the BOLD fMRI signal to flashing checkboards in visual cortex in migraine relative to headache free controls[73]. Related work shows hyperresponsiveness in migraine through

electrophysiology[74] and TMS[75]. Interestingly, many of these studies attribute the hyperresponsiveness to a failure of neural adaptation, suggesting the pathology results from aberrant temporal processing.

These studies represent significant progress in our understanding of the pathophysiology of light sensitivity, but it must be emphasized that not all responses to light are the same. Indeed, significant inferential value is added by comparing different light-mediated responses. For example, consider the pupillary light reflex. Although it shares the same sensory apparatus (i.e. the retina), the rest of the anatomy underlying it and cortical hyperresponsiveness largely differs. Comparing pupillometry and presumably cortically mediated responses then may help localize light sensitivity within the central nervous system.

There have been numerous studies to date that look at the pupillary light reflex in people with migraine between headache episodes. The majority show no difference in the resting pupil size or amplitude of pupil constriction following a light pulse[76–80]. Other studies show more subtle alterations in the way the pupil changes size over time[78,79,81]. When considered together, however, there is no evidence for similar hyperresponsiveness at the level of the pupil. Contextualizing any more subtle changes in the pupillary light reflex is challenging, and could relate to autonomic disturbances prominent in migraine[82,83] rather than the visual system itself per se. Further careful quantitative measures of the pupillary light reflex in migraine, especially those that dissect the contributions of individual photoreceptor classes, are needed.

References

1. Provencio I, Jiang G, De Grip WJ, Pär Hayes W, Rollag MD. Melanopsin: An opsin in melanophores, brain, and eye. *Proc Natl Acad Sci U S A*. 1998. doi:10.1073/pnas.95.1.340
2. Provencio I, Rodriguez IR, Jiang G, Hayes WP, Moreira EF, Rollag MD. A Novel Human Opsin in the Inner Retina. *J Neurosci*. 2000;20(2):600-605. http://www.jneurosci.org/content/20/2/600%5Cnhttp://www.jneurosci.org/content/20/2/600.full%5Cnhttp://www.jneurosci.org/content/20/2/600.full.pdf%5Cnhttp://www.ncbi.nlm.nih.gov/pubmed/10632589.
3. Liao HW, Ren X, Peterson BB, et al. Melanopsin-expressing ganglion cells on macaque and human retinas form two morphologically distinct populations. *J Comp Neurol*. 2016;524(14):2845-2872. doi:10.1002/cne.23995
4. La Morgia C, Ross-Cisneros FN, Sadun AA, et al. Melanopsin retinal ganglion cells are resistant to neurodegeneration in mitochondrial optic neuropathies. *Brain*. 2010;133(8):2426-2438. doi:10.1093/brain/awq155
5. Hannibal J, Hindersson P, Østergaard J, et al. Melanopsin is expressed in PACAP-containing retinal ganglion cells of the human retinohypothalamic tract. *Investig Ophthalmol Vis Sci*. 2004;45(11):4202-4209. doi:10.1167/iovs.04-0313
6. Nasir-Ahmad S, Lee SCS, Martin PR, Grünert U. Melanopsin-expressing ganglion cells in human retina: Morphology, distribution, and synaptic connections. *J Comp Neurol*. 2017. doi:10.1002/cne.24176
7. Perez-Leon JA, Warren EJ, Allen CN, Robinson DW, Lane Brown R. Synaptic inputs to retinal ganglion cells that set the circadian clock. *Eur J Neurosci*. 2006. doi:10.1111/j.1460-9568.2006.04999.x
8. Wong KY, Dunn FA, Graham DM, Berson DM. Synaptic influences on rat ganglion-cell photoreceptors. *J Physiol*. 2007. doi:10.1113/jphysiol.2007.133751
9. Weng S, Estevez ME, Berson DM. Mouse Ganglion-Cell Photoreceptors Are Driven by the Most Sensitive Rod Pathway and by Both Types of Cones. *PLoS One*. 2013. doi:10.1371/journal.pone.0066480
10. Dacey DM, Liao H-W, Peterson BB, et al. Melanopsin-expressing ganglion cells in primate retina signal colour and irradiance and project to the LGN. *Nature*. 2005;433(7027):749-754. doi:10.1038/nature03387
11. Berson DM. Phototransduction by Retinal Ganglion Cells That Set the Circadian Clock. *Science (80-)*. 2002;295(5557):1070-1073. doi:10.1126/science.1067262
12. Provencio I, Rollag MD, Castrucci AM. Photoreceptive net in the mammalian retina. *Nature*. 2002. doi:10.1038/415493a
13. Arendt D. Evolution of eyes and photoreceptor cell types. *Int J Dev Biol*. 2003. doi:10.1387/ijdb.14756332
14. Graham DM, Wong KY, Shapiro P, Frederick C, Pattabiraman K, Berson DM. Melanopsin ganglion cells use a membrane-associated rhabdomeric phototransduction cascade. *J Neurophysiol*. 2008.

doi:10.1152/jn.01066.2007
15. Do MTH, Kang SH, Xue T, et al. Photon capture and signalling by melanopsin retinal ganglion cells. *Nature*. 2009;457(7227):281-287. doi:10.1038/nature07682
16. Wang JS, Kefalov VJ. The Cone-specific visual cycle. *Prog Retin Eye Res*. 2011. doi:10.1016/j.preteyeres.2010.11.001
17. Mure LS, Rieux C, Hattar S, Cooper HM. Melanopsin-dependent nonvisual responses: Evidence for photopigment bistability in vivo. *J Biol Rhythms*. 2007. doi:10.1177/0748730407306043
18. Matsuyama T, Yamashita T, Imamoto Y, Shichida Y. Photochemical properties of mammalian melanopsin. *Biochemistry*. 2012. doi:10.1021/bi3004999
19. Zhao X, Pack W, Khan NW, Wong KY. Prolonged inner retinal photoreception depends on the visual retinoid cycle. *J Neurosci*. 2016. doi:10.1523/JNEUROSCI.2629-14.2016
20. Fu Y, Zhong H, Wang MHH, et al. Intrinsically photosensitive retinal ganglion cells detect light with a vitamin A-based photopigment, melanopsin. *Proc Natl Acad Sci U S A*. 2005. doi:10.1073/pnas.0501866102
21. Schmidt TM, Chen SK, Hattar S. Intrinsically photosensitive retinal ganglion cells: Many subtypes, diverse functions. *Trends Neurosci*. 2011. doi:10.1016/j.tins.2011.07.001
22. Wong KY. A retinal ganglion cell that can signal irradiance continuously for 10 hours. *J Neurosci*. 2012. doi:10.1523/JNEUROSCI.1423-12.2012
23. Lucas RJ, Hattar S, Takao M, Berson DM, Foster RG, Yau KW. Diminished pupillary light reflex at high irradiances in melanopsin-knockout mice. *Science (80-)*. 2003;299(5604):245-247. doi:10.1126/science.1077293
24. Gamlin PDR, McDougal DH, Pokorny J, Smith VC, Yau KW, Dacey DM. Human and macaque pupil responses driven by melanopsin-containing retinal ganglion cells. *Vision Res*. 2007;47(7):946-954. doi:10.1016/j.visres.2006.12.015
25. Hattar S, Liao HW, Takao M, Berson DM, Yau KW. Melanopsin-containing retinal ganglion cells: architecture, projections, and intrinsic photosensitivity. *Science (80-)*. 2002;295(5557):1065-1070. doi:10.1126/science.1069609
26. Güler AD, Ecker JL, Lall GS, et al. Melanopsin cells are the principal conduits for rod/cone input to non-image forming vision. *Nature*. 2008;453(7191):102-105. doi:10.1038/nature06829.Melanopsin
27. Hatori M, Le H, Vollmers C, et al. Inducible ablation of melanopsin-expressing retinal ganglion cells reveals their central role in non-image forming visual responses. *PLoS One*. 2008. doi:10.1371/journal.pone.0002451
28. Lall GS, Revell VL, Momiji H, et al. Distinct contributions of rod, cone, and melanopsin photoreceptors to encoding irradiance. *Neuron*. 2010. doi:10.1016/j.neuron.2010.04.037

29. Baver SB, Pickard GE, Sollars PJ, Pickard GE. Two types of melanopsin retinal ganglion cell differentially innervate the hypothalamic suprachiasmatic nucleus and the olivary pretectal nucleus. *Eur J Neurosci*. 2008;27(7):1763-1770. doi:10.1111/j.1460-9568.2008.06149.x
30. Spitschan M, Lazar R, Yetik E, Cajochen C. No evidence for an S cone contribution to acute neuroendocrine and alerting responses to light. *Curr Biol*. 2019. doi:10.1016/j.cub.2019.11.031
31. Walmsley L, Hanna L, Mouland J, et al. Colour As a Signal for Entraining the Mammalian Circadian Clock. *PLoS Biol*. 2015. doi:10.1371/journal.pbio.1002127
32. Mouland JW, Martial F, Watson A, Lucas RJ, Brown TM. Cones Support Alignment to an Inconsistent World by Suppressing Mouse Circadian Responses to the Blue Colors Associated with Twilight. *Curr Biol*. 2019. doi:10.1016/j.cub.2019.10.028
33. Chen SK, Badea TC, Hattar S. Photoentrainment and pupillary light reflex are mediated by distinct populations of ipRGCs. *Nature*. 2011. doi:10.1038/nature10206
34. Spitschan M, Bock AS, Ryan J, Frazzetta G, Brainard DH, Aguirre GK. The human visual cortex response to melanopsin-directed stimulation is accompanied by a distinct perceptual experience. *Proc Natl Acad Sci*. 2017;114(46):12291-12296. doi:10.1073/pnas.1711522114
35. Brown TM, Tsujimura SI, Allen AE, et al. Melanopsin-based brightness discrimination in mice and humans. *Curr Biol*. 2012;22(12):1134-1141. doi:10.1016/j.cub.2012.04.039
36. Zele AJ, Adhikari P, Feigl B, Cao D. Cone and melanopsin contributions to human brightness estimation. *J Opt Soc Am A*. 2018. doi:10.1364/josaa.35.000b19
37. Yamakawa M, Tsujimura S ichi, Okajima K. A quantitative analysis of the contribution of melanopsin to brightness perception. *Sci Rep*. 2019. doi:10.1038/s41598-019-44035-3
38. Lei S, Goltz HC, Chen X, Zivcevska M, Wong AMF. The relation between light-induced lacrimation and the melanopsin-driven postillumination pupil response. *Investig Ophthalmol Vis Sci*. 2017;58(3):1449-1454. doi:10.1167/iovs.16-21285
39. Johnson J, Wu V, Donovan M, et al. Melanopsin-dependent light avoidance in neonatal mice. *Proc Natl Acad Sci U S A*. 2010. doi:10.1073/pnas.1008533107
40. Matynia A, Parikh S, Chen B, et al. Intrinsically photosensitive retinal ganglion cells are the primary but not exclusive circuit for light aversion. *Exp Eye Res*. 2012. doi:10.1016/j.exer.2012.09.012
41. Noseda R, Kainz V, Jakubowski M, et al. A neural mechanism for exacerbation of headache by light. *Nat Neurosci*. 2010;13(2):239-245. http://dx.doi.org/10.1038/nn.2475.
42. Ksendzovsky A, Pomeraniec IJ, Zaghloul KA, Provencio JJ, Provencio I. Clinical implications of the melanopsin-based non-image-forming visual

system. *Neurology*. 2017. doi:10.1212/WNL.0000000000003761
43. Digre KB, Brennan KC. Shedding light on photophobia. *J Neuro-Ophthalmology*. 2012. doi:10.1097/WNO.0b013e3182474548
44. McDougal DH, Gamlin PD. The influence of intrinsically-photosensitive retinal ganglion cells on the spectral sensitivity and response dynamics of the human pupillary light reflex. *Vis Res*. 2010;50(1):72-87. doi:10.1016/j.visres.2009.10.012
45. Kankipati L, Girkin CA, Gamlin PD. Post-illumination pupil response in subjects without ocular disease. *Investig Ophthalmol Vis Sci*. 2010;51(5):2764-2769. doi:10.1167/iovs.09-4717
46. Joyce DS, Feigl B, Kerr G, Roeder L, Zele AJ. Melanopsin-mediated pupil function is impaired in Parkinson's disease. *Sci Rep*. 2018;8(1). doi:10.1038/s41598-018-26078-0
47. Park JC, Moss HE, McAnany JJ. The Pupillary Light Reflex in Idiopathic Intracranial Hypertension. *Invest Ophthalmol Vis Sci*. 2016;57(1):23-29. doi:10.1167/iovs.15-18181
48. Yuhas PT, Shorter PD, Mcdaniel CE, Earley MJ, Hartwick ATE. Blue and Red Light-Evoked Pupil Responses in Photophobic Subjects with TBI. 2016;93(00):108-117. doi:10.1097/OPX.0000000000000934
49. Kankipati L, Girkin CA, Gamlin PD. The post-illumination pupil response is reduced in glaucoma patients. *Investig Ophthalmol Vis Sci*. 2011;52(5):2287-2292. doi:10.1167/iovs.10-6023
50. Feigl B, Mattes D, Thomas R, Zele AJ. Intrinsically photosensitive (melanopsin) retinal ganglion cell function in glaucoma. *Investig Ophthalmol Vis Sci*. 2011;52(7):4362-4367. doi:10.1167/iovs.10-7069
51. Feigl B, Zele AJ, Fader SM, et al. The post-illumination pupil response of melanopsin-expressing intrinsically photosensitive retinal ganglion cells in diabetes. *Acta Ophthalmol*. 2012;90(3). doi:10.1111/j.1755-3768.2011.02226.x
52. Kawasaki A, Crippa S V., Kardon R, Leon L, Hamel C. Characterization of pupil responses to blue and red light stimuli in autosomal dominant retinitis pigmentosa due to NR2E3 mutation. *Investig Ophthalmol Vis Sci*. 2012;53(9):5562-5569. doi:10.1167/iovs.12-10230
53. Moura ALA, Nagy B V., La Morgia C, et al. The Pupil Light Reflex in Leber's Hereditary Optic Neuropathy: Evidence for Preservation of Melanopsin-Expressing Retinal Ganglion Cells. *Investig Opthalmology Vis Sci*. 2013;54(7):4471. doi:10.1167/iovs.12-11137
54. Barboni MTS, Bueno C, Nagy BV, et al. Melanopsin System Dysfunction in Smith-Magenis Syndrome Patients. *Invest Ophthalmol Vis Sci*. 2018;59(1):362-369.
55. Berman G, Muttuvelu D, Berman D, et al. Decreased retinal sensitivity in depressive disorder: a controlled study. *Acta Psychiatr Scand*.:n/a--n/a. doi:10.1111/acps.12851
56. Schroeder MM, Harrison KR, Jaeckel ER, et al. The roles of rods, cones, and melanopsin in photoresponses of M4 intrinsically photosensitive retinal

ganglion cells (ipRGCs) and optokinetic visual behavior. *Front Cell Neurosci*. 2018;12:203.
57. Estévez O, Spekreijse H. The “silent substitution” method in visual research. *Vision Res*. 1982;22(6):681-691. doi:10.1016/0042-6989(82)90104-3
58. Spitschan M, Aguirre GK, Brainard DH. Selective stimulation of penumbral cones reveals perception in the shadow of retinal blood vessels. *PLoS One*. 2015;10(4). doi:10.1371/journal.pone.0124328
59. Lipton RB, Stewart WF, Diamond S, Diamond ML, Reed M. Prevalence and burden of migraine in the United States: Data from the American Migraine Study II. *Headache*. 2001;41(7):646-657. doi:10.1046/j.1526-4610.2001.041007646.x
60. Munjal S, Singh P, Reed ML, et al. Most Bothersome Symptom in Persons With Migraine: Results From the Migraine in America Symptoms and Treatment (MAST) Study. *Headache*. 2020. doi:10.1111/head.13708
61. Main A, Dowson A, Gross M. Photophobia and phonophobia in migraineurs between attacks. *Headache*. 1997;37(8):492-495. doi:10.1046/j.1526-4610.1997.3708492.x
62. Stringham JM, Fuld K, Wenzel AJ. Action spectrum for photophobia. *J Opt Soc Am A*. 2003. doi:10.1364/josaa.20.001852
63. Bernstein C, Burstein R. Sensitization of the trigeminovascular pathway: Perspective and implications to migraine pathophysiology. *J Clin Neurol*. 2012. doi:10.3988/jcn.2012.8.2.89
64. Rossi HL, Recober A. Photophobia in primary headaches. *Headache*. 2015. doi:10.1111/head.12532
65. Drummond P d., Woodhouse A. Painful Stimulation of the Forehead Increases Photophobia in Migraine Sufferers. *Cephalalgia*. 1993. doi:10.1046/j.1468-2982.1993.1305321.x
66. Okamoto K, Thompson R, Tashiro A, Chang Z, Bereiter DA. Bright light produces Fos-positive neurons in caudal trigeminal brainstem. *Neuroscience*. 2009. doi:10.1016/j.neuroscience.2009.03.003
67. Okamoto K, Tashiro A, Chang Z, Bereiter DA. Bright light activates a trigeminal nociceptive pathway. *Pain*. 2010. doi:10.1016/j.pain.2010.02.004
68. Matynia A, Nguyen E, Sun X, et al. Peripheral Sensory Neurons Expressing Melanopsin Respond to Light. *Front Neural Circuits*. 2016;10(August):60. doi:10.3389/fncir.2016.00060
69. Noseda R, Bernstein CA, Nir RR, et al. Migraine photophobia originating in cone-driven retinal pathways. *Brain*. 2016. doi:10.1093/brain/aww119
70. Bernstein CA, Nir RR, Noseda R, et al. The migraine eye: Distinct rod-driven retinal pathways’ response to dim light challenges the visual cortex hyperexcitability theory. *Pain*. 2019. doi:10.1097/j.pain.0000000000001434
71. Goadsby PJ, Holland PR, Martins-Oliveira M, Hoffmann J, Schankin C, Akerman S. Pathophysiology of migraine: A disorder of sensory processing. *Physiol Rev*. 2017. doi:10.1152/physrev.00034.2015
72. Recober A, Kuburas A, Zhang Z, Wemmie JA, Anderson MG, Russo AF.

Role of calcitonin gene-related peptide in light-aversive behavior: Implications for migraine. *J Neurosci*. 2009. doi:10.1523/JNEUROSCI.1727-09.2009
73. Datta R, Aguirre GK, Hu S, Detre J a, Cucchiara B. Interictal cortical hyperresponsiveness in migraine is directly related to the presence of aura. *Cephalalgia*. 2013;33(6):365-374. doi:10.1177/0333102412474503
74. Ambrosini A, Schoenen J. Electrophysiological response patterns ofprimary sensory cortices in migraine. *J Headache Pain*. 2006;7(6):377-388. doi:10.1007/s10194-006-0343-x
75. Coppola G, Pierelli F, Schoenen J. Is the cerebral cortex hyperexcitable or hyperresponsive in migraine? *Cephalalgia*. 2007;27(12):1429-1439. doi:10.1111/j.1468-2982.2007.01500.x
76. Cambron M, Maertens H, Paemeleire K, Crevits L. Autonomic function in migraine patients: Ictal and interictal pupillometry. *Headache*. 2014;54(4):655-662. doi:10.1111/head.12139
77. Harle DE, Wolffsohn JS, Evans BJW. The pupillary light reflex in migraine. *Ophthalmic Physiol Opt*. 2005;25(3):240-245. doi:10.1111/j.1475-1313.2005.00291.x
78. Eren OE, Ruscheweyh R, Schankin C, Schöberl F, Straube A. The cold pressor test in interictal migraine patients - different parasympathetic pupillary response indicates dysbalance of the cranial autonomic nervous system. *BMC Neurol*. 2018. doi:10.1186/s12883-018-1043-2
79. Cortez MM, Rea NA, Hunter LA, Digre KB, Brennan KC. Altered pupillary light response scales with disease severity in migrainous photophobia. *Cephalalgia*. 0(0):0333102416673205. doi:10.1177/0333102416673205
80. Drummond PD. Pupil diameter in migraine and tension headache. *J Neurol Neurosurg Psychiatry*. 1987. doi:10.1136/jnnp.50.2.228
81. Cortez MM, Rae N, Millsap L, McKean N, Brennan KC. Pupil cycle time distinguishes migraineurs from subjects without headache. *Front Neurol*. 2019. doi:10.3389/fneur.2019.00478
82. Peroutka SJ. Migraine: A Chronic Sympathetic Nervous System Disorder. *Headache*. 2004. doi:10.1111/j.1526-4610.2004.04011.x
83. Miglis MG. Migraine and Autonomic Dysfunction: Which Is the Horse and Which Is the Jockey? *Curr Pain Headache Rep*. 2018. doi:10.1007/s11916-018-0671-y

Chapter 2 - Pulses of melanopsin-directed contrast produce highly reproducible pupil responses that are insensitive to a change in background radiance

Citation:

McAdams, H., Igdalova, A., Spitschan, M., Brainard, D. H., & Aguirre, G. K. (2018). Pulses of melanopsin-directed contrast produce highly reproducible pupil responses that are insensitive to a change in background radiance. *Investigative ophthalmology & visual science*, *59*(13), 5615-5626.

Authors:

Harrison McAdams: BA, Perelman School of Medicine at the University of Pennsylvania, Department of Neurology

Aleksandra “Sasha” Igdalova: BA, Perelman School of Medicine at the University of Pennsylvania, Department of Neurology

Manuel Spitschan: PhD, Department of Experimental Psychology, University of Oxford

David H. Brainard: PhD, Department of Psychology, University of Pennsylvania

Geoffrey K. Aguirre: MD/PhD, Perelman School of Medicine at the University of Pennsylvania, Department of Neurology. Corresponding author. Address: 3400 Spruce Street, Philadelphia, PA 19104. Phone: 215-662-3390. Fax: 215-349-8260. Email: aguirreg@upenn.edu

Grant support: R01EY024681 - Melanopsin and cone signals in human visual processing, supported by the NIH

Commercial relationships: n/a

Abstract

Purpose

To measure the pupil response to pulses of melanopsin-directed contrast, and compare this response to those evoked by cone-directed contrast and spectrally-narrowband stimuli.

Methods

3-second unipolar pulses were used to elicit pupil responses in human subjects across 3 sessions. Thirty subjects were studied in Session 1, and most returned for Sessions 2 and 3. The stimuli of primary interest were “silent substitution” cone- and melanopsin-directed modulations. Red and blue narrowband pulses delivered using the post-illumination pupil response (PIPR) paradigm were also studied. Sessions 1 and 2 were identical, while Session 3 involved modulations around higher radiance backgrounds. The pupil responses were fit by a model whose parameters described response amplitude and temporal shape.

Results

Group average pupil responses for all stimuli overlapped extensively across Sessions 1 and 2, indicating high reproducibility. Model fits indicate that the response to melanopsin-directed contrast is prolonged relative to that elicited by cone-directed contrast. The group average cone- and melanopsin-directed pupil responses from Session 3 were highly similar to those from Sessions 1 and 2,

suggesting that these responses are insensitive to background radiance over the range studied. The increase in radiance enhanced persistent pupil constriction to blue light.

Conclusions

The group average pupil response to stimuli designed through silent substitution provides a reliable probe of the function of a melanopsin-mediated system in humans. As disruption of the melanopsin system may relate to clinical pathology, the reproducibility of response suggests that silent substitution pupillometry can test if melanopsin signals differ between clinical groups.

Introduction

Melanopsin is a photopigment found within the intrinsically photosensitive retinal ganglion cells (ipRGCs; Figure 1a). While they represent a small fraction (~1-3%) of the total retinal ganglion cell population[1–4], ipRGCs are critical for entrainment of circadian rhythm[5,6], aversive responses to light[7], light-induced lacrimation[8], and control of pupil diameter[9–11]. Disruption of these reflexive visual functions is seen in many clinical conditions, leading to the speculation that dysfunction in the melanopsin system is responsible[7,12–17]. Consequently there is interest in measuring, in humans, a signal that reflects melanopsin function and testing if this signal varies between groups.

The post-illumination pupil response (PIPR) paradigm is one method to assess melanopsin function in humans[11,18,19]. The PIPR paradigm exploits the differing spectral sensitivities of the melanopsin photopigment and the cone-based luminance mechanism: the medium and long-wavelength cones (M and L)—which are the primary input to the luminance mechanism—are more sensitive to light of longer wavelengths ('red'), while melanopsin sensitivity is greatest in the short-wavelength ('blue') range. The PIPR paradigm measures the response of the pupil to pulses of narrowband blue and red light presented against steady dark backgrounds. Particular attention is paid to the behavior of the pupil at relatively delayed time periods, including after stimulus offset (i.e., 'post-illumination'), when melanopsin is found to exert greater and more sustained influence over pupil size relative to the cones[11,20]. In fact, this relative persistence of the melanopsin response as compared to the more rapidly

adapting cone response is a key property of signaling within ipRGCs. PIPR measurements have been made in numerous clinical conditions, including multiple sclerosis, Parkinson's disease, idiopathic intracranial hypertension, traumatic brain injury, glaucoma, diabetes, retinitis pigmentosa, Leber's hereditary optic neuropathy, Smith-Magenis syndrome, and depression[21–32].

While relatively simple to deploy and measure, interpretation of the PIPR as a melanopsin-specific signal is less straightforward. Because the blue stimulus is presented against a dark background, the pupil response will include a rod contribution[33,34]. Blue light also drives S-cones, which, like melanopsin, produce delayed and sustained pupil responses[35]. While there is convincing evidence that sustained pupil constriction can be produced by melanopsin alone[11], cones may also contribute (perhaps via the ipRGCs) to a sustained response[36–38]. Therefore, while the PIPR response reflects (perhaps overwhelmingly) the contribution of melanopsin signals, it cannot be concluded that differences between clinical populations in PIPR responses are attributable solely to the melanopsin system.

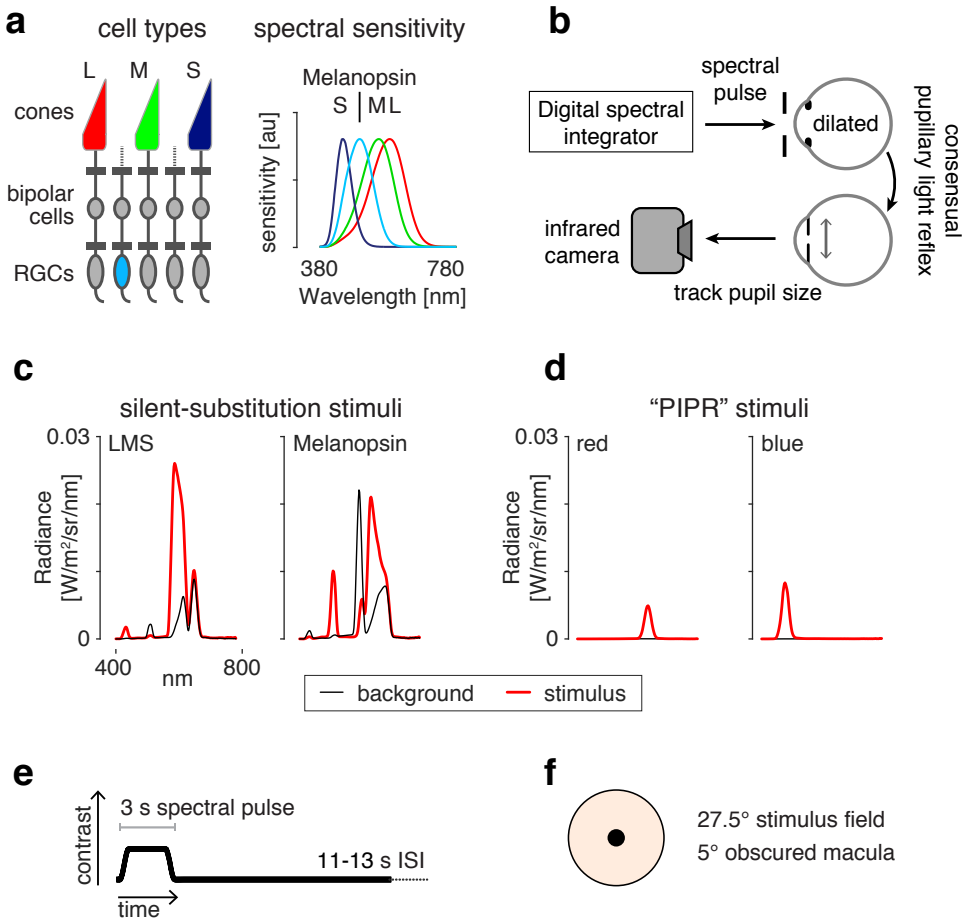

Figure 1. Overview and experimental design. (a, left) L, M, and S cones as well as melanopsin-containing ipRGCs (blue) mediate visual function at daytime light levels. (a, right) The spectral sensitivity functions of these photoreceptors. (b) A digital light integrator delivers spectral pulses to the pharmacologically dilated right eye of the subject's pupil. The consensual pupil- lary reflex from the left eye is recorded via an infrared camera. (c) We use silent substitution to selectively target either the L, M and S cones and thus the postreceptoral luminance channel (left) or melanopsin (right). (d) The PIPR stimuli consist of narrowband pulses of long wavelength red light (left) or short wavelength blue light (right). Note that the stimuli are equated in terms of retinal irradiance, but because the number of quanta/Watt and pre-receptoral filtering are wavelength dependent, the blue stimulus has higher measured radiance. All stimuli are from Session 1. The particular spectra plotted here and in panel d are an example from one subject; the spectra varied by subject age to account for preceptoral filtering. (e) We delivered 3 s spectral pulses smoothed by a 500 ms half-cosine window, with an inter-stimulus interval between trials ranging from 11 to 13 s. (f) Stimuli were presented through an eyepiece with a 27.5° with the central 5° obscured to prevent activation of the macula.

Silent substitution spectral modulations[39] provide an alternate approach to the study of the melanopsin contribution to the human pupil response[35,40–45]. Light spectra are tailored to modulate the response of one or more targeted photoreceptor mechanisms (e.g., melanopsin), while holding the response of the remaining photoreceptor mechanisms (e.g., L-, M- and S-cones) constant. Subjects first adapt to a background light spectrum. When the silent substitution modulation is presented around that background, the subsequent response is attributable to the targeted photoreceptor(s). Here, we measured the temporal properties and reliability of the across-subject average pupil response to pulses of melanopsin contrast delivered via silent substitution. We compared the response to melanopsin stimulation to that evoked by cone-directed contrast that was silent for melanopsin, and by narrowband PIPR stimuli. To anticipate, we find that the silent substitution approach produces a highly reproducible measure of melanopsin-driven pupil response that is insensitive to a change in background radiance.

These experiments were the subject of pre-registration documents. The pre-registered protocol was followed (with small exceptions, see Methods) in subject recruitment, screening, exclusion, stimulus validation, and pupil data pre-processing. The analyses described in the pre-registration examined the reliability of between subject differences in response. We found relatively low reliability and present those results in the supplementary materials (Supplementary Figures 5, 6). We focus here upon population level analyses that were not pre-registered.

Methods

Subjects

Subjects were recruited from the community of students and staff at the University of Pennsylvania. Exclusion criteria for enrollment included a prior history of glaucoma or a negative reaction to pupil-dilating eye drops. During an initial screening session, subjects were also excluded for abnormal color vision as determined by the Ishihara plates[46] or visual acuity below 20/40 in each eye as determined using a distance Snellen eye chart. Subjects completed a brief, screening pupillometry session. We excluded at this preliminary stage subjects who were unable to provide high-quality pupil tracking data (details below). Poor data quality was found to result from difficulty suppressing blinks or from poor infra-red contrast between the pupil and iris.

A total of 32 subjects were recruited and completed initial screening. Two of these subjects were excluded after screening due to poor data quality (e.g., excessive loss of data points from blinking) as determined by pre-registered criteria. Thirty subjects thus successfully completed Session 1 and provided data for analysis. These subjects were between 19-33 years of age (mean 25.93 ± 4.24 SD). Fourteen subjects identified as male, 15 female, and one declined to provide a gender identification. Of this group of 30 subjects, 24 completed an identical second session of testing and 21 completed a third session at higher light levels. The time between participation in Session 1 and Session 2 was on average 110 days, and between Session 1 and Session 3 on average 296 days. The study was approved by the Institutional Review Board of the University of

Pennsylvania, with all subjects providing informed written consent, and all experiments adhered to the tenets of the Declaration of Helsinki.

When a subject arrived for a session of primary data collection, the right eye was first anesthetized with 0.5% proparacaine and dilated with 1% tropicamide ophthalmic solution. Subjects then had their right eye dark adapted by wearing swimming goggles with the right eye obscured while sitting in a dark room for 20 minutes. In an attempt to minimize variation in circadian cycle across sessions, testing for Sessions 2 and 3 started within three hours of the time of day when the same subject started Session 1.

Stimuli

The experiments used two classes of stimuli: 1) silent substitution spectral modulations that targeted either the melanopsin photopigment or the cone-mediated luminance post-receptoral mechanism; 2) narrow-band blue and red stimuli designed to elicit the post-illumination pupil response (PIPR).

The silent substitution stimuli were a subset of those used in a prior report[42], and full details of their generation may be found there. Briefly, we used the method of silent substitution together with a digital light synthesis engine (OneLight Spectra) to stimulate targeted photoreceptors. The device produces stimulus spectra as mixtures of 56 independent primaries (~16 nm FWHM) under digital control, and can modulate between these spectra at 256 Hz. Details regarding the device, stimulus generation, and estimates of precision have been previously reported[35,47,48]. Our estimates of photoreceptor spectral sensitivities

were as previously described[48], with those for the cones based on the field size and age dependent CIE physiological cone fundamentals[49]. The estimates account for subject age, pupil size (which was fixed at 6 mm diameter through the use of an artificial pupil) and our field size of 27.5 degrees. Although the standard specifies fundamentals only for field sizes up to 10 degrees, we obtained the 27.5 degree estimates by extrapolating using the formula from the standard using routines in the open-source Psychophysics Toolbox[50–52]. Separate background and modulation spectra were identified to provide nominal 400% Weber contrast on melanopsin while silencing the cones for the melanopsin-directed background/modulation pair (Mel), and 400% contrast on each of the L-, M-, and S-cone classes while silencing melanopsin for the luminance-directed modulation/background pair (LMS) (Figure 1c). The xy chromaticities of the background spectra for the Mel and LMS stimuli were similar (Mel: ~0.56, ~0.40; LMS: ~0.58, ~0.38)[49]. The background for Mel and LMS pulses were nominally rod-saturating (~110 photopic cd/m^2 or 3.10 log scoptopic trolands for Mel and ~40 photopic cd/m^2 or 2.99 log scotopic trolands for LMS for Sessions 1 and 2; ~270 photopic cd/m^2 or 3.59 log scotopic trolands and ~90 photopic cd/m^2 or 3.46 log scotopic trolands for Session 3). The xy chromaticities and photopic luminances reported above were calculated using the proposed XYZ functions associated with the CIE 2006 10-degree cone fundamentals (https://cvrl.org)[49]. The modulations did not explicitly silence rods or penumbral cones[48].

The PIPR stimuli consisted of narrowband pulses of blue (475 ± 25 nm peak ± Gaussian FWHM) and red (623 ± 25 nm) light (Figure 1d). These stimuli were each designed to produce 12.30 log quanta·cm^{-2}·sec^{-1} retinal irradiance for Sessions 1 and 2, and12.85 log quanta·cm^{-2}·sec^{-1} for Session 3, in a manner that accounted for differences in lens density due to subject age. These stimuli were presented against a dim background (~0.5 cd/m^2 for the first 2 sessions, ~1 cd/m^2 for the third session). The irradiance of the PIPR stimuli was limited by the gamut of the device at short wavelengths, and the requirement to match the retinal irradiance of the red and blue stimuli. Background light levels were the minimum possible with our apparatus, as some light is emitted by the light engine even when all primaries are set to their minimum level.

Due to imperfections in device control, the actual stimuli presented differed in photoreceptor contrast and irradiance from their nominal designed values. Before and after each subject's measurement session, spectroradiometric validation measurements of the background and modulation spectra were obtained. From these, we calculated the actual contrast upon targeted and nominally silenced photoreceptors for that subject (using age-based photoreceptor sensitivities) for the silent substitution stimuli, as well as the retinal irradiance of the PIPR stimuli. Following our pre-registered protocol, we excluded data for a given session if the post-experiment validation measurements showed that the silent substitution stimuli were of insufficient quality. Specifically, if the contrast on the targeted post-receptoral mechanism (Mel or LMS) was less than 350% (as compared to the nominal 400%), or if contrast upon an ostensibly

silenced post-receptoral mechanism (Mel, LMS, L–M, or S) was greater than 20%. Data from five sessions were discarded (and subsequently recollected) as a consequence of this procedure. We did not evaluate the PIPR stimuli for the purposes of data exclusion. Supplementary Table 1 provides the results of the stimulus validations for all subjects, sessions, and stimuli. These calculations do not account for the biological variability in individual photoreceptor spectral sensitivity that can produce further departures from nominal stimulus contrasts[42].

Three-second pulses of spectral change were presented during individual trials of 17 s duration (Figure 1e). During each trial, a transition from the background to the stimulation spectrum (Mel, LMS, blue, or red) would occur starting at either 0, 1, or 2 seconds after trial onset (randomized uniformly across trials); this jitter was designed to reduce the ability of the subject to anticipate the moment of stimulus onset. The transition from the background to the stimulation spectrum, and the return to background, was smoothed by a 500 msec half-cosine window. The half-cosine windowing of the stimulus was designed to minimize perception of a Purkinje tree percept in the melanopsin-directed stimulus[48].

Each session consisted of three blocks of stimuli: PIPR (consisting of both red and blue stimuli counterbalanced in order within subject), LMS, and Mel, in this fixed order. At the start of each block the subject adapted to the background spectrum for 4.5 minutes. The block consisted of twenty-four, 17 second trials. Within each block, after every 6 trials, participants were invited to take a break before resuming the experiment. During the break they could lift their head from

the chin rest. The duration of each break was determined by the subject, and was less than a few minutes. Light adaptation was not maintained during the break. Before continuing with the experiment, subjects re-adapted to the background spectrum for 30 seconds, whether or not they took a break.

Stimuli were presented through a custom-made eyepiece with a circular, uniform field of 27.5° diameter and the central 5° diameter obscured (Figure 1f). The central area of the stimulus was obscured to minimize stimulation within the macula, where macular pigment alters the spectral properties of the stimulus arriving at the photoreceptors. Subjects viewed the field through a 6 mm diameter artificial pupil and were asked to maintain fixation on the center of the obscured central region.

Pupillometry

Pupil diameter was measured using an infrared video pupillometry system (Video Eye Tracker; Cambridge Research Systems Ltd.), sampled at 50 Hz. Following acquisition, the raw measured pupil response was adjusted in time to account for the stimulus onset time within each trial and normalized by the baseline pupil size for that trial (with baseline size taken as the mean pupil diameter for 1 second prior to stimulus onset). Data points in the resulting response for which the velocity of constriction or dilation exceeded 2500% change/s were rejected and replaced via linear interpolation. The responses across trials were averaged.

Pupillometry data were excluded from analysis on the basis of the number of rejected data points. Trials containing 10% or more rejected data points were

deemed incomplete and excluded from the average; if more than 75% of the trials for a given stimulus type were excluded, then the entire session was judged to be incomplete and the subject was either re-studied or excluded, following our pre-registered procedure. Additionally, if more than 50% of trials across all stimulus types were excluded, then the subject was either re-studied or excluded. Data from four sessions were discarded for this reason; 2 of these subjects were re-studied.

As noted briefly under Subjects above, screening pupillometry was also performed prior to primary data collection to exclude subjects for whom good quality pupil tracking data could not be obtained. In a screening session, subjects were presented two sets of six trials of the PIPR stimuli. Subjects with 4 or more incomplete trials assessed by the same criterion above were excused from the experiment. Two subjects were excused from the study in this manner.

Analysis

We fit the pupil response for each stimulus and subject using a three-component temporal model (Figure 3a)[42]. The stimulus profile passes through the model and, under the control of six parameters, is transformed into a predicted pupil response. The six parameters include two time constants that influence the shape of each component, three gain parameters that adjust the scaling of each component, and one onset delay parameter that shifts the entire modeled response in time. The transient component captures the initial peak of pupil constriction, the sustained component tracks the shape of the stimulus profile,

and the persistent component describes the slow dilation of the pupil back to baseline. Each component has an amplitude parameter. The shape of the components are under the control of two temporal parameters. The τ_{gamma} parameter controls the rate of onset and width of all components. The $\tau_{exponential}$ controls the rate of exponential decay of the persistent component. The three components are summed to create the model response, which is then temporally shifted in time by the overall delay parameter. We fit this model to the average response for each subject for each stimulus condition. In analyzing group differences of model parameters, the median value was used as parameters were not normally distributed across subjects.

Model fits were performed using MATLAB's fmincon function. Fits were initialized from 6 different starting positions and the fit with the highest proportion variance explained (R^2) was retained. Additionally, bounds were placed on each parameter, as informed by an initial inspection of the data. The bounds of the τ_{gamma} were different for responses elicited through silent substitution and PIPR stimuli. Specifically, the upper boundary of τ_{gamma} for fits to responses elicited by PIPR stimuli was greater than that for fits to responses elicited through silent substitution to reflect the generally wider shape of these responses. This choice improved the quality of fits to each stimulus type. As we were interested exclusively in comparisons within a stimulus type (LMS vs. Mel, red vs. blue), the differing parameter boundaries would not influence any subsequent conclusions. We also performed additional analyses in which we locked and freed different

sets of parameters as part of control tests. These procedures are described in the Supplementary Materials (Supplementary Figure 3).

To test for significance of observed group differences of metrics derived from our model, we used label permutation. For a given group comparison, we took the observed metric aggregated across all trials for a given stimulus type for each subject and randomly assigned each metric to the correct stimulus label or the opposite stimulus label. After performing this for all subjects, we computed the median difference. We performed this simulation 1,000,000 times, and asked the percentage of simulations in which the simulated median difference is more extreme than the observed median difference.

Pre-registration of studies

Our studies (composed of three sessions of data collection) were the subject of pre-registration documents (https://osf.io/9umq4/) and annotated addenda (https://osf.io/bg76w/). The pre-registered protocol dictated subject recruitment, screening, data exclusion, and stimulus validation. Session 1 was designed to test if we could measure the melanopsin mediated pupil response to silent substitution and PIPR stimuli in individuals. Data collection for Session 1 commenced in September 2016. An addendum (https://osf.io/hyj89/) detailed an improvement in our approach to generating stimuli that accurately described stimulus production for both the initial and subsequent subjects; this document is dated September 2016 but was not uploaded until October 2016. A January of

2017 addendum clarified an ambiguity in our original description of the stimulus validation procedure (https://osf.io/b4r3q/).

Session 2 was designed to determine if the magnitude of pupil response to melanopsin stimulation was a reliable individual subject difference (https://osf.io/z2vj7/). Session 3 repeated the measurements at a higher light level in an attempt to evoke a larger response to the PIPR stimuli and to further test the reliability of any individual differences in pupil response (https://osf.io/angyu/).

Our original motivation for these studies was to measure individual differences in pupil response. We ultimately determined that this test was limited by within-session measurement noise. Therefore, this paper focuses on comparisons at the group level. In keeping with our pre-registered protocols, however, we provide in the supplementary material the results of individual subject analyses (Supplementary Figures 5, 6).

There was ambiguity in our initial protocol regarding the interpretation of post-experimental stimulus validations. Five validation measurements were made after each experimental session. Our pre-registration initially failed to delineate how to interpret all five validation values; our procedure was later clarified to specify that data from a session would be excluded if the median value across all five post-experiment validation values was larger than the cutoff criterion. Data from one session were discarded and re-collected based upon an initial interpretation of the validation procedure in which a single validation measurement that exceeded criterion led to data rejection. Following the

clarification of our procedure to use the median validation measurement, data from four subsequent sessions were discarded and recollected because of stimulus quality.

Availability of data and analysis code

Data will be available via figshare upon publication. Analysis code that operates upon the raw data and produces the results and figures may be found here: https://github.com/gkaguirrelab/pupilPIPRAnalysis.

Results

In each of 30 subjects we measured consensual pupil responses in the left eye to spectral modulations presented to the pharmacologically dilated right eye (Figure 1b). Two of the modulations targeted the post-receptoral luminance or melanopsin pathway using a silent substitution spectral exchange (Figure 1c, left), and two of the modulations were narrowband red or blue increments typical of PIPR studies (Figure 1c, right). We presented these spectral modulations as half-cosine windowed, 3 second pulses (Figure 1d) on a spatially uniform field, except for masking of the central 5° of visual angle to minimize stimulation of the macula (Figure 1e). We recorded the ensuing pupil response for each of many trials in 30 subjects (Session 1) and a subset of these subjects in Sessions 2 (24 subjects) and 3 (21 subjects). We derived the average pupil response for each subject across the 24 trials presented in a session. In supplementary analyses

(Supplementary Figures 1, 2) we examined the dependence of pupil size and pupil response upon trial order.

Silent substitution and PIPR stimuli elicit highly reproducible pupil responses at the group level

We first examined the form of group (averaged over subjects) pupil responses to pulsed spectral modulations designed to selectively target the cones or melanopsin (Figure 2a, top row). We measured pupil responses during the 13 seconds that followed the onset of a 3 second stimulus pulse, and expressed pupil size as the percentage change in diameter relative to the pre-stimulus period. For our silent substitution stimuli, which were equated in contrast, the LMS-mediated pupil response was of overall larger amplitude than that evoked by the melanopsin-directed stimulus. The responses also differed in their shape, with the offset of the stimulus producing a more rapid dilation for LMS stimulation as compared to melanopsin stimulation.

The red and blue PIPR stimuli also produced pupil constriction. These stimuli were equated in retinal irradiance but the amplitude of pupil constriction was smaller in response to the red stimulus as compared to the blue stimulus. The shape of these responses also differed subtly, as the pupil began to dilate during the red stimulus, while the constriction in response to the blue stimulus continued to increase during stimulus presentation.

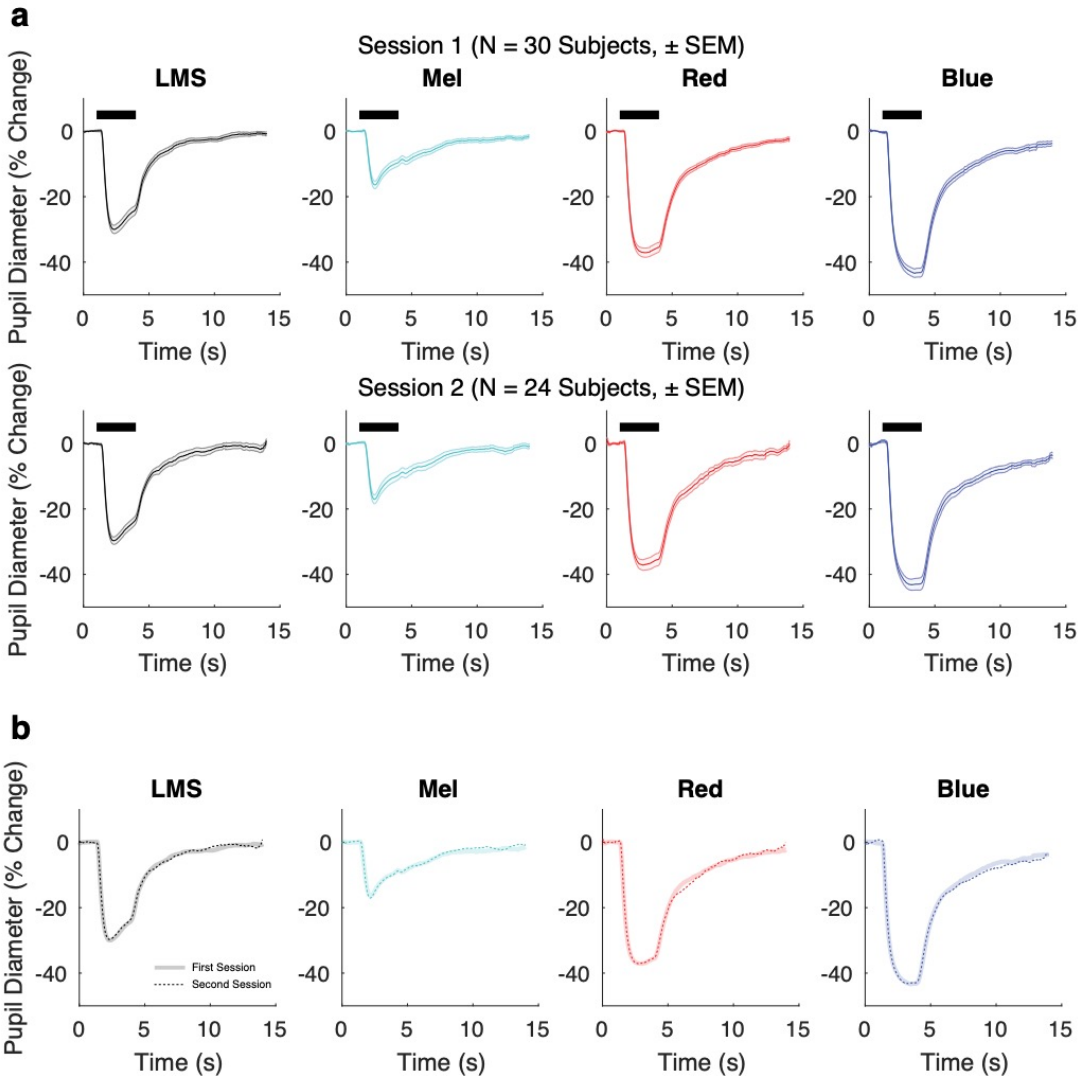

Figure 2. Reproducibility of group average pupil responses by stimulation/The group average pupil response is stable over time. (a) Group average pupil responses (± standard error of the mean) for each stimulus condition from session 1 (top, N = 30 subjects) and session 2 (bottom, N = 24 subjects). (b) Group average responses from session 2 in saturated, dotted lines are plotted on top of group average responses from session 1.

The standard error of the mean across subjects was quite small relative to the amplitude of response. While this might suggest that the measurements would be reproducible in this group, it is possible that variation in subject state

(e.g., due seasonal or circadian changes) or drift in our apparatus would reduce reproducibility across sessions. We tested for reproducibility by repeating the measurements during Session 2 in 24 of the 30 subjects between 54 and 175 days later (Figure 2a, bottom row). The amplitude, shape, and within-session standard error of the mean measured in Session 2 was quite similar to that measured in Session 1. Figure 2b presents the group average from Session 2 plotted directly on top of that from Session 1 for each stimulus condition. The reproducibility of the pupil response to all stimuli is evident, both in amplitude (max absolute difference in amplitude of group-averaged responses: 1.47% for LMS, 1.64% for Mel, 2.24% for red 1.74%, for blue), and in shape (Pearson correlation coefficient of the Session 1 group average with the Session 2 group average: r = 0.999 for LMS, r = 0.995 for Mel, 0.998 for red, r = 0.999 for blue).

The melanopsin response is more persistent than the cone response

Melanopsin-driven activation of ipRGCs results in notably prolonged responses[5,20]. Here we asked if a difference in the temporal profile of the pupil response to cone and melanopsin stimulation is apparent at the group level. We fit the data from each subject with a three-component model of the pupil response (Figure 3a)[42]. The model has amplitude parameters for transient, sustained, and persistent components, as well as three temporal parameters that specify the overall timing and influence the shape of the components. Figure 3b illustrates the model fits for the data from Session 1. The fit line is given by the median of the model parameters across subjects. There is good agreement

between the model and the across-subject average response. The amplitude and shape of the three model components are shown inset in each panel. After combining the data from Sessions 1 and 2 for those subjects studied twice, we tested for differences in the amplitude and temporal parameters evoked by the different stimuli.

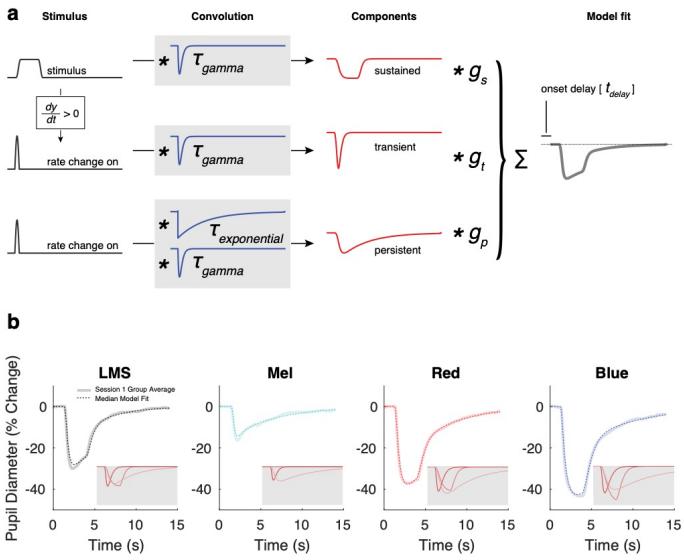

Figure 3. A three-component model fits the group average pupil responses. (a) Within-subject average evoked responses to each stimulus type was fit with a six-parameter, three-component model using a non-linear temporal fitting engine (https://github.com/gkaguirrelab/temporalFittingEngine). The model was designed to capture the three, visually apparent and temporally separated components of the evoked pupil response. The elements of the model are not intended to directly correspond to any particular biological mechanism. The input to the model was the stimulus profile (black). An additional input vector, representing the rate of stimulus change at onset, was created by differentiating the stimulus profile and retaining the positive elements. These three vectors were then subjected to convolution operations composed of a gamma and exponential decay function (blue), each under the control of a single time-constant parameter (τgamma and τexponential). The resulting three components (red) were normalized to have unit area, and then subjected to multiplicative scaling by a gain parameter applied to each component (gtransient, gsustained, and gpersistent). The scaled components were summed to produce the modeled response (gray), which was temporally shifted (tdelay). (b) The model fit, computed from the median response parameter across all 30 subjects from Session 1, is plotted in saturated, dotted lines on top of the group average response from Session 1. The gray inset shows each model component of the fit (transient, sustained, and persistent from most to least saturated).

The transient, sustained, and persistent components of the model reflect different temporal domains. The persistent component captures the slow return to baseline of the pupil response following the offset of the stimulus. We considered that stimulation of the ipRGCs might produce pupil responses with a relatively enhanced persistent component. For each subject for each stimulus type, we computed the proportion of the total pupil response area made up of the persistent component (Figure 4a). Across subjects, the median pupil response to LMS stimulation had 50% of its total response area fit by the persistent component. In contrast, the response to melanopsin stimulation was 76% persistent ($p = 0.0015$ established by permutation of stimulus labels). This difference reflects primarily a larger sustained component in the pupil response to luminance; the absolute response area of the persistent component was similar for the cone and melanopsin-driven responses (Supplementary Table 2). Unexpectedly, for the PIPR stimuli, the persistent component was larger in response to the red as compared to the blue stimulus (median 'percent persistent' for red: 65%; for blue: 58%; $p = 0.00047$ by label permutation).

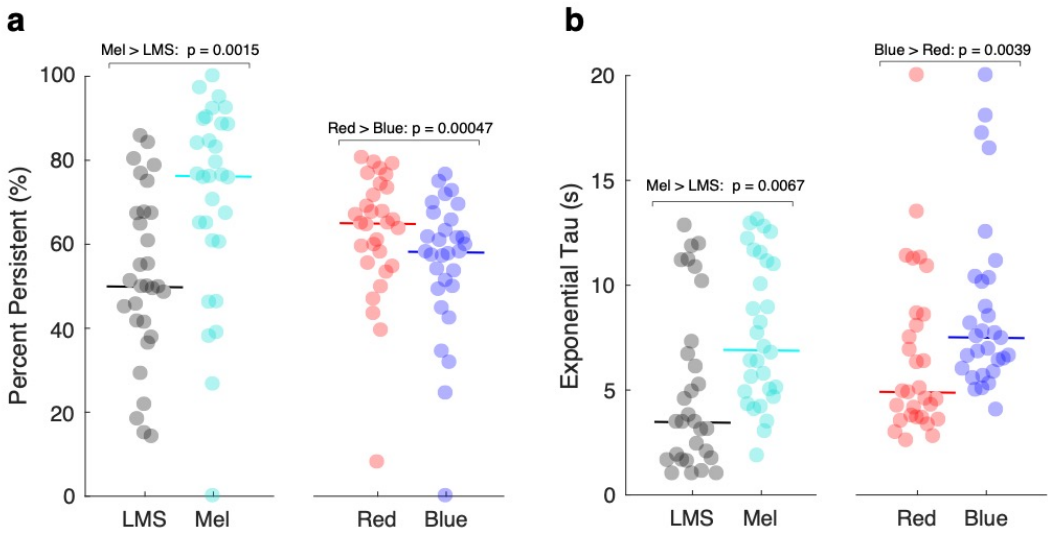

Figure 4. The melanopsin-mediated pupil response is more persistent than the cone-mediated pupil response. The (a) 'percent persistent' (b) and average exponential tau per subject of the model fit from Session 1 and Session 2 is plotted by stimulus type (N = 30 subjects); solid horizontal lines show the median value across subjects. Permutation testing was used to assess the significance of median differences in response across stimulus conditions at the group level.

We considered that the temporal profile of the persistent response, as opposed to its magnitude alone, would reflect the influence of melanopsin. The model parameter $\tau_{exponential}$ influences the rate at which the persistent component of pupil diameter dilates back to baseline following stimulus offset. We tested if this time constant differed in the responses to the stimulus types. Consistent with the expected properties of the ipRGCs, the melanopsin-driven response had a slower return to baseline as compared to the LMS-driven response (Figure 4b, median $\tau_{exponential}$ for LMS: 3.46 s; for Mel: 6.90 s; p = 0.0067 by label permutation). This slower return to baseline was also observed for the response to the blue stimulus as compared to the red stimulus (red: 4.89 s; blue: 7.50 s; p

= 0.0039 by label permutation). Supplementary Table 2 contains the amplitude and temporal parameters for all conditions and stimuli.

A property of our analysis is that the temporal parameters are allowed to vary between the compared stimulus conditions to best fit the data. It is therefore possible that observed differences in the $\tau_{exponential}$ or 'percent persistent' measurements arise as a consequence of differences in other model parameters. To evaluate this possibility, we re-ran the analyses holding the other temporal parameters fixed between the two compared stimulus conditions. This analysis revealed very similar results (Supplementary Figure 3).

Silent substitution and PIPR methods are differently sensitive to stimulus radiance

We considered the possibility that the pupil response evoked by the silent substitution stimuli would be relatively insensitive to the overall spectral power of the stimuli, as long as the contrast was held constant. For Session 3, we modified our apparatus to increase the radiance of all stimuli. Although the background luminance of the silent substitution stimuli more than doubled (mean background luminance for LMS from ~40 cd/m^2 to ~90 cd/m^2 or 2.99 log scotopic trolands to 3.46 log scotopic trolands; for Mel increased from ~110 cd/m^2 to ~270 cd/m^2 or 3.10 log scoptopic trolands to 3.59 log scotopic trolands), the calculated LMS and melanopsin contrast remained the same. For the PIPR stimuli, the nominal intensity of the spectral pulse increased from 12.30 to 12.85 log

quanta·cm^{-2}·sec^{-1}, and the background luminance increased from 0.5 cd/m^2 to 0.9 cd/m^2.

We then repeated the pupil measurements in 21 of the 30 subjects between 238 and 352 days after their initial enrollment (Session 3). Figure 5 presents the group average response collapsed across the first two sessions, compared to the pupil response measured in Session 3. For the LMS and Mel stimuli the average group response was essentially unchanged (max absolute difference in amplitude of group-averaged responses: 1.10% for LMS, 1.27% for Mel; Pearson correlation of the evoked response between Session 1/2 and Session 3: LMS, r = 0.999; Mel, r = 0.994). This high degree of reproducibility suggests that the pupil response to the silent substitution stimuli is insensitive to this change in absolute light intensity and instead reflects stimulus contrast.

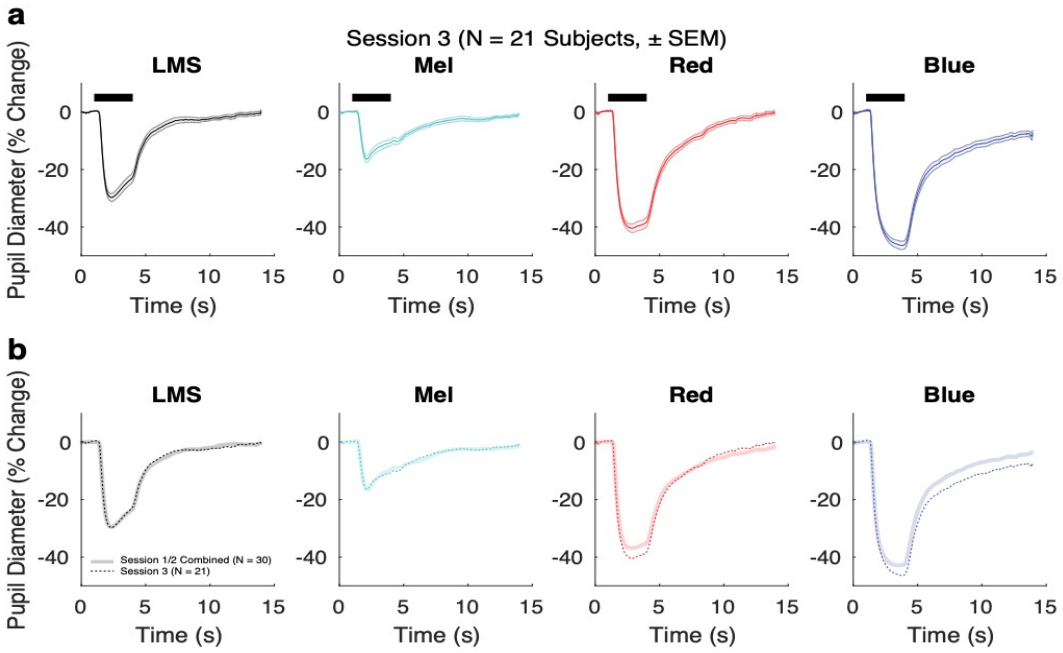

Figure 5. The pupil response is invariant to background luminance. (a) Group average pupil responses (± standard error of the mean) for each stimulus condition from session 3 (N = 21 subjects). (b) Group average responses from session 3 (back- ground luminance for Mel and LMS were ~270 cd/m2 and ~ 100 cd/m2, respectively) in saturated, dotted lines are plotted on top of group average responses from sessions 1 and 2 combined (N = 30 subjects; background luminance for Mel and LMS were ~100 cd/m2 and ~40 cd/m2, respectively).

In distinction, the increase in the radiance of the PIPR stimuli produced a larger amplitude of pupil response (max absolute difference in amplitude of group-averaged responses: 3.60% for red, 4.89% for blue). Many studies that use the PIPR stimuli attempt to isolate the melanopsin-specific component by taking the difference of the blue and red responses. Figure 6 presents the difference in pupil response evoked by the red and blue stimuli at the two radiance levels. This PIPR effect, especially at the later time points, grows in magnitude from Sessions 1 and 2 to Session 3 (Figure 6). We quantified the

PIPR effect as the difference in the total response area of the model fits to blue and red stimuli for each subject, for each session. The median PIPR was larger in Session 3 as stimulus radiance was increased (Sessions 1/2 median PIPR: 35 % change * s; Session 3 median PIPR: 74 % change * s; p = 0.0002 by label permutation).

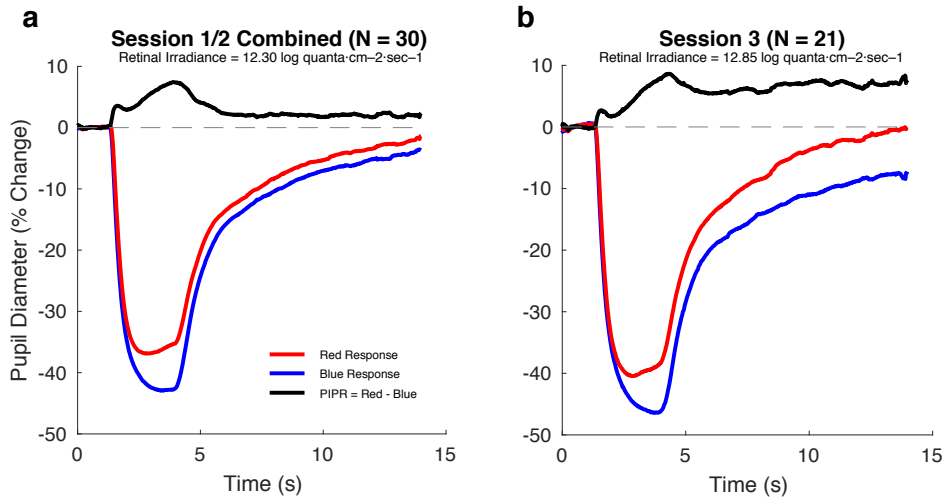

Figure 6. The differential PIPR increases with stimulus intensity. The differential PIPR (black) was calculated by subtracting the blue response from the red response (this order was chosen to provide a positive differential). The average responses from Session 1 and 2 were elicited from pulses with retinal irradiances of 12.30 log quanta·cm–2·sec–1 (a). Session 3 used pulses with retinal irradiances of 12.85 log quanta·cm–2·sec–1 (b).

Discussion

We find that pulsed spectral modulations that target the cones and melanopsin evoke distinctive pupil responses. At a group level, the average responses to these silent substitution stimuli are highly reliable. Consistent with the known temporal properties of the ipRGCs, the response to melanopsin-directed as

compared to cone-directed stimulation features a relatively larger persistent response that returns to baseline more slowly.

Our findings indicate the feasibility of using pupillometry with silent substitution stimuli to test for group differences in cone and melanopsin physiology. As compared to the PIPR stimuli, the silent substitution approach more directly targets and isolates the melanopsin and cone systems. Further, the highly reproducible responses seen at the group level indicate that differences between groups should be detected with good statistical power. Indeed, the extent to which this group average signal is reliable can be seen in the highly similar responses elicited from a different cohort of subjects using the same stimuli as part of a previous study[42] (Supplementary Figure 4).

We applied a model to the temporal profile of pupil responses to derive amplitude and timing parameters. This model accounts well for the form of response to both silent substitution and PIPR stimuli. Although we use 'percent persistent' to describe differences between the cone- and melanopsin-driven pupil responses, we find that all stimuli evoke some degree of persistent response. This observation is consistent with prior work, both in previous PIPR studies that show that the red stimulus evokes persistent pupil constriction, as well as neurophysiologic studies that show ipRGCs generate persistent firing from non-melanopsin inputs[38]. We examined as well the $\tau_{exponential}$ timing parameter of our model fits. The melanopsin-directed and PIPR blue stimuli produced responses with greater $\tau_{exponential}$ values as compared to their cone-directed and PIPR red counterparts. Therefore, while all stimulus types evoked

some amount of persistent pupil response, slower resolution of this response was seen for the stimuli thought to drive melanopsin. We anticipate that the temporal model may be used to test for differences in the amplitude and temporal properties of melanopsin-driven responses in clinical populations.

Although these results suggest that a key feature of the melanopsin response is its persistence, the delay to response onset was also found to differ between melanopsin- and cone-driven pupil responses. The relatively longer delay to response onset for the melanopsin-driven response is broadly consistent with prior work, although the absolute magnitude is less than might be expected[5,20,53,54]. Comparing the latency of neural responses within the ipRGCs to that within pupil responses is not straightforward. Neural response latency is dependent upon stimulus intensity, and can be as short as several hundred milliseconds for melanopsin-driven ipRGC activation[5]. Further, nonlinearities in the conversion of retinal ganglion cell signals to pupil response would complicate the interpretation of absolute latency differences between cone- and melanopsin-driven signals.

An original motivation for our study was to examine individual differences in the pupil response. While average responses at the group level were highly reliable, we found that there was relatively poor reproducibility for individual subjects (Supplementary Figure 5). We examined the reproducibility of total pupil response amplitude across subjects. While there was a reasonable correlation of this measure between Sessions 1 and 2, these responses did not correlate with the measurements from Session 3. Our results do not reject the possibility that

there are in fact reliable individual differences in the pupil response. Simulations suggest that within-session measurement noise could have obscured a true individual difference effect. Analysis of individual subject data also failed to show a relationship between individual differences in melanopsin function as elicited through the silent substitution and PIPR approaches (Supplementary Figure 6). In future studies, increasing the number of trials and improving pupillometry quality could reduce within-session measurement error and perhaps reveal reproducible individual differences in response.

In Session 3, we examined the effect of a multiplicative increase in stimulus intensity. This manipulation increased the radiance of both the stimulus and the background. For the silent substitution stimuli that targeted either the cones or melanopsin, this change in stimulus intensity did not alter the pupil response. While retinal irradiance was increased in Session 3, the contrast of the silent substitution modulations remained constant at 400%. Therefore, within this stimulus regime, the pupil response to silent substitution stimuli appears to be best characterized in terms of the photoreceptor contrast of the modulation.

These results also allow us to discount the possibility of inadvertent rod stimulation by the melanopsin-directed stimulus. The spectral sensitivity functions of melanopsin and rhodopsin overlap. Consequently, the melanopsin-directed silent substitution stimulus has substantial calculated contrast (~320%) upon the rod photoreceptors. Because the stimulus background is in the photopic range, we generally assume that the rods are saturated, and thus this rod contrast does not contribute to the observed pupil response. This assumption, however, may

be challenged by recent work that finds rods can signal above their nominal saturation threshold[55]. It is therefore reassuring to observe in the current study that the pupil response is unchanged with the increased stimulus intensity used in Session 3. If there were a substantial rod contribution to the pupil response measured to the melanopsin-directed stimulus in Sessions 1 and 2, we would expect that this contribution would become smaller at the higher background level. The equivalence of the pupil response suggests that any rod signals are minimal under these conditions. There remain other mechanisms through which rods could impact our measured pupil responses, including through the possibility of light scatter onto rods in the obscured parafoveal region or in the periphery beyond our 27.5 degree field. Prior work suggests, however, that any rod signaling produced through scattered light would have a small and transient effect upon the measured response[56].

Conversely, the post illumination pupil response (PIPR) evoked by the chromatic stimuli was enhanced by the increase in stimulus intensity in Session 3. Similar to the silent substitution stimuli, the photoreceptor contrast produced by the red and blue stimuli is in principle unchanged in Session 3. However, small imperfections in the control of the dim background light levels used for the PIPR stimuli could produce substantial changes in stimulus contrast. While our stimulus measurements indicate fairly consistent calculated contrast between the experimental sessions (Supplementary Table 1), actual variation in the contrasts produced by the PIPR stimuli remains a possible explanation for the enhanced responses to the PIPR stimuli seen in Session 3. It is also possible, however,

that the increased pupil response to the PIPR stimuli is a real effect of the change in stimulus intensity. When stimuli are presented against dark backgrounds, changes in intensity can lead to substantial changes in rod activation, which could then alter the response.

We note that our implementation of the PIPR paradigm differs from that used in many other studies, due to the particular nature of our apparatus. For example, the change in stimulus intensity examined in Session 3 increased both the stimulus and background light levels. This is unlike previous studies of the dependence of the PIPR upon intensity[29,57], in which the background presumably was held fixed across changes in the intensity of the chromatic pulses. Our apparatus also imposes gamut limits that restrict how dark we can make the background and how intense we can make the chromatic pulses. Additionally, many PIPR studies make use of a Ganzfeld dome and thus provide a greater spatial extent of stimulation than used here. These difference likely account for the smaller magnitude of post-illumination pupil response that we obtain in comparison to other studies[18,29,58]. That the PIPR depends on the specifics of the stimuli is an important consideration when comparing results obtained with this paradigm.

Overall, we find that the melanopsin-mediated pupil response at the group level is stable over time, consistent across stimulus conditions, and reflective of known melanopsin physiology. Various clinical conditions, including light sensitivity, may result from an alteration of melanopsin function. Our results suggest that silent substitution pupillometry can be used to test such hypotheses.

Supplementary Materials:

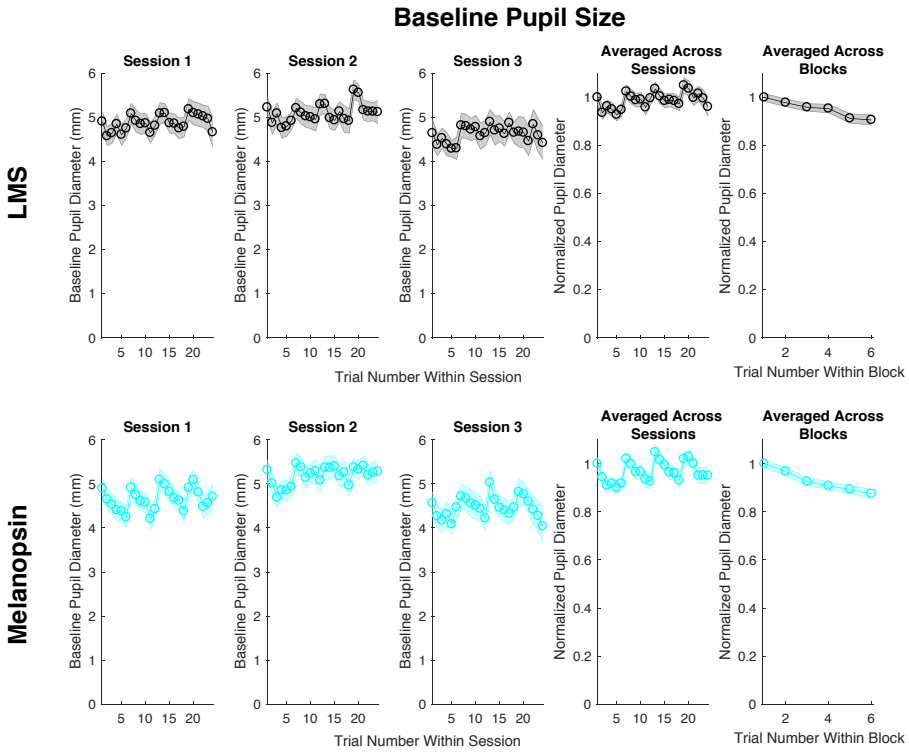

Supplementary Figure 1. Baseline pupil size as a function of trial number. We examined the baseline pupil size averaged over the 1 second prior to stimulus onset. For each trial, we averaged across subjects for each stimulus condition. This average baseline pupil size is plotted against trial number. The first three columns show the average baseline size for Sessions 1-3. The fourth column plots the data after normalizing pupil diameter within each session by the average baseline pupil diameter from the first trial within that session, and then averaging across sessions. The final column averages these normalized data across the 6-trial blocks. A general trend of decreasing baseline pupil size across trials within a block is seen for both LMS-directed (top) and melanopsin-directed (bottom) stimulation. Error bars reflect standard error of the mean.

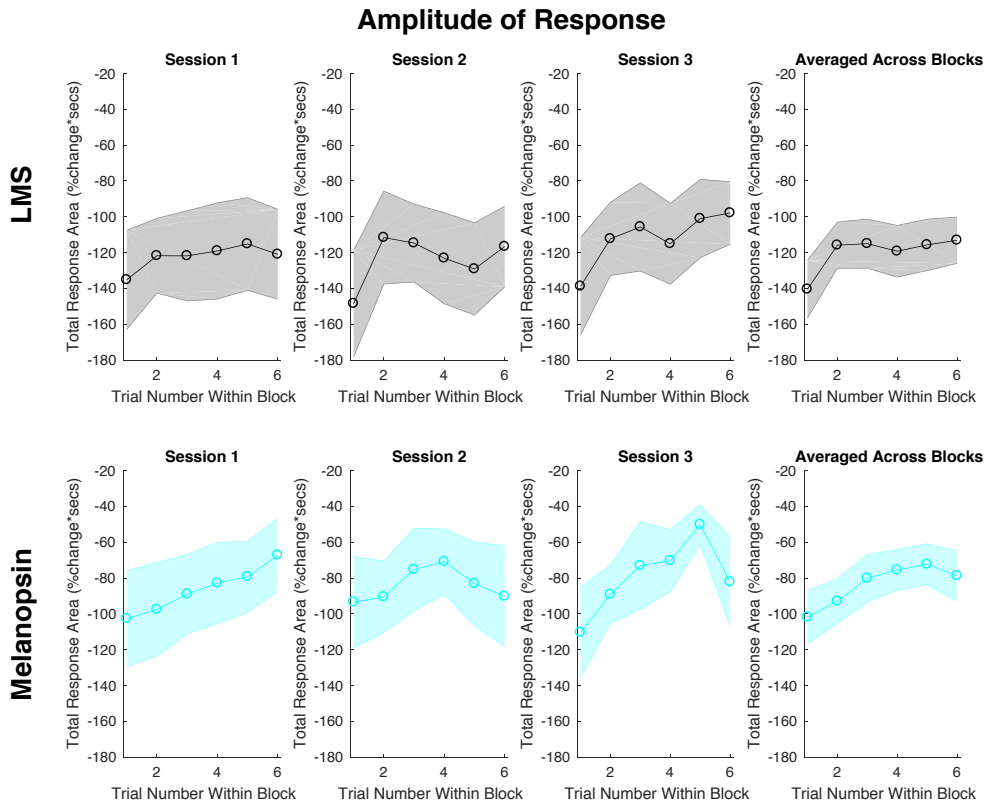

Supplementary Figure 2. Amplitude of evoked pupil response as a function of trial number within a block. We fit the three component model to the average pupil response across all trials of the same position within a block. The first three columns are these results for each session, while the fourth column represents the average values collapsed across sessions. A general trend of increasing evoked response across trials within a block is seen for both LMS-directed (top) and melanopsin-directed (bottom) stimulation. Error bars reflect standard error of the mean.

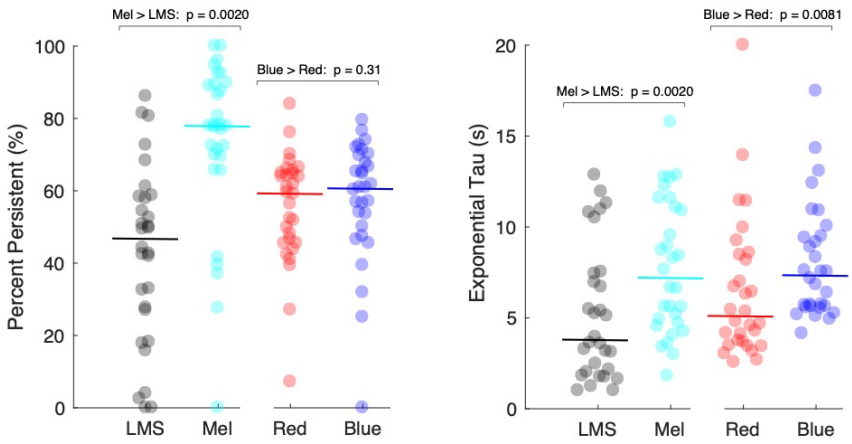

Supplementary Figure 3. The effect of parameter locking upon model results. Figure 4 presents two model-derived measures ('percent persistent' and $\tau_{exponential}$) compared between stimuli. This model fitting included other parameters, and it is possible that the observed results reflect a change in these other parameters as opposed to the parameters of interest. To examine this possibility, we re-ran the analysis holding the remaining parameters constant between our compared stimulus conditions. (a) The percent persistent measurement was made for the silent substitution data while fixing the three temporal parameters ($\tau_{exponential}$, τ_{gamma}, τ_{delay}) at the average value across the Mel and LMS response. Similarly, the amplitude of response evoked from the PIPR stimuli was modeled while fixing the temporal parameters at the mean value across the red and blue stimuli. The results of this analysis are largely consistent with the results presented in Figure 4. (b) The complementary analysis, now conducted by holding all model parameters fixed except for $\tau_{exponential}$.

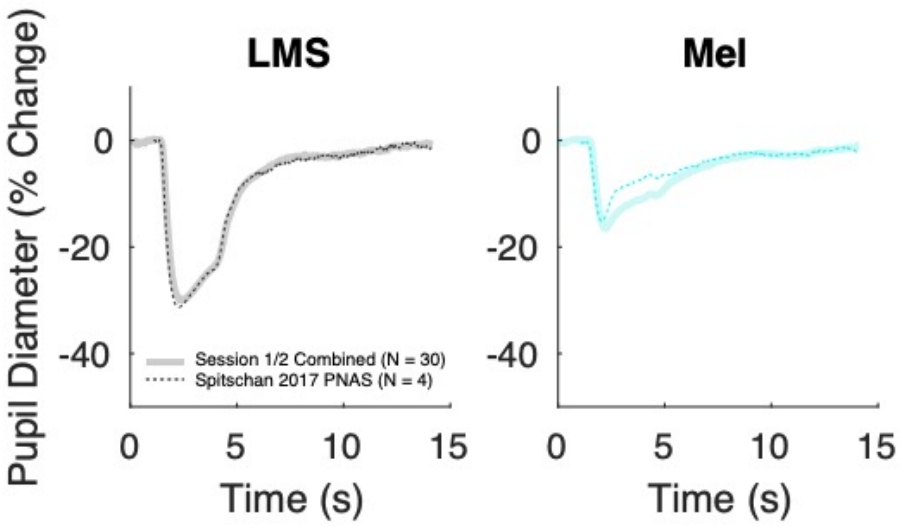

Supplementary Figure 4. The pupil response is consistent with a prior report. The pupil response evoked by the silent substitution stimuli in Session 3 of the current study was compared to that observed in a prior study of a small number of subjects (N=4)[42]. The amplitude and form of response is similar. As compared to the current study, the prior study featured a larger stimulus field (64° vs. 27.5°), but was otherwise similar in stimulus contrast and stimulus background radiance.

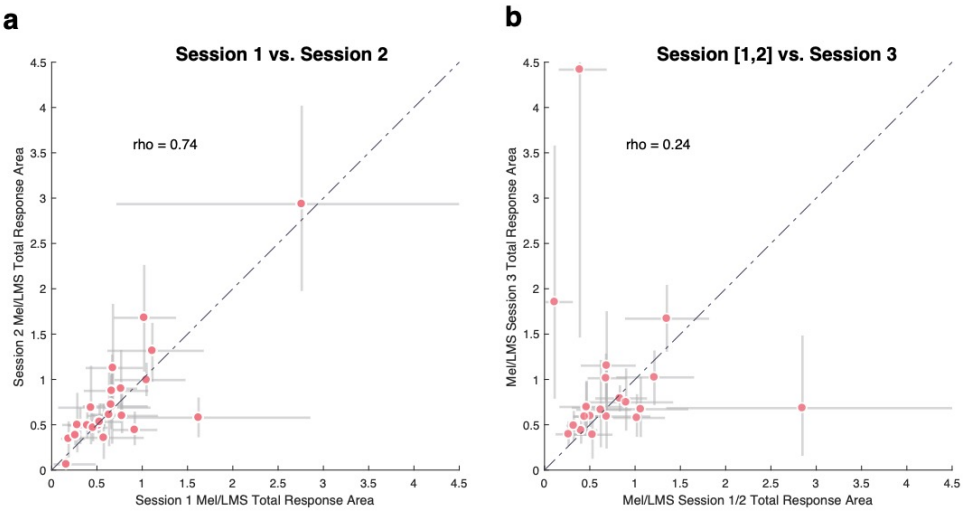

Supplementary Figure 5. Individual differences in amplitude of pupil response. We tested for individual differences in the relative pupil response to the melanopsin- and cone-directed stimuli. The total modeled area of pupil response to the melanopsin and cone stimulus was obtained and expressed as a ratio. (a) When compared between Sessions 1 and 2, individual differences in response ratio were well reproduced (Spearman's rho = 0.74, N = 24 subjects). (b) The same analysis, now comparing the average measurement from Sessions 1 and 2 with the measurement from Session 3 (Spearman's rho = 0.24, N = 21 subjects). A weaker correlation was seen. The error bars reflect the 10-90% confidence interval, obtained via bootstrap analysis across trials within a subject. As the magnitude of these error bars are large relative to the variation across subjects, it is possible that within-session measurement noise limits our ability to detect if there is in fact a stable individual difference in relative pupil response to melanopsin and cone stimulation.

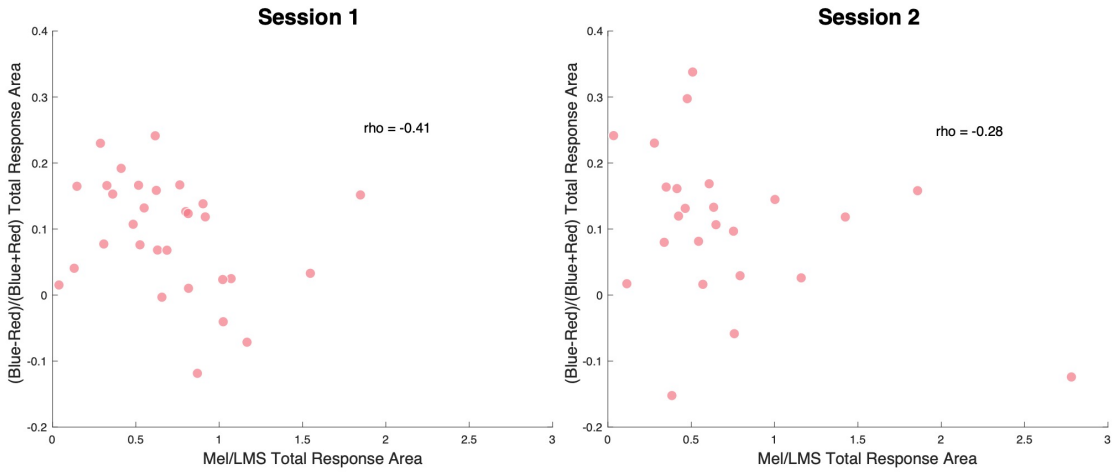

Supplementary Figure 6. A test for individual differences in melanopsin function as elicited by the silent substitution and PIPR approaches. We fit the three-component model to the average response for each subject to all trials of each stimulus type across Sessions 1 and 2. The PIPR effect was expressed as the difference in the area of response to the blue and red stimuli, divided by the sum of the response areas. This normalization was needed to account for individual differences in overall pupil responses, independent of variation in melanopsin sensitivity *per se*. The melanopsin effect in the response to the silent substitution stimuli was expressed as the ratio of the response area for the melanopsin-directed stimulus divided by that evoked by the cone-directed stimulus. While a correlation with a positive slope would be expected if these two measurements reflect an underlying individual difference in melanopsin sensitivity, this was not observed (Spearman's rho = -0.28).

References

1. Liao HW, Ren X, Peterson BB, et al. Melanopsin-expressing ganglion cells on macaque and human retinas form two morphologically distinct populations. *J Comp Neurol*. 2016;524(14):2845-2872. doi:10.1002/cne.23995.
2. La Morgia C, Ross-Cisneros FN, Sadun AA, et al. Melanopsin retinal ganglion cells are resistant to neurodegeneration in mitochondrial optic neuropathies. *Brain*. 2010;133(8):2426-2438. doi:10.1093/brain/awq155.
3. Hannibal J, Hindersson P, Østergaard J, et al. Melanopsin is expressed in PACAP-containing retinal ganglion cells of the human retinohypothalamic tract. *Investig Ophthalmol Vis Sci*. 2004;45(11):4202-4209. doi:10.1167/iovs.04-0313.
4. Nasir-Ahmad S, Lee SCS, Martin PR, Grünert U. Melanopsin-expressing ganglion cells in human retina: Morphology, distribution, and synaptic connections. *J Comp Neurol*. 2017. doi:10.1002/cne.24176.
5. Berson DM. Phototransduction by Retinal Ganglion Cells That Set the Circadian Clock. *Science (80-)*. 2002;295(5557):1070-1073. doi:10.1126/science.1067262.
6. Thapan K, Arendt J, Skene DJ. An action spectrum for melatonin suppression: Evidence for a novel non-rod, non-cone photoreceptor system in humans. *J Physiol*. 2001;535(1):261-267. doi:10.1111/j.1469-7793.2001.t01-1-00261.x.
7. Noseda R, Kainz V, Jakubowski M, et al. A neural mechanism for exacerbation of headache by light. *Nat Neurosci*. 2010;13(2):239-245. http://dx.doi.org/10.1038/nn.2475.
8. Lei S, Goltz HC, Chen X, Zivcevska M, Wong AMF. The relation between light-induced lacrimation and the melanopsin-driven postillumination pupil response. *Investig Ophthalmol Vis Sci*. 2017;58(3):1449-1454. doi:10.1167/iovs.16-21285.
9. Lucas RJ, Douglas RH, Foster RG. Characterization of an ocular photopigment capable of driving pupillary constriction in mice. *Nat Neurosci*. 2001;4(6):621-626. doi:10.1038/88443.
10. Lucas RJ. Diminished Pupillary Light Reflex at High Irradiances in Melanopsin-Knockout Mice. *Science (80-)*. 2003;299(5604):245-247. doi:10.1126/science.1077293.
11. Gamlin PDR, McDougal DH, Pokorny J, Smith VC, Yau KW, Dacey DM. Human and macaque pupil responses driven by melanopsin-containing retinal ganglion cells. *Vision Res*. 2007;47(7):946-954. doi:10.1016/j.visres.2006.12.015.
12. Main A, Dowson A, Gross M. Photophobia and phonophobia in migraineurs between attacks. *Headache*. 1997;37(8):492-495. doi:10.1046/j.1526-

4610.1997.3708492.x.
13. Vanagaite J, Pareja JA, Støren O, White LR, Sand T, Stovner LJ. Light-induced discomfort and pain in migraine. *Cephalalgia*. 1997;17(7):733-741. doi:10.1046/j.1468-2982.1997.1707733.x.
14. Cortez MM, Rea NA, Hunter LA, Digre KB, Brennan KC. Altered pupillary light response scales with disease severity in migrainous photophobia. *Cephalalgia*. 0(0):0333102416673205. doi:10.1177/0333102416673205.
15. Cambron M, Maertens H, Paemeleire K, Crevits L. Autonomic function in migraine patients: Ictal and interictal pupillometry. *Headache*. 2014;54(4):655-662. doi:10.1111/head.12139.
16. Harle DE, Wolffsohn JS, Evans BJW. The pupillary light reflex in migraine. *Ophthalmic Physiol Opt*. 2005;25(3):240-245. doi:10.1111/j.1475-1313.2005.00291.x.
17. Wulff K, Gatti S, Wettstein JG, Foster RG. Sleep and circadian rhythm disruption in psychiatric and neurodegenerative disease. *Nat Rev Neurosci*. 2010;11(8):589-599. doi:10.1038/nrn2868.
18. Kankipati L, Girkin CA, Gamlin PD. Post-illumination pupil response in subjects without ocular disease. *Investig Ophthalmol Vis Sci*. 2010;51(5):2764-2769. doi:10.1167/iovs.09-4717.
19. McDougal DH, Gamlin PD. The influence of intrinsically-photosensitive retinal ganglion cells on the spectral sensitivity and response dynamics of the human pupillary light reflex. *Vision Res*. 2010;50(1):72-87. doi:10.1016/j.visres.2009.10.012.
20. Dacey DM, Liao H-W, Peterson BB, et al. Melanopsin-expressing ganglion cells in primate retina signal colour and irradiance and project to the LGN. *Nature*. 2005;433(7027):749-754. doi:10.1038/nature03387.
21. Meltzer E, Sguigna P V., Subei A, et al. Retinal Architecture and Melanopsin-Mediated Pupillary Response Characteristics. *JAMA Neurol*. 2017;354(9):942-955. doi:10.1001/jamaneurol.2016.5131.
22. Park JC, Moss HE, McAnany JJ. The Pupillary Light Reflex in Idiopathic Intracranial Hypertension. *Invest Ophthalmol Vis Sci*. 2016;57(1):23-29. doi:10.1167/iovs.15-18181.
23. Feigl B, Zele AJ, Fader SM, et al. The post-illumination pupil response of melanopsin-expressing intrinsically photosensitive retinal ganglion cells in diabetes. *Acta Ophthalmol*. 2012;90(3). doi:10.1111/j.1755-3768.2011.02226.x.
24. Joyce DS, Feigl B, Kerr G, Roeder L, Zele AJ. Melanopsin-mediated pupil function is impaired in Parkinson's disease. *Sci Rep*. 2018;8(1). doi:10.1038/s41598-018-26078-0.
25. Yuhas PT, Shorter PD, Mcdaniel CE, Earley MJ, Hartwick ATE. Blue and Red Light-Evoked Pupil Responses in Photophobic Subjects with TBI. 2016;93(00):108-117. doi:10.1097/OPX.0000000000000934.
26. Kankipati L, Girkin CA, Gamlin PD. The post-illumination pupil response is reduced in glaucoma patients. *Investig Ophthalmol Vis Sci*. 2011;52(5):2287-2292. doi:10.1167/iovs.10-6023.

27. Feigl B, Mattes D, Thomas R, Zele AJ. Intrinsically photosensitive (melanopsin) retinal ganglion cell function in glaucoma. *Investig Ophthalmol Vis Sci*. 2011;52(7):4362-4367. doi:10.1167/iovs.10-7069.
28. Kawasaki A, Crippa S V., Kardon R, Leon L, Hamel C. Characterization of pupil responses to blue and red light stimuli in autosomal dominant retinitis pigmentosa due to NR2E3 mutation. *Investig Ophthalmol Vis Sci*. 2012;53(9):5562-5569. doi:10.1167/iovs.12-10230.
29. Park JC, Moura AL, Raza AS, Rhee DW, Kardon RH, Hood DC. Toward a clinical protocol for assessing rod, cone, and melanopsin contributions to the human pupil response. *Investig Ophthalmol Vis Sci*. 2011;52(9):6624-6635. doi:10.1167/iovs.11-7586.
30. Moura ALA, Nagy B V., La Morgia C, et al. The Pupil Light Reflex in Leber's Hereditary Optic Neuropathy: Evidence for Preservation of Melanopsin-Expressing Retinal Ganglion Cells. *Investig Opthalmology Vis Sci*. 2013;54(7):4471. doi:10.1167/iovs.12-11137.
31. Barboni MTS, Bueno C, Nagy BV, et al. Melanopsin System Dysfunction in Smith-Magenis Syndrome Patients. *Invest Ophthalmol Vis Sci*. 2018;59(1):362-369.
32. Berman G, Muttuvelu D, Berman D, et al. Decreased retinal sensitivity in depressive disorder: a controlled study. *Acta Psychiatr Scand*.:n/a--n/a. doi:10.1111/acps.12851.
33. Adhikari P, Feigl B, Zele AJ. Rhodopsin and melanopsin contributions to the early redilation phase of the post-illumination pupil response (PIPR). *PLoS One*. 2016;11(8). doi:10.1371/journal.pone.0161175.
34. Alpern M, Campbell FW. The spectral sensitivity of the consensual light reflex. *J Physiol*. 1962;164(3):478-507. doi:10.1113/jphysiol.1962.sp007033.
35. Spitschan M, Jain S, Brainard DH, Aguirre GK. Opponent melanopsin and S-cone signals in the human pupillary light response. *Proc Natl Acad Sci*. 2014;111(43):15568-15572. doi:10.1073/pnas.1400942111.
36. Sabbah S. All bipolar cells encode irradiance in their output [ARVO Abstract]. *Investig Ophthalmol Vis Sci*. 2017;58(8):2973.
37. Lucas RJ, Hattar S, Takao M, Berson DM, Foster RG, Yau KW. Diminished pupillary light reflex at high irradiances in melanopsin-knockout mice. *Science (80-)*. 2003;299(5604):245-247. doi:10.1126/science.1077293.
38. Schroeder MM, Harrison KR, Jaeckel ER, et al. The roles of rods, cones, and melanopsin in photoresponses of M4 intrinsically photosensitive retinal ganglion cells (ipRGCs) and optokinetic visual behavior. *Front Cell Neurosci*. 2018;12:203.
39. Estévez O, Spekreijse H. The "silent substitution" method in visual research. *Vision Res*. 1982;22(6):681-691. doi:10.1016/0042-6989(82)90104-3.
40. Barrionuevo PA, Nicandro N, McAnany JJ, Zele AJ, Gamlin P, Cao D. Assessing rod, cone, and melanopsin contributions to human pupil flicker responses. *Investig Ophthalmol Vis Sci*. 2014;55(2):719-727.

doi:10.1167/iovs.13-13252.
41. Viénot F, Bailacq S, Rohellec J Le. The effect of controlled photopigment excitations on pupil aperture. In: *Ophthalmic and Physiological Optics*. Vol 30. ; 2010:484-491. doi:10.1111/j.1475-1313.2010.00754.x.
42. Spitschan M, Bock AS, Ryan J, Frazzetta G, Brainard DH, Aguirre GK. The human visual cortex response to melanopsin-directed stimulation is accompanied by a distinct perceptual experience. *Proc Natl Acad Sci*. 2017;114(46):12291-12296. doi:10.1073/pnas.1711522114.
43. Viénot F, Brettel H, Dang T-V, Le Rohellec J. Domain of metamers exciting intrinsically photosensitive retinal ganglion cells (ipRGCs) and rods. *J Opt Soc Am A*. 2012. doi:10.1364/JOSAA.29.00A366.
44. Tsujimura SI, Ukai K, Ohama D, Nuruki A, Yunokuchi K. Contribution of human melanopsin retinal ganglion cells to steady-state pupil responses. In: *Proceedings of the Royal Society B: Biological Sciences*. ; 2010. doi:10.1098/rspb.2010.0330.
45. Cao D, Nicandro N, Barrionuevo PA. A five-primary photostimulator suitable for studying intrinsically photosensitive retinal ganglion cell functions in humans. *J Vis*. 2015. doi:10.1167/15.1.27.
46. Ishihara S. series of plates designed as tests for colour-blindness. 1936.
47. Spitschan M, Datta R, Stern AM, Brainard DH, Aguirre GK. Human Visual Cortex Responses to Rapid Cone and Melanopsin-Directed Flicker. *J Neurosci*. 2016;36(5):1471-1482. doi:10.1523/JNEUROSCI.1932-15.2016.
48. Spitschan M, Aguirre GK, Brainard DH. Selective stimulation of penumbral cones reveals perception in the shadow of retinal blood vessels. *PLoS One*. 2015;10(4). doi:10.1371/journal.pone.0124328.
49. CIE. Fundamental chromaticity diagram with physiological axes – Part 1. Technical Report 170-1 (Central Bureau of the Commission Internationale de l'Éclairage, Vienna). 2006.
50. Kleiner M, Brainard DH, Pelli DG, Broussard C, Wolf T, Niehorster D. What's new in Psychtoolbox-3? *Perception*. 2007. doi:10.1068/v070821.
51. Brainard DH. The Psychophysics Toolbox. *Spat Vis*. 1997. doi:10.1163/156856897X00357.
52. Pelli DG. The VideoToolbox software for visual psychophysics: Transforming numbers into movies. *Spat Vis*. 1997. doi:10.1163/156856897X00366.
53. Do MTH, Kang SH, Xue T, et al. Photon capture and signalling by melanopsin retinal ganglion cells. *Nature*. 2009;457(7227):281-287. doi:10.1038/nature07682.
54. Tsujimura S, Tokuda Y. Delayed response of human melanopsin retinal ganglion cells on the pupillary light reflex. *Ophthalmic Physiol Opt*. 2011. doi:10.1111/j.1475-1313.2011.00846.x.
55. Tikidji-Hamburyan A, Reinhard K, Storchi R, et al. Rods progressively escape saturation to drive visual responses in daylight conditions. *Nat Commun*. 2017;8(1). doi:10.1038/s41467-017-01816-6.
56. McDougal DH, Gamlin PD. The influence of intrinsically-photosensitive

retinal ganglion cells on the spectral sensitivity and response dynamics of the human pupillary light reflex. *Vis Res*. 2010;50(1):72-87. doi:10.1016/j.visres.2009.10.012.
57. Lei S, Goltz HC, Chandrakumar M, Wong AMF. Full-field chromatic pupillometry for the assessment of the postillumination pupil response driven by melanopsin-containing retinal ganglion cells. *Investig Ophthalmol Vis Sci*. 2014;55(7):4496-4503. doi:10.1167/iovs.14-14103.
58. Adhikari P, Zele AJ, Feigl B. The post-illumination pupil response (PIPR). *Investig Ophthalmol Vis Sci*. 2015;56(6):3838-3849. doi:10.1167/iovs.14-16233.

Chapter 3 - Selective amplification of ipRGC signals accounts for interictal photophobia in migraine

Harrison McAdams[1], Eric A Kaiser[2], Aleksandra Igdalova[2], Edda B Haggerty[2], Brett Cucchiara[2], David H Brainard[3], Geoffrey K Aguirre[2]*

Citation:

McAdams, Harrison M., et al. "Selective amplification of ipRGC signals accounts for interictal photophobia in migraine." *BioRxiv* (2020).
Submitted to *PNAS*

Departments of [1]Neuroscience and [2]Neurology, Perelman School of Medicine, University of Pennsylvania, Philadelphia, PA 19104.

Department of [3]Psychology, University of Pennsylvania, Philadelphia, PA 19104

*Address correspondence to:

Geoffrey K Aguirre, MD, PhD

aguirreg@upenn.edu

Department of Neurology

3400 Spruce Street

Hospital of the University of Pennsylvania

Philadelphia, Pennsylvania 19104

Abstract

Second only to headache, photophobia is the most debilitating symptom reported by people with migraine. While the melanopsin-containing, intrinsically photosensitive retinal ganglion cells (ipRGCs) are thought to play a role, how cone and melanopsin signals are integrated in this pathway to produce visual discomfort is poorly understood.

We studied 60 people: 20 without headache and 20 each with interictal photophobia from migraine with or without aura. Participants viewed pulses of spectral change that selectively targeted melanopsin, the cones, or both, and rated the degree of visual discomfort produced by these stimuli while we also recorded pupil responses.

We examined the data within a model that describes how cone and melanopsin signals are weighted and combined at the level of the retina, and how this combined signal is transformed into a rating of discomfort or pupil response. Our results indicate that people with migraine do not differ from headache-free controls in the manner in which melanopsin and cone signals are combined. Instead, people with migraine demonstrate an amplification of integrated ipRGC signals for discomfort. This effect of migraine is selective for ratings of visual discomfort, in that an amplification of pupil responses was not seen in the migraine group, nor were group differences found in surveys of other behaviors

putatively linked to ipRGC function (chronotype, seasonal sensitivity, presence of a photic sneeze reflex).

By revealing a dissociation in the amplification of discomfort versus pupil response, our findings suggest a post-retinal alteration in processing of ipRGC signals for photophobia in migraine.

Significance

The melanopsin-containing, intrinsically photosensitive retinal ganglion cells (ipRGCs) may contribute to photophobia in migraine. We measured visual discomfort and pupil responses to cone and melanopsin stimulation—the photoreceptor inputs to the ipRGCs—in people with and without migraine. We find that people with migraine do not differ from those without headaches in how cone and melanopsin signals are weighted and combined to produce visual discomfort. Instead, migraine is associated with an amplification of ipRGC signals for discomfort. This effect of migraine upon ipRGC signals is limited to photophobia, as we did not find an enhancement of pupil responses or a change in other behaviors linked to ipRGC function. Our findings suggest a post-retinal amplification of ipRGC signals for photophobia in migraine.

Introduction

People find bright light uncomfortable and sometimes even painful. This experience of light-induced discomfort is exacerbated in numerous clinical conditions and can be debilitating[1]. We refer here to discomfort from light as photophobia, which is typically manifest as a somatic sensation localized to the eyes or head[2]. A common cause of photophobia is migraine[3]. Photophobia is reported by 80-90% of individuals during a migraine attack[4–6], and 50% of individuals report it as their most burdensome symptom[7]. Even between headaches, people with migraine have a lowered threshold for pain from light as compared to headache-free controls[8–11].

The signals that ultimately result in photophobia presumably begin with photoreceptors in the eye. Under daylight conditions, the cone photoreceptors capture photons and relay signals via retinal ganglion cells to thalamic and brainstem targets (Figure 1a). A subset of retinal ganglion cells express the photopigment melanopsin[12]. These “intrinsically photosensitive” retinal ganglion cells (ipRGCs) are capable of responding to light without synaptic input[13]. There is evidence from rodent studies that ipRGCs project to the somatosensory thalamus, where they innervate neurons that are also sensitive to dural stimulation carried by trigeminal afferents[14] (Figure 1a). This finding offers a neural mechanism by which light stimulation creates somatic discomfort. The ipRGCs contribute to other “reflexive” functions of vision as well, including photo-entrainment of the circadian rhythm[15,16] and control of pupil size[17–19].

The ipRGCs may play a role in human photophobia. People who have migraine and are also blind from inherited rod-cone degeneration experience photophobia during a headache[14], implicating spared ipRGCs as the source of this sensation. In people without visual impairment, Stringham and colleagues found that shorter wavelengths of light (closer to the peak spectral sensitivity of the melanopsin photopigment) tend to produce greater discomfort in healthy observers[20]. Studies that use narrow-band light stimuli, however, are limited in their ability to probe the specific contribution of melanopsin to photophobia in the intact visual system. This is due to the considerable overlap of the cone and melanopsin spectral sensitivity functions (Figure 1b). Moreover, some classes of ipRGCs also receive input from the cones[13,21–23]. As a consequence, photophobia may result from both melanopsin and cone signals after their integration within ipRGCs. It is unknown how these photoreceptor classes are weighted and combined to produce photophobia, and how this process might be altered in migraine.

In previous work we have shown that carefully tailored modulations of the spectral content of light may be used to selectively target melanopsin or the cones.[24,25] Here, we examine the contribution of cone and melanopsin signals to visual discomfort, and to pupil responses, in people who have migraine with interictal photophobia. Participants reported the discomfort they experienced from viewing pulses of light that selectively targeted melanopsin, the cones, or their combination (Figure 1c, d). Pupillometry in response to these pulses was

also obtained (Figure 1e). We recruited 20 participants in each of three groups: migraine with visual aura, migraine without aura, and headache-free controls. All of the participants with migraine endorsed interictal sensitivity to light. Our findings demonstrate that both melanopsin and cone stimulation in isolation produce visual discomfort. By examining the effect of separate and simultaneous stimulation of melanopsin and the cones, we quantified how these photoreceptor signals are weighted and combined to produce visual discomfort and pupil responses. We find that the enhanced interictal light sensitivity observed in migraine is well described as an amplification of photoreceptor signals after their combination. We further demonstrate that pupil responses are governed by different combination parameters, and do not demonstrate amplification in migraine. These results indicate that interictal photophobia in migraine is a selective amplification of a sub-set of ipRGC outputs, most plausibly at a post-retinal locus.

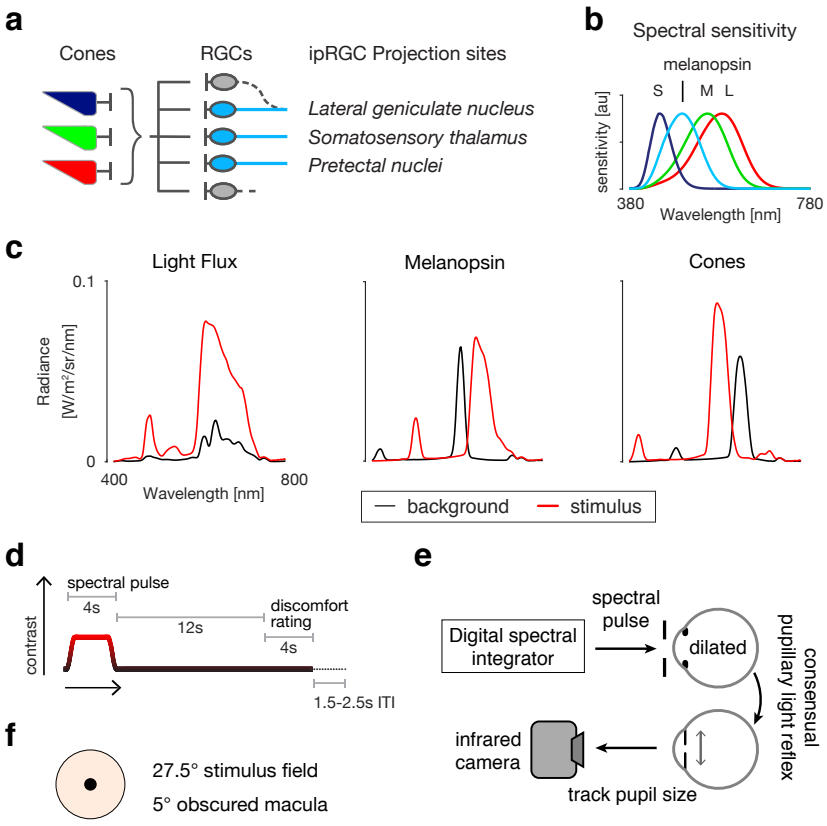

Figure 1. Experiment Overview. a. There are several classes of melanopsin-containing ipRGCs which vary in their central projections, function, and extent to which they receive input from cones. Among other sites, the ipRGCs project to the somatosensory thalamus and the lateral geniculate nucleus, where their signals may contribute to light sensitivity. Other ipRGCs project to the pretectal nuclei to control the size of the pupil. **b.** The spectral sensitivity functions of the relevant photoreceptors under daylight conditions. **c.** Shown are pairs of spectra (background: black; stimulus: red) that differ in excitation for the targeted photoreceptors. From left to right, the stimuli produce: equal contrast on the cones and melanopsin (termed light flux); contrast only on melanopsin; and equal contrast across all three classes of cones but no contrast on melanopsin. **d.** Each trial featured a four-second period during which the stimulus transitioned from the background to the stimulation spectrum and back. Twelve seconds after stimulus offset, the subject provided a discomfort rating. There was an inter-trial interval that varied between 1.5 and 2.5 s. **e.** The light from a digital spectral integrator was presented to the pharmacologically dilated right eye of the subject through an artificial pupil. The consensual pupillary light response of left eye was recorded with an infrared camera. **f.** The stimulus spectra were presented in an eyepiece with a 27.5 degree diameter field, with the central 5 degrees obscured to minimize macular stimulation.

Results

Participant demographic and clinical characteristics

Group	# women	Age in years	Headache Days per 3 Months	Disability		Medication use			
				MIDAS	HIT-6	NSAID	Excedrin	Triptan	Preventive
Controls	13/20	31 (5)	1.3 (1.4)	0.5 (0.8)	40.7 (4.1)	15	0	0	0
MwA	19/20	31 (4)	13.1 (8.9)	18.6 (15.3)	60.6 (8.0)	16	6	5	1
MwoA	17/20	30 (4)	11.7 (9.7)	16.0 (13.7)	60.0 (8.8)	18	1	1	3

Table 1. Subject demographic and clinical characteristics. Participants were asked to report the number of headaches they had experienced over the prior three months. The Migraine Disability Assessment Test (MIDAS)[28] and the Headache Impact Test (HIT-6)[29] measure headache disability. Medication use is summarized within four categories. Where appropriate, the mean value (and standard deviation) across subjects is reported.

We studied 20 people from each of three groups: migraine with aura (MwA), without (MwoA) aura, and headache free controls (HAf). The three groups (Table 1) were well-matched in age ($F[2,57] = 0.2$, $p = 0.820$), but differed in gender distribution ($F[2,57] = 3.3$, $p = 0.0439$), with fewer women in the control group. The greater proportion of women in the migraine groups is consistent with migraine epidemiology[26]. Headache frequency was similar in the two migraine groups with 12 ($\pm$ 10) and 13 ($\pm$ 9) days with headache reported within a 90 day period by MwA and MwoA subjects, respectively (~4 headache days per month), consistent with a classification of episodic (as opposed to chronic) migraine[27]. Acetaminophen and NSAID use for any indication were similar across all three groups. Triptan use was reported by 5 MwA and 1 MwoA participants. Similarly, combined aspirin/acetaminophen/caffeine use was reported by 5 MwA and 1 MwoA participants. Preventive medication use (e.g., tricyclics, beta-blockers, etc.) was reported by 1 MwA and 3 MwoA participants. We quantified headache disease burden using the MIDAS[28] and HIT-6[29] surveys. The migraine groups

unsurprisingly had higher scores on both instruments relative to headache-free controls (MIDAS: F[2,57] = 13.65, p = 1.43e-5; HIT-6: F[2,57] = 48.82, p = 4.43e-13). The two migraine groups did not differ in disease impact (MIDAS: t = 1.00, p = 0.76; HIT-6: t = 0.40, p = 0.96). The distribution of these values suggests moderate disability from migraine in both groups.

Participants with migraine have interictal photophobia, but do not differ from controls in surveys of circadian and seasonal behavior

Group	VDS	PAQ-Photophobia	PAQ-Photophilia	SPAQ	Morningness-Eveningness	Photic Sneeze Reflex
Controls	3.45 (1.76)	0.15 (0.19)	0.71 (0.21)	6.10 (3.81)	51.55 (10.28)	4
MwA	16.55 (10.00)	0.46 (0.28)	0.65 (0.22)	8.90 (5.53)	48.80 (10.53)	3
MwoA	13.15 (8.88)	0.51 (0.31)	0.63 (0.23)	8.65 (4.55)	48.75 (8.32)	3

Table 2. Surveys of behaviors that may be related to ipRGC function. The Visual Discomfort Scale (VDS) measures reported light sensitivity across several domains of visual function[30]. The Photosensitivity Assessment Questionnaire (PAQ) measures reported "photophobia" and "photophilia" behaviors [31]. The Seasonal Pattern Assessment Questionnaire (SPAQ)[33] measures the reported degree to which mood and behavior varies over course of a year, and the Morningness-Eveningness Questionnaire provides a "chronotype" score[32]. Values are the mean (and standard deviation) across subjects within each group. Finally, we asked subjects if they "tend to sneeze when [they] step out of a dark room into bright sunlight" and report here the number of subjects in each group who responded "yes".

The Visual Discomfort Scale (VDS) measures symptoms of discomfort from reading, patterns, and light on a 0-69 scale[30]. We required our control participants to have a low score on this instrument (less than or equal to 7) but did not impose a requirement for migraineurs. Symptoms of visual discomfort were correspondingly greater in the migraine population as compared to the controls (Table 2, F[2,57] = 15.23, p = 5.02e-6). Participants also completed the Photosensitivity Assessment Questionnaire (PAQ) which measures light-avoiding

("photophobia") and light-seeking ("photophilia") behavior on a 0-8 scale[31]. Migraine participants again reported greater light avoidance as compared to controls (Table 2, F[2,57] = 10.95, p = 9.44e-5), although there was no difference in reported light-seeking behavior (Table 2, F[2,57] = 0.75, p = 0.448).

As we are interested in how migraine and photophobia may relate to ipRGC function, we examined if our participant groups differed in other functions thought to be mediated by ipRGCs. In the rodent, multiple classes of ipRGCs have been identified that differ in their subcortical projections and in their functional properties. Projections of the ipRGCs to the suprachiasmatic nucleus are thought to control circadian photoentrainment[15]. As variation in this function is speculated to relate to sleep alterations and seasonal affective disorder, we gathered information about the sleep habits and seasonal preferences of our participants (Table 2). The Morningness-Eveningness Questionnaire[32] characterizes chronotype on a scale of 16-86, with the extremes corresponding to evening and morning preference, respectively. The median scores for the three groups all were in the mid-range (~50), and were not significantly different (F[2,57] = 0.54, p = 0.586). The Seasonal Pattern Assessment Questionnaire[33] provides a Global Seasonality Score, which assesses on a 0-24 scale the degree to which mood and physiology varies across seasons; a score of 16 or higher is typical in patients with seasonal affective disorder. The central tendency of our participants (a score of ~7) indicates a mild degree of seasonal sensitivity, and this did not differ between the groups (F[2,57] = 2.19, p = 0.121). Finally, the photic sneeze

reflex has been hypothesized to be related to ipRGC function[34]. We asked our participants if they experience this phenomenon and did not find any difference between groups in the proportion of participants (15-20%) who have this experience ($F[2,57] = 0.04$, $p = 0.962$).

Overall, apart from photophobia, our studied populations were well matched in behaviors hypothesized to be related to ipRGC function.

Melanopsin and cone contrast produce mild discomfort in control participants

Our participants rated the degree of discomfort they experienced while viewing pulses of spectral change that targeted melanopsin, the cones, or combined stimulation of both sets of photoreceptors (termed light flux). The stimuli were designed to increase excitation in the targeted photoreceptor(s) by 100%, 200% or 400%. Participants rated the amount of discomfort produced by each type of light pulse on a 0 (none) to 10 (extreme) scale.

The light flux stimulus combines melanopsin and cone stimulation. In the HAf control participants, light flux pulses evoked mild discomfort, increasing with contrast, reaching a mean discomfort rating of 3.15 out of 10 for 400% contrast (Figure 2, left-top). To determine whether this discomfort was a consequence of melanopsin or cone-based signaling, we examined the discomfort ratings in response to stimuli designed to target these photoreceptor classes in isolation. Discomfort ratings to both melanopsin (Figure 2, left-middle) and cone-directed

stimuli (Figure 2, left-bottom) also increased with contrast, but only with mild discomfort at 400% (Figure 2, center row, left column: mean rating of 2.18 for melanopsin; bottom row, left column: 2.80 for cones). This result suggests that both cone and melanopsin signals contribute to light-induced discomfort. For all stimuli, we further observed that logarithmic changes in stimulus contrast produced linear changes in mean rated discomfort, as illustrated by the good agreement between the fit lines and the data (Figure 2).

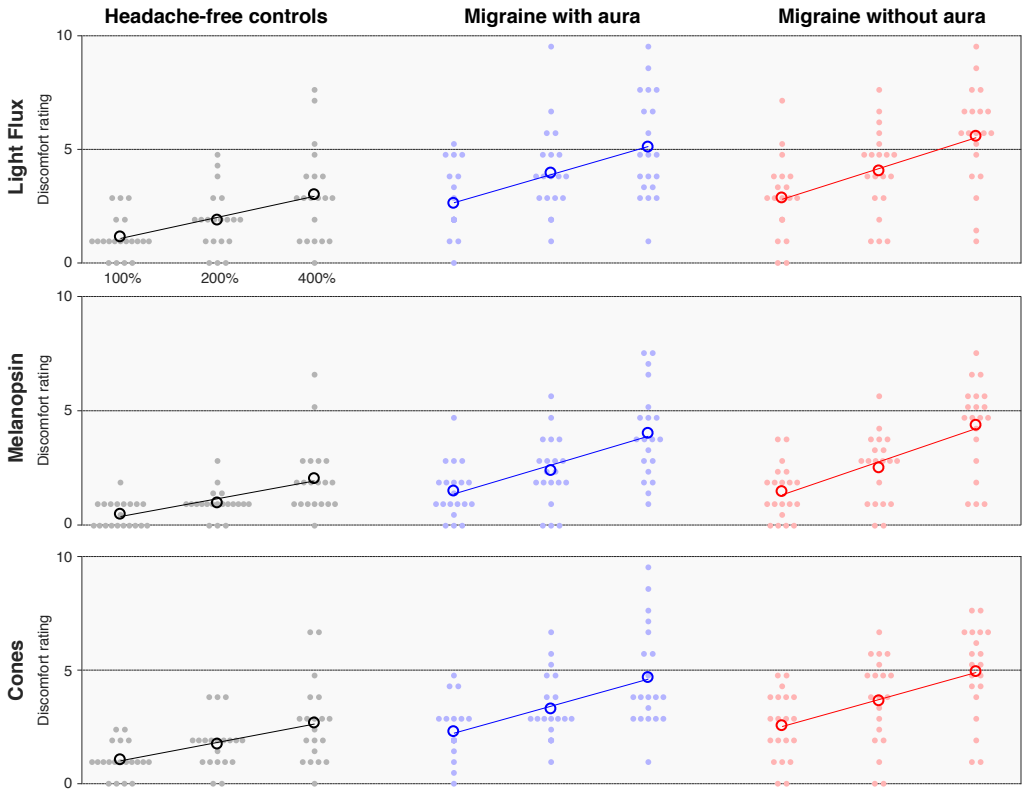

Figure 2. Discomfort ratings by stimulus and group. Each row presents the discomfort ratings elicited by stimuli that targeted a particular combination of photoreceptors, and each column contains the data from each individual group (n = 20 participants per group). The stimuli were presented at three different contrast levels (100, 200, and 400%), and these (log-spaced) values define the x-axis of each subplot. The median (across trial) discomfort rating for a given stimulus and contrast is shown for each participant (filled circle), as is the mean rating across participants (open circle). The best fit line to the mean discomfort rating across participants as a function of log contrast is shown in each subplot.

Cone and melanopsin signals contribute to interictal photophobia in migraine

We next asked if people with photophobic migraine would experience greater discomfort in response to our stimuli, and if so, whether the enhanced discomfort signal is attributable to the cones, melanopsin, or both. Both migraine groups showed increased discomfort in response to the combined light flux stimuli at all contrast levels (Figure 2, center and right, top: at 400% contrast, mean of 5.35 for MwA and 5.85 for MwoA vs. 3.15 for controls). The mean rating across participants was also increased in both migraine groups in response to melanopsin-directed stimulation (Figure 2, middle row: at 400% contrast, mean of 4.28 for MwA and 4.65 for MwoA vs. 2.18 for controls) and cone-directed stimulation (Figure 2, bottom row: at 400% contrast, mean of 4.90 for MwA and 5.18 for MwoA vs. 2.80 for controls). Both migraine groups also showed a linear relationship between log-spaced contrast and mean discomfort ratings for all stimulus types, which is again illustrated by the fit lines (Figure 2).

There was a higher proportion of women in the migraine groups as compared to the control group. We considered if this unequal distribution of gender could account for the differences in discomfort ratings between the groups. The mean discomfort rating reported by female control participants (across all stimuli) was not higher than the ratings provided by male participants (mean rating men: 1.79, women: 1.74), indicating that differing gender ratios do not account for the increased discomfort in the migraine groups.

Discomfort ratings are well fit by a two-stage, non-linear, log-linear model

We observe that mean discomfort ratings for all stimuli are well described as a linear function of log-scaled stimulus contrast, consistent with the Weber–Fechner law of perception. It is also apparent that a light flux stimulus, which combines melanopsin and cone contrast, evokes less discomfort than would be predicted given the discomfort produced by each stimulus component alone. These properties of the data may be explained by non-linear combination of melanopsin and cone signals prior to the stage at which photoreceptor signals are interpreted as discomfort.

We examined these impressions within the context of a quantitative, two-stage model governed by four parameters. The first stage is based upon psychophysical measures of combined stimulus dimensions[35,36], and the second on the Weber-Fechner Law. The model provides a discomfort rating for stimuli with arbitrary combinations of melanopsin and cone contrast.

The first stage of the model (Figure 3a, left) considers the combination of melanopsin and cone signals within ipRGCs. The inputs to this stage are the contrasts on the melanopsin and cone photoreceptors created by a stimulus. A light flux stimulus of (e.g.) 200% contrast has the property of providing 200% contrast input on both of these photoreceptor classes. A scaling factor (α) adjusts the relative potency of melanopsin contrast as compared to cone contrast. The two contrast types are then combined using a Minkowski distance metric with

exponent β. This integrated, “ipRGC contrast” is log-transformed and then passed to the second stage of the model (Figure 3a, right), which transforms input into a discomfort rating under the control of a slope and offset parameter (which is the intercept transformed to describe the modeled response to 200% contrast).

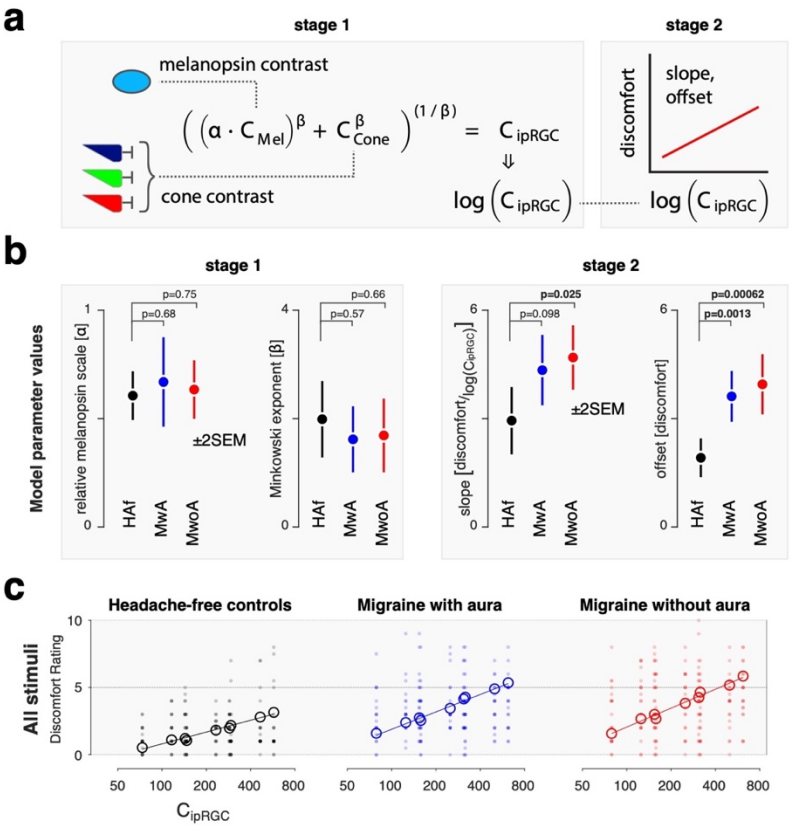

Figure 3. A two-stage model of discomfort ratings. We developed a two-stage model that describes discomfort ratings as a function of melanopsin and cone stimulation. **a.** In the first stage, (left) melanopsin contrast (C_{Mel}) is weighted by a scaling factor (α) and then combined with cone contrast (C_{Cone}) under the control of the Minkoswki exponent (β). The output of this stage is "ipRGC contrast", which is log-transformed and passed to the second stage (right). Here, the signal undergoes an affine transform to produce a discomfort rating, under the control of a slope and offset parameter (the latter being expressed as the modelled discomfort rating at 200% ipRGC contrast). **b.** The model was fit to the discomfort data from each group, yielding estimates of the model parameters (±2SEM obtained via bootstrapping). The p-value associated with a two-tailed t-value, taken with respect to the pooled standard errors, is presented for the comparison of each of the migraine groups to the control group for each parameter (n = 20 participants per group). **c.** Stage 1 of the model transforms the stimuli used in the experiment to common units of ipRGC contrast. Each plot presents the discomfort ratings (individual participants in filled circles, group means in open circles) in terms of ipRGC contrast, with the parameters at stage 1 forced to be the same across groups. The fit of the second stage of the model (which can vary across groups) provides the fit line.

We fit this model to the discomfort ratings across trials for all stimuli and participants within a particular group, using bootstrap resampling across participants to characterize the variability of the model parameters. Fitting was

performed separately for the data from each group (Figure 3b). The model performed equally well for each group in accounting for the mean (across participant) discomfort ratings across stimuli (model R-squared, ±SEM: HAf controls: 0.95 ± 0.03; MwA: 0.96 ± 0.03; MwoA: 0.97 ± 0.01).

Migraine groups differ from headache-free controls in the response to integrated melanopsin and cone signals

We examined the fitted parameters of the model and compared these values across groups (Figure 3b). The discomfort data from all three groups is best fit by first scaling (α) the influence of melanopsin contrast by ~60%. The scaled melanopsin and cone contrast is then combined with a sub-additive Minkowski exponent (β) of ~1.75, intermediate between simple additivity (β=1), and a Euclidean distance metric (β=2). We find that these parameter values do not significantly differ between the three groups (Figure 3b, left). Therefore, we do not find that people with photophobic migraine differ from headache-free controls in the manner in which melanopsin and cone signals are combined at this initial stage.

The second pair of parameters convert log-transformed, ipRGC contrast into discomfort ratings. Here, substantial differences between the migraine and control groups were found. The MwoA group had a greater slope and a higher offset of discomfort rating, and the MwA group a higher offset, for a given amount

of ipRGC contrast (Figure 3b, right). The migraine groups reported discomfort that was roughly twice as great overall and had a slope that was 50% steeper as compared to controls for the increase in discomfort with ipRGC contrast.

Based upon these results, we re-fit the model, forcing the stage 1 parameters to be the same across the three groups, but allowing the stage 2 parameters to vary. The output of stage 1 allows us to describe all the stimuli used in the experiment in terms of a single value of ipRGC contrast. Figure 3c re-plots the discomfort data for all participants and all stimuli from each group in terms of the stage 1 value of ipRGC contrast. The stage 2 model fits differ for each group and are used to generate the solid lines on the plots. Open circles mark the mean, across-participant discomfort ratings for each of the nine stimulus types. There is good agreement between the model fit and the across-participant mean discomfort. Forcing the stage 1 parameters to be the same across groups had minimal impact upon the fit of the model to the data (model R-squared, ±SEM: HAf controls: 0.95 ± 0.03; MwA: 0.96 ± 0.02; MwoA: 0.97 ± 0.01), supporting the claim that the stage 1 model parameters do not meaningfully differ between the groups.

Overall, these findings indicate that people with migraine with interictal photophobia do not differ from controls in the manner in which cone and melanopsin signals are scaled relative to each other and combined, but experience greater discomfort from this integrated signal.

Migraine groups do not have enhanced pupil responses, indicating a selective enhancement of ipRGC discomfort signals

We considered the possibility that people with migraine have a general amplification of ipRGC signals at the level of the retina, of which visual discomfort is one aspect. If so, then we might expect an amplification of pupil responses to be seen in this population as well. To test this idea, we compared pupil constriction in the migraine groups to that observed in the headache-free control participants.

Figure 4a presents the mean, across-participant pupil responses observed in each of the three groups to the stimuli used in the experiment. The temporal profile of the pupil response to stimuli that target melanopsin, the cones, or their combination is in good agreement with prior reports[25]. There is also a clear increase in the amplitude of the pupil constriction produced by stimuli with increasing (100%, 200%, 400%) contrast.

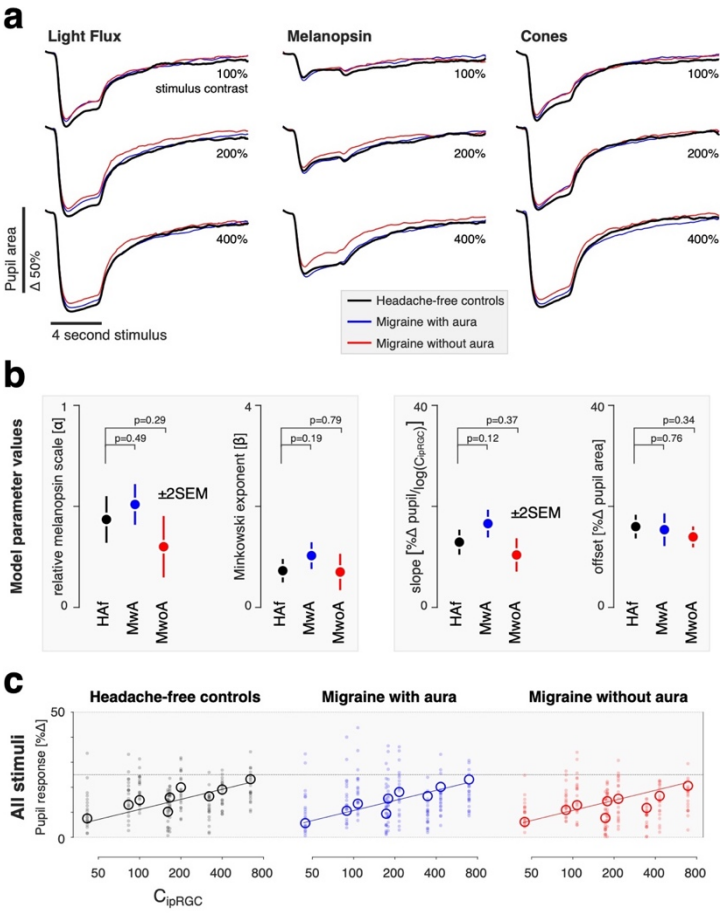

Figure 4. Pupil response by stimulus and group. a. The average pupil response across participants within each group (n = 20 participants per group) is shown for each stimulus type (columns) at each contrast level (rows). The responses from the three groups for each stimulus type are superimposed. **b.** We summarized the pupil responses by taking the mean of the percent change in amplitude of the pupil area across the recording period. These data were then fit with the two-stage model (see Figure 3). No significant differences between the groups in the parameter estimates were found (±2SEM obtained via bootstrapping), although both the relative melanopsin scaling and Minkowski exponent values are smaller for pupil responses than was observed for discomfort ratings. **c.** As no significant differences between groups was found for the parameters, we re-fit our model to the data forcing all parameters to be the same across groups. The plots report individual (filled circles) and mean (open circles) pupil response as a function of modeled ipRGC contrast.

The responses obtained from each studied group are close to overlapping in the plots for each combination of stimulus direction and contrast. We did not observe a greater amplitude of pupil response in the migraine groups as compared to the controls. Indeed, if anything, the pupil response in the migraine groups (particularly MwoA) is slightly attenuated compared to that of the headache free controls. We quantified the pupil response for each participant by measuring the

mean percent change in pupil area following stimulus onset (Supplementary Figure 1). Similar to what was observed for visual discomfort ratings, the relationship between pupil response and stimulus contrast is well described as log-linear.

We next examined how cone and melanopsin signals are combined to produce the overall amplitude of pupil constriction, using the same two-stage model that we developed for the discomfort ratings (Figure 4b). The model fit the data from the three groups well (model R-squared, ±SEM: HAf controls: 0.95 ± 0.03; MwA: 0.98 ± 0.01; MwoA: 0.94 ± 0.02). We found no significant differences between the groups in the parameters of the model for pupil response. Therefore, we re-fit the model to the pupil data, forcing all parameters to be the same across the groups (Figure 4c). The agreement between the data and the model was quite good, despite requiring that all three groups be described using the same model parameters (model R-squared, ±SEM: HAf controls: 0.96 ± 0.01; MwA: 0.95 ± 0.001; MwoA: 0.91 ± 0.06).

The stage 1 parameters in control of the pupil describe a scaling factor for melanopsin (α) of ~40%, which is somewhat less than the influence that melanopsin has upon discomfort (~60%). The Minkowski exponent for the combination of melanopsin and cone signals in the pupil response is ~0.8, compared to its value of ~1.75 for the discomfort ratings. The value of ~0.8 indicates a combination rule for cone and melanopsin signals that is reasonably

close to linear, consistent with prior observations of the additivity of cone and melanopsin signals in the pupil response[24,37]. The fact that the stage 1 parameters differ between the model fits to the two measures indicates that discomfort and pupil control are mediated by mechanisms that combine signals from melanopsin and the cones in different ways. A possible neural basis for these mechanisms would be distinct classes of ipRGCs.

Separately from the matter of how signals from melanopsin and the cones are combined across the two measures, the fact that the stage 2 parameters differ between controls and people with migraine for the production of discomfort but not for pupil constriction argues against the idea that a common, single amplification of retinal signals mediates increased interictal photophobia in migraine.

Discussion

Our study indicates that the enhanced, interictal light sensitivity experienced by people with migraine is due to a selective amplification of a subset of ipRGC signals. Photophobia in migraine is not the result of an omnibus change in cone or melanopsin signals *per se*, but instead a change in the response to these photoreceptor inputs after they have been weighted and combined. Moreover, this amplification of retinal signaling is specific for discomfort signals, in that it is not observed for ipRGC outputs that control other reflexive responses to light, in particular pupil constriction.

Distinct ipRGC classes

Studies in rodents[38–40], primates[13,41–43], and in the post-mortem human eye[44,45] have demonstrated the existence of multiple classes and subclasses of ipRGCs, which differ in their photoreceptor inputs, signaling kinetics, and central projections. Control of circadian photoentrainment and the pupil response, for example, is attributable to distinct subsets of ipRGCs in rodents[38,46].

We examined how melanopsin and cone inputs contribute separately and in combination to visual discomfort and to the pupil response within the context of a quantitative model. The first stage of our model estimates how melanopsin signals are weighted relative to cone signals, and the metric with which melanopsin and cone signals are combined. We did not find a difference at this stage between people with or without migraine. We did find, however, that the model parameters differ substantially when measured for the pupil response and for ratings of visual discomfort. A plausible explanation for these differences in photoreceptor combination is that different classes of ipRGCs contribute to visual discomfort and pupil responses in the human.

In the current study, we find that melanopsin and cone signals are combined approximately additively in control of the pupil, consistent with prior reports[24,37]. Melanopsin contrast was 40% as effective as cone contrast in modulating the pupil for these pulsed stimuli, as compared to a prior report of an overall 26%

effectiveness of melanopsin relative to L+M cone modulations for driving pupil responses with sinusoidal modulations of contrast at low and high temporal frequencies[24]. We note that our index of pupil change here was across the entire time course of evoked response. While it is likely that the relative contribution of melanopsin to the amplitude of pupil constriction varies as a function of time following stimulus onset[19,25,37,47,48], such a dissection of the components of the pupil response is beyond the scope of the current report.

In contrast to the pupil response, melanopsin and cone signals exhibit a nearly Euclidean combination metric in our measure of discomfort, and we find that the influence of melanopsin signals (relative to the cones) is ~1.5x greater in producing visual discomfort as compared to pupil responses. A Euclidean combination metric is a feature of stimulus dimensions that produce a single, integrated percept[35], suggesting that cone and melanopsin signals are combined into a unitary experience of discomfort.

We have previously found that observers describe targeted melanopsin stimulation as “uncomfortable brightness”[49]. It may be the case that the “brightness” and “discomfort” percepts, while each integrating cone and melanopsin signals, reflect the action of distinct retinal ganglion cell populations. Our present data, however, do not directly address such a dissociation.

Several studies have demonstrated that melanopsin contrast contributes to a sensation of brightness[50–53]. The melanopic component of brightness is presumably combined with the post-receptoral luminance channel that is derived from the sum of L and M cone excitations and carried by the classical (non-melanopsin containing) retinal ganglion cells. Yamakawa and colleagues measured the perceptual brightness of lights that varied in melanopic and luminance content[51]. A roughly additive effect of luminance and melanopsin content upon brightness is present in their data, although the form of the response departed from linear. The interpretation of these measurements is complicated, however, as the observers did not undergo pharmacologic dilation of the pupil, causing retinal irradiance to vary systematically with the stimulus.

Zele and colleagues also examined how cone and melanopsin signals combine in the perception of brightness[53]. Their work shows a log-linear relationship between isolated melanopsin and cone stimulus intensity and brightness. However, when presented in combination, they report two contribution components of cones to brightness, one of which is negative and may imply an adaptation process.

Selective amplification

The ipRGCs are known to manifest linear changes in firing rates with logarithmic changes in retinal irradiance[54]. In our measurements, we find that ratings of visual discomfort, and the amplitude of evoked pupil response, vary linearly with

log changes in stimulus contrast, consistent with an output system that receives these log-transformed signals from the ipRGCs.

While participant groups did not differ in the manner in which cone and melanopsin signals were combined, we find that people with episodic migraine with interictal photophobia have an amplification of the effect of this integrated signal upon ratings of visual discomfort. This amplification is similar in migraine with or without visual aura.

Importantly, we did not find evidence of a general amplification of ipRGC signals in migraine. The ipRGCs are the dominant, and perhaps exclusive, route for photoreceptor signals influencing the light-evoked pupil response via the pre-tectal nuclei[55,56]. If migraine is accompanied by a general amplification of ipRGC signals, then an enhanced light-evoked pupil response in this population might be predicted. Instead, we find that the amplitude of evoked pupil responses is not increased in people with migraine in response to stimulation of melanopsin, the cones, or their combination. Indeed, the trend in the data was towards smaller evoked pupil responses in migraine, especially in migraine without aura. Prior studies of pupil response in migraine have obtained varying results. Prior studies have not found migraine group differences in the amplitude of pupil constriction or steady-state pupil size[57–60], although more subtle changes in pupil dynamics have been reported[58,61,62]. Our study differs from many prior reports in that we measured open-loop, consensual pupil responses by combining pharmacologic

dilation with an artificial pupil, thus controlling retinal irradiance across the studied groups.

We also surveyed our participants regarding other behaviors that may be related to ipRGC function. A general alteration in ipRGC function in people with migraine might be predicted to be manifest in these measures as well. The ipRGCs have been implicated in circadian photoentrainment[15], seasonal variation in mood and physiology[63–65], and in the photic sneeze reflex. Our participants with migraine did not differ from headache-free controls in these behaviors, again suggesting that the amplification of ipRGC signals in migraine is specific to visual discomfort.

The neural locus of amplification

While no specific ipRGC subtype has been identified as carrying the signal for visual discomfort, various lines of evidence implicate non-M1 ipRGCs[66–68]. The ipRGCs co-innervate neurons within the posterior thalamus of the rodent that also receive trigeminal afferents. These thalamic neurons then project onward to both somatosensory and visual cortices. Classes of ipRGCs also project to the lateral geniculate nucleus[13,69] and are capable of modulating visual cortex responses[49]. Our findings of amplified discomfort to visual stimulation in people with migraine could reflect alteration of signals derived from the ipRGCs at any one of these sites.

A physiologic hallmark of migraine is alteration in the excitability of cortex, as manifest both in the phenomenon of cortical spreading depression of aura, and a tendency towards enhanced responses to sensory stimulation as compared to headache free controls[70]. Enhanced cortical responses to sensory stimulation has been observed in migraine with[70] and possibly without[71] aura, and for multiple sensory modalities. A natural locus, therefore, for the amplification of ipRGC signals for visual discomfort is at cortical sites. This could take place within primary visual or somatosensory cortex, or further downstream at the integration of these signals into a report of discomfort.

An ipRGC signal of visual discomfort might also be amplified at the level of the thalamus. Altered thalamic gating has been proposed as a mechanism for altered sensory perception in migraine, including photophobia[3,72]. Enhanced signaling within the trigeminal system may also contribute to amplification of ipRGC signals. In rodents, bright light activates the trigeminal ganglion and trigeminal nucleus caudalis[73–75]. Human studies suggest an interaction of the peripheral trigeminal system and light-mediated pathways, as noxious trigeminal stimulation lowers the visual discomfort threshold, and light stimulation lowers trigeminal pain thresholds[11,76]. Studies in the rodent implicate the ipRGCs in this interaction, as light aversion following corneal surface damage is attenuated in mice lacking ipRGCs[77]. Migraine may induce photophobia through the action of neuropeptides within this trigeminal-thalamic system[78].

We might finally consider the possibility that ipRGC signals for visual discomfort are amplified at the level of the retina. This possibility strikes us as less plausible, given that our results would require a mechanism for selective enhancement of only the class of ipRGC that produces photophobia. Our results also argue against a change in the sensitivity of melanopsin or the cones in migraine under photopic conditions.

There have been varying reports of alteration of cone electroretinogram responses in people with migaine[79,80], although these studies are also difficult to interpret given possible differences in retinal irradiance between the studied groups[81].

We interpret our results within a modeling approach that assumes that melanopsin and cone signals are integrated within the ipRGCs, and that post-retinal sites act upon the integrated, log-transformed signal. While this model was not a component of our pre-registered experimental protocol, we find that it provides an excellent account of the data. There is abundant evidence in support of the view that melanopsin and cone signals are integrated in the ipRGCs in this manner[13,21–23,82]. We cannot, however, exclude the possibility that cone and melanopsin signals are transmitted from the retina by separate channels, and that we are measuring the integration of these signals at some downstream site. Such a post-retinal integration is likely to be the case for the perception of the "brightness" of stimuli that combine melanopsin and cone contrast, as the post-retinal luminance channel originates in signals from the "classical" retinal

ganglion cells, and must be integrated with signals from melanopsin-containing ipRGCs, perhaps at the level of the lateral geniculate nucleus.

More broadly, there is evidence that expression of melanopsin in eye tissues apart from the retina contributes to photophobia in rodent models[83]. Because we placed an artificial pupil between the stimulus and the pharmacologically dilated pupil of the observer, our stimuli illuminated only a small area of the cornea, and minimally the iris. There has also been interest in the contribution of the rods to photophobia in migraine[80], and there is evidence that the rods provide inputs to ipRGCs[84]. We sought to minimize the influence of the rods upon our measurements by modulating our stimuli around a photopic background. While there is evidence that rod signals can modulate RGC firing at any light level[85], the amplitude of these effects under photopic conditions is quite small relative to the cones. Further, our prior work indicates that rod signals do not make a measurable contribution to the pupil response at these background light levels[25].

Conclusion

Our study demonstrates that discomfort from light does not arise as the exclusive action of melanopsin, but instead reflects a signal that integrates cone and melanopsin inputs. The interictal photophobia of migraine is a selective amplification of this integrated signal, and one which does not extend to other domains of ipRGC function. We suspect that the amplification in migraine of ipRGC signals for discomfort occurs at a post-retinal site but cannot yet identify

the locus. The modeling approach we adopted here provides a mechanism by which this localization might be pursued, by identifying central sites in which log changes in modeled ipRGC contrast are related to linear modulations of neural activity.

Materials and Methods

We studied 20 participants in each of three groups: migraine with aura, migraine without aura, and headache-free controls (Table 1). Participants were between 25 and 40 years old and were recruited via digital social media. Headache classification was established using the Penn Online Evaluation of Migraine[86]. Participants with migraine were also required to endorse interictal photophobia[87]. Participants completed surveys that assessed behaviors putatively related to ipRGC function (Table 2).

Participants viewed stimuli that targeted specific photoreceptor classes using the technique of silent substitution[88] (Figure 1c). Each stimulus type was presented at three, log-spaced contrast levels: 100%, 200%, and 400%. These stimuli were produced by a digital light synthesis engine (OneLight Spectra, Vancouver, BC, Canada) and tailored for the lens transmittance predicted for the age of each subject. The stimuli were presented through a custom-made eyepiece with a circular, uniform field of 27.5° diameter with the central 5° diameter of the field obscured to minimize macular stimulation. Spectroradiographic measurements

were made before and after each session to ensure stimulus quality (Supplementary Table 1).

On each of many trials, the participant viewed a pulsed spectral modulation, at one of three contrast levels, designed to target melanopsin, the cones, or both (Figure 1c). The transition from the background to the stimulation spectrum (melanopsin, cones, or light flux), and the subsequent return to the background, were windowed with a 500 ms half-cosine. The total duration of the pulse was 4 seconds, after which the stimulus field returned to and remained at the background spectrum (Figure 1d). Twelve seconds after the pulse ended, participants were prompted by an auditory cue to verbally rate their visual discomfort on a 0-10 scale. Participants viewed the stimuli through their pharmacologically dilated right eye and a 6 mm diameter artificial pupil to control retinal irradiance. Infrared video recording of the left eye measured the consensual pupil response during each trial. Each participant viewed at least 12 trials for each crossing of photoreceptor target and contrast, and at least 6 of those trials were required to possess good quality pupillometry for the subject to be included in the study.

Pupil response was quantified for each trial as the mean percent change in pupil area during the period of 0 to 16 seconds from stimulus onset, relative to the 0.5 seconds before stimulus onset. We obtained the median pupil and discomfort response across trials within participant, and across participants within groups.

We examined the discomfort and pupil data within a two stage, non-linear model (Figure 3a). The response to a stimulus (either discomfort rating or pupil constriction) is given by:

$$\text{Response} = m^* \log_{10}\left(\sqrt[\beta]{(\alpha^* C_{Mel})^{\beta} + C_{Cone}{}^{\beta}}\right) + b$$

where C_{Mel} and C_{Cone} are the contrasts produced upon the melanopsin and cone photoreceptors by a stimulus, and α, β, m, and b are the four parameters of the model. Non-linear fitting was performed in MATLAB using *fmincon*, and the variability of parameter estimates within each group obtained by bootstrap resampling of the data across subjects.

This study was pre-registered (Supplementary Table 2). The analysis code is available (https://github.com/gkaguirrelab/melSquintAnalysis), as will be the data following publication.

Detailed methods are described in *SI Appendix*, *SI Text Online Methods*.

Funding

This work was supported by grants from the National Eye Institute (R01EY024681 to GKA and DHB; Core Grant for Vision Research P30

EY001583), National Institute of Neurological Disorders and Stroke (R25 NS065745), National Institute on Aging (5T32AG000255-13), and the Department of Defense (W81XWH-151-0447 to GKA).

References

1. Digre KB, Brennan KC. Shedding light on photophobia. *J Neuro-Ophthalmology*. 2012. doi:10.1097/WNO.0b013e3182474548
2. Noseda R, Burstein R. Advances in understanding the mechanisms of migraine-type photophobia. *Curr Opin Neurol*. 2011. doi:10.1097/WCO.0b013e3283466c8e
3. Rossi HL, Recober A. Photophobia in primary headaches. *Headache*. 2015. doi:10.1111/head.12532
4. Selby G, Lance JW. Observations on 500 cases of migraine and allied vascular headache. *J Neurol Neurosurg Psychiatry*. 1960. doi:10.1136/jnnp.23.1.23
5. Drummond PD. A Quantitative Assessment of Photophobia in Migraine and Tension Headache. *Headache J Head Face Pain*. 1986. doi:10.1111/j.1526-4610.1986.hed2609465.x
6. Rasmussen BK, Jensen R, Olesen J. A population-based analysis of the diagnostic criteria of the international headache society. *Cephalalgia*. 1991. doi:10.1046/j.1468-2982.1991.1103129.x
7. Munjal S, Singh P, Reed ML, et al. Most Bothersome Symptom in Persons With Migraine: Results From the Migraine in America Symptoms and Treatment (MAST) Study. *Headache*. 2020. doi:10.1111/head.13708
8. Main A, Dowson A, Gross M. Photophobia and phonophobia in migraineurs between attacks. *Headache*. 1997;37(8):492-495. doi:10.1046/j.1526-4610.1997.3708492.x
9. Vanagaite J, Pareja JA, Støren O, White LR, Sand T, Stovner LJ. Light-induced discomfort and pain in migraine. *Cephalalgia*. 1997;17(7):733-741. doi:10.1046/j.1468-2982.1997.1707733.x
10. Vingen JV, Sand T, Stovner LJ. Sensitivity to various stimuli in primary headaches: A questionnaire study. *Headache*. 1999. doi:10.1046/j.1526-4610.1999.3908552.x
11. Kowacs PA, Piovesan EJ, Werneck LC, et al. Influence of intense light stimulation on trigeminal and cervical pain perception thresholds. *Cephalalgia*. 2001. doi:10.1046/j.1468-2982.2001.00178.x
12. Provencio I, Rodriguez IR, Jiang G, Hayes WP, Moreira EF, Rollag MD. A Novel Human Opsin in the Inner Retina. *J Neurosci*. 2000;20(2):600-605.
13. Dacey DM, Liao H-W, Peterson BB, et al. Melanopsin-expressing ganglion cells in primate retina signal colour and irradiance and project to the LGN.

Nature. 2005;433(7027):749-754. doi:10.1038/nature03387
14. Noseda R, Kainz V, Jakubowski M, et al. A neural mechanism for exacerbation of headache by light. *Nat Neurosci*. 2010;13(2):239-245. http://dx.doi.org/10.1038/nn.2475.
15. Berson DM. Phototransduction by Retinal Ganglion Cells That Set the Circadian Clock. *Science (80-)*. 2002;295(5557):1070-1073. doi:10.1126/science.1067262
16. Thapan K, Arendt J, Skene DJ. An action spectrum for melatonin suppression: Evidence for a novel non-rod, non-cone photoreceptor system in humans. *J Physiol*. 2001;535(1):261-267. doi:10.1111/j.1469-7793.2001.t01-1-00261.x
17. Lucas RJ, Hattar S, Takao M, Berson DM, Foster RG, Yau KW. Diminished pupillary light reflex at high irradiances in melanopsin-knockout mice. *Science (80-)*. 2003;299(5604):245-247. doi:10.1126/science.1077293
18. Lucas RJ, Douglas RH, Foster RG. Characterization of an ocular photopigment capable of driving pupillary constriction in mice. *Nat Neurosci*. 2001;4(6):621-626. doi:10.1038/88443
19. Gamlin PDR, McDougal DH, Pokorny J, Smith VC, Yau KW, Dacey DM. Human and macaque pupil responses driven by melanopsin-containing retinal ganglion cells. *Vision Res*. 2007;47(7):946-954. doi:10.1016/j.visres.2006.12.015
20. Stringham JM, Fuld K, Wenzel AJ. Action spectrum for photophobia. *J Opt Soc Am A*. 2003. doi:10.1364/josaa.20.001852
21. Perez-Leon JA, Warren EJ, Allen CN, Robinson DW, Lane Brown R. Synaptic inputs to retinal ganglion cells that set the circadian clock. *Eur J Neurosci*. 2006. doi:10.1111/j.1460-9568.2006.04999.x
22. Wong KY, Dunn FA, Graham DM, Berson DM. Synaptic influences on rat ganglion-cell photoreceptors. *J Physiol*. 2007. doi:10.1113/jphysiol.2007.133751
23. Weng S, Estevez ME, Berson DM. Mouse Ganglion-Cell Photoreceptors Are Driven by the Most Sensitive Rod Pathway and by Both Types of Cones. *PLoS One*. 2013. doi:10.1371/journal.pone.0066480
24. Spitschan M, Jain S, Brainard DH, Aguirre GK. Opponent melanopsin and S-cone signals in the human pupillary light response. *Proc Natl Acad Sci*. 2014;111(43):15568-15572. doi:10.1073/pnas.1400942111
25. McAdams H, Igdalova A, Spitschan M, Brainard DH, Aguirre GK. Pulses of melanopsin-directed contrast produce highly reproducible pupil responses that are insensitive to a change in background radiance. *Investig Ophthalmol Vis Sci*. 2018. doi:10.1167/iovs.18-25219
26. Lipton RB, Bigal ME. Migraine: Epidemiology, impact, and risk factors for progression. *Headache*. 2005;45(SUPPL. 1). doi:10.1111/j.1526-4610.2005.4501001.x
27. Olesen J, Steiner TJ. The international classification of headache disorders, 2nd edn (ICDH-II). *J Neurol Neurosurg Psychiatry*. 2004. doi:10.1136/jnnp.2003.031286

28. Stewart WF, Lipton RB, Dowson AJ, Sawyer J. Development and testing of the Migraine Disability Assessment (MIDAS) Questionnaire to assess headache-related disability. *Neurology*. 2001. doi:10.1212/wnl.56.suppl_1.s20
29. Yang M, Rendas-Baum R, Varon SF, Kosinski M. Validation of the Headache Impact Test (HIT-6™) across episodic and chronic migraine. *Cephalalgia*. 2011. doi:10.1177/0333102410379890
30. Conlon EG, Lovegrove WJ, Chekaluk E, Pattison PE. Measuring visual discomfort. *Vis cogn*. 1999. doi:10.1080/135062899394885
31. Bossini L, Valdagno M, Padula L, De Capua A, Pacchierotti C, Castrogiovanni P. Sensibilità alla luce e psicopatologia: Validazione del Questionario per la Valutazione della Fotosensibilità (Q.V.F.). *Med Psicosom*. 2006.
32. Horne JA, Ostberg O. A self assessment questionnaire to determine Morningness Eveningness in human circadian rhythms. *Int J Chronobiol*. 1976.
33. Rosenthal NE, Bradt GH, Wehr TA. Seasonal pattern assessment questionnaire. *Washington, DC Natl Inst Ment Heal*. 1987.
34. Matynia A, Nguyen E, Sun X, et al. Peripheral sensory neurons expressing melanopsin respond to light. *Front Neural Circuits*. 2016. doi:10.3389/fncir.2016.00060
35. Shepard RN. Toward a universal law of generalization for psychological science. *Science (80-)*. 1987. doi:10.1126/science.3629243
36. Quick RF. A vector-magnitude model of contrast detection. *Kybernetik*. 1974. doi:10.1007/BF00271628
37. Zele AJ, Adhikari P, Cao D, Feigl B. Melanopsin and cone photoreceptor inputs to the afferent pupil light response. *Front Neurol*. 2019. doi:10.3389/fneur.2019.00529
38. Baver SB, Pickard GE, Sollars PJ, Pickard GE. Two types of melanopsin retinal ganglion cell differentially innervate the hypothalamic suprachiasmatic nucleus and the olivary pretectal nucleus. *Eur J Neurosci*. 2008. doi:10.1111/j.1460-9568.2008.06149.x
39. Hattar S, Liao HW, Takao M, Berson DM, Yau KW. Melanopsin-containing retinal ganglion cells: architecture, projections, and intrinsic photosensitivity. *Science (80-)*. 2002;295(5557):1065-1070. doi:10.1126/science.1069609
40. Zhao X, Stafford BK, Godin AL, King WM, Wong KY. Photoresponse diversity among the five types of intrinsically photosensitive retinal ganglion cells. *J Physiol*. 2014. doi:10.1113/jphysiol.2013.262782
41. Grnert U, Jusuf PR, Lee SCS, Nguyen DT. Bipolar input to melanopsin containing ganglion cells in primate retina. *Vis Neurosci*. 2011. doi:10.1017/S095252381000026X
42. Neumann S, Haverkamp S, Auferkorte ON. Intrinsically photosensitive ganglion cells of the primate retina express distinct combinations of inhibitory neurotransmitter receptors. *Neuroscience*. 2011.

doi:10.1016/j.neuroscience.2011.10.027
43. Jusuf PR, Lee SCS, Hannibal J, Grünert U. Characterization and synaptic connectivity of melanopsin-containing ganglion cells in the primate retina. *Eur J Neurosci*. 2007. doi:10.1111/j.1460-9568.2007.05924.x
44. Hannibal J, Christiansen AT, Heegaard S, Fahrenkrug J, Kiilgaard JF. Melanopsin expressing human retinal ganglion cells: Subtypes, distribution, and intraretinal connectivity. *J Comp Neurol*. 2017. doi:10.1002/cne.24181
45. Hannibal J, Hindersson P, Østergaard J, et al. Melanopsin is expressed in PACAP-containing retinal ganglion cells of the human retinohypothalamic tract. *Investig Ophthalmol Vis Sci*. 2004;45(11):4202-4209. doi:10.1167/iovs.04-0313
46. Chen SK, Badea TC, Hattar S. Photoentrainment and pupillary light reflex are mediated by distinct populations of ipRGCs. *Nature*. 2011. doi:10.1038/nature10206
47. Barrionuevo PA, Nicandro N, McAnany JJ, Zele AJ, Gamlin P, Cao D. Assessing rod, cone, and melanopsin contributions to human pupil flicker responses. *Investig Ophthalmol Vis Sci*. 2014;55(2):719-727. doi:10.1167/iovs.13-13252
48. Barrionuevo PA, Cao D. Luminance and chromatic signals interact differently with melanopsin activation to control the pupil light response. *J Vis*. 2016. doi:10.1167/16.11.29
49. Spitschan M, Bock AS, Ryan J, Frazzetta G, Brainard DH, Aguirre GK. The human visual cortex response to melanopsin-directed stimulation is accompanied by a distinct perceptual experience. *Proc Natl Acad Sci*. 2017;114(46):12291-12296. doi:10.1073/pnas.1711522114
50. Brown TM, Tsujimura SI, Allen AE, et al. Melanopsin-based brightness discrimination in mice and humans. *Curr Biol*. 2012;22(12):1134-1141. doi:10.1016/j.cub.2012.04.039
51. Yamakawa M, Tsujimura S ichi, Okajima K. A quantitative analysis of the contribution of melanopsin to brightness perception. *Sci Rep*. 2019. doi:10.1038/s41598-019-44035-3
52. DeLawyer T, Tsujimura S, Shinomori K. Relative contributions of melanopsin to brightness discrimination when hue and luminance also vary. *J Opt Soc Am A*. 2020. doi:10.1364/josaa.382349
53. Zele AJ, Adhikari P, Feigl B, Cao D. Cone and melanopsin contributions to human brightness estimation. *J Opt Soc Am A*. 2018. doi:10.1364/josaa.35.000b19
54. Storchi R, Milosavljevic N, Eleftheriou CG, et al. Melanopsin-driven increases in maintained activity enhance thalamic visual response reliability across a simulated dawn. *Proc Natl Acad Sci*. 2015;112(42):E5734-E5743. doi:10.1073/pnas.1505274112
55. Hatori M, Le H, Vollmers C, et al. Inducible ablation of melanopsin-expressing retinal ganglion cells reveals their central role in non-image forming visual responses. *PLoS One*. 2008. doi:10.1371/journal.pone.0002451

56. Lucas RJ. Diminished Pupillary Light Reflex at High Irradiances in Melanopsin-Knockout Mice. *Science (80-)*. 2003;299(5604):245-247. doi:10.1126/science.1077293
57. Cambron M, Maertens H, Paemeleire K, Crevits L. Autonomic function in migraine patients: Ictal and interictal pupillometry. *Headache*. 2014;54(4):655-662. doi:10.1111/head.12139
58. Harle DE, Wolffsohn JS, Evans BJW. The pupillary light reflex in migraine. *Ophthalmic Physiol Opt*. 2005;25(3):240-245. doi:10.1111/j.1475-1313.2005.00291.x
59. Eren OE, Ruscheweyh R, Schankin C, Schöberl F, Straube A. The cold pressor test in interictal migraine patients - different parasympathetic pupillary response indicates dysbalance of the cranial autonomic nervous system. *BMC Neurol*. 2018. doi:10.1186/s12883-018-1043-2
60. Drummond PD. Pupil diameter in migraine and tension headache. *J Neurol Neurosurg Psychiatry*. 1987. doi:10.1136/jnnp.50.2.228
61. Cortez MM, Rea NA, Hunter LA, Digre KB, Brennan KC. Altered pupillary light response scales with disease severity in migrainous photophobia. *Cephalalgia*. 0(0):0333102416673205. doi:10.1177/0333102416673205
62. Cortez MM, Rae N, Millsap L, McKean N, Brennan KC. Pupil cycle time distinguishes migraineurs from subjects without headache. *Front Neurol*. 2019. doi:10.3389/fneur.2019.00478
63. Roecklein KA, Wong PM, Franzen PL, et al. Melanopsin Gene Variations Interact With Season to Predict Sleep Onset and Chronotype. *Chronobiol Int*. 2012;29(8):1036-1047. doi:10.3109/07420528.2012.706766
64. Roecklein KA, Rohan KJ, Duncan WC, et al. A missense variant (P10L) of the melanopsin (OPN4) gene in seasonal affective disorder. *J Affect Disord*. 2009;114(1-3):279-285. doi:10.1016/j.jad.2008.08.005
65. Roecklein KA, Wong PM, Miller MA, Donofry SD, Kamarck ML, Brainard GC. Melanopsin, photosensitive ganglion cells, and seasonal affective disorder. *Neurosci Biobehav Rev*. 2013. doi:10.1016/j.neubiorev.2012.12.009
66. Johnson J, Wu V, Donovan M, et al. Melanopsin-dependent light avoidance in neonatal mice. *Proc Natl Acad Sci U S A*. 2010. doi:10.1073/pnas.1008533107
67. Routtenberg A, Strop M, Jerdan J. Response of the infant rat to light prior to eyelid opening: Mediation by the superior colliculus. *Dev Psychobiol*. 1978. doi:10.1002/dev.420110510
68. McNeill DS, Sheely CJ, Ecker JL, et al. Development of melanopsin-based irradiance detecting circuitry. *Neural Dev*. 2011. doi:10.1186/1749-8104-6-8
69. Storchi R, Milosavljevic N, Eleftheriou CG, et al. Melanopsin-driven increases in maintained activity enhance thalamic visual response reliability across a simulated dawn. *Proc Natl Acad Sci U S A*. 2015. doi:10.1073/pnas.1505274112
70. Goadsby PJ, Holland PR, Martins-Oliveira M, Hoffmann J, Schankin C,

Akerman S. Pathophysiology of migraine: A disorder of sensory processing. *Physiol Rev*. 2017. doi:10.1152/physrev.00034.2015
71. Mulleners WM, Chronicle EP, Palmer JE, Koehler PJ, Vredeveld JW. Visual cortex excitability in migraine with and without aura. *Headache*. 2001. doi:10.1046/j.1526-4610.2001.041006565.x
72. Hodkinson DJ, Wilcox SL, Veggeberg R, et al. Increased amplitude of thalamocortical low-frequency oscillations in patients with migraine. *J Neurosci*. 2016. doi:10.1523/JNEUROSCI.1038-16.2016
73. Marek V, Reboussin E, Dégardin-Chicaud J, et al. Implication of Melanopsin and Trigeminal Neural Pathways in Blue Light Photosensitivity in vivo. *Front Neurosci*. 2019. doi:10.3389/fnins.2019.00497
74. Okamoto K, Thompson R, Tashiro A, Chang Z, Bereiter DA. Bright light produces Fos-positive neurons in caudal trigeminal brainstem. *Neuroscience*. 2009. doi:10.1016/j.neuroscience.2009.03.003
75. Okamoto K, Tashiro A, Chang Z, Bereiter DA. Bright light activates a trigeminal nociceptive pathway. *Pain*. 2010. doi:10.1016/j.pain.2010.02.004
76. Drummond P d., Woodhouse A. Painful Stimulation of the Forehead Increases Photophobia in Migraine Sufferers. *Cephalalgia*. 1993. doi:10.1046/j.1468-2982.1993.1305321.x
77. Matynia A, Parikh S, Deot N, et al. Light aversion and corneal mechanical sensitivity are altered by intrinscally photosensitive retinal ganglion cells in a mouse model ofcorneal surface damage. *Exp Eye Res*. 2015. doi:10.1016/j.exer.2015.05.025
78. Kaiser EA, Russo AF. CGRP and migraine: Could PACAP play a role too? *Neuropeptides*. 2013. doi:10.1016/j.npep.2013.10.010
79. Noseda R, Bernstein CA, Nir RR, et al. Migraine photophobia originating in cone-driven retinal pathways. *Brain*. 2016. doi:10.1093/brain/aww119
80. Bernstein CA, Nir RR, Noseda R, et al. The migraine eye: Distinct rod-driven retinal pathways' response to dim light challenges the visual cortex hyperexcitability theory. *Pain*. 2019. doi:10.1097/j.pain.0000000000001434
81. Mahroo OA. Pupil area and photopigment spectral sensitivity are relevant to study of migraine photophobia. *Brain*. 2017. doi:10.1093/brain/aww274
82. Wong KY. A retinal ganglion cell that can signal irradiance continuously for 10 hours. *J Neurosci*. 2012. doi:10.1523/JNEUROSCI.1423-12.2012
83. Matynia A, Nguyen E, Sun X, et al. Peripheral Sensory Neurons Expressing Melanopsin Respond to Light. *Front Neural Circuits*. 2016;10(August):60. doi:10.3389/fncir.2016.00060
84. Lee SK, Sonoda T, Schmidt TM. M1 Intrinsically Photosensitive Retinal Ganglion Cells Integrate Rod and Melanopsin Inputs to Signal in Low Light. *Cell Rep*. 2019. doi:10.1016/j.celrep.2019.11.024
85. Tikidji-Hamburyan A, Reinhard K, Storchi R, et al. Rods progressively escape saturation to drive visual responses in daylight conditions. *Nat Commun*. 2017;8(1). doi:10.1038/s41467-017-01816-6
86. Kaiser EA, Igdalova A, Aguirre GK, Cucchiara B. A web-based, branching logic questionnaire for the automated classification of migraine.

Cephalalgia. 2019. doi:10.1177/0333102419847749
87. Choi JY, Oh K, Kim BJ, Chung CS, Koh SB, Park KW. Usefulness of a photophobia questionnaire in patients with migraine. *Cephalalgia*. 2009. doi:10.1111/j.1468-2982.2008.01822.x
88. Estévez O, Spekreijse H. The “silent substitution” method in visual research. *Vision Res*. 1982;22(6):681-691. doi:10.1016/0042-6989(82)90104-3

Supplmental Material:

Supplementary Figures:

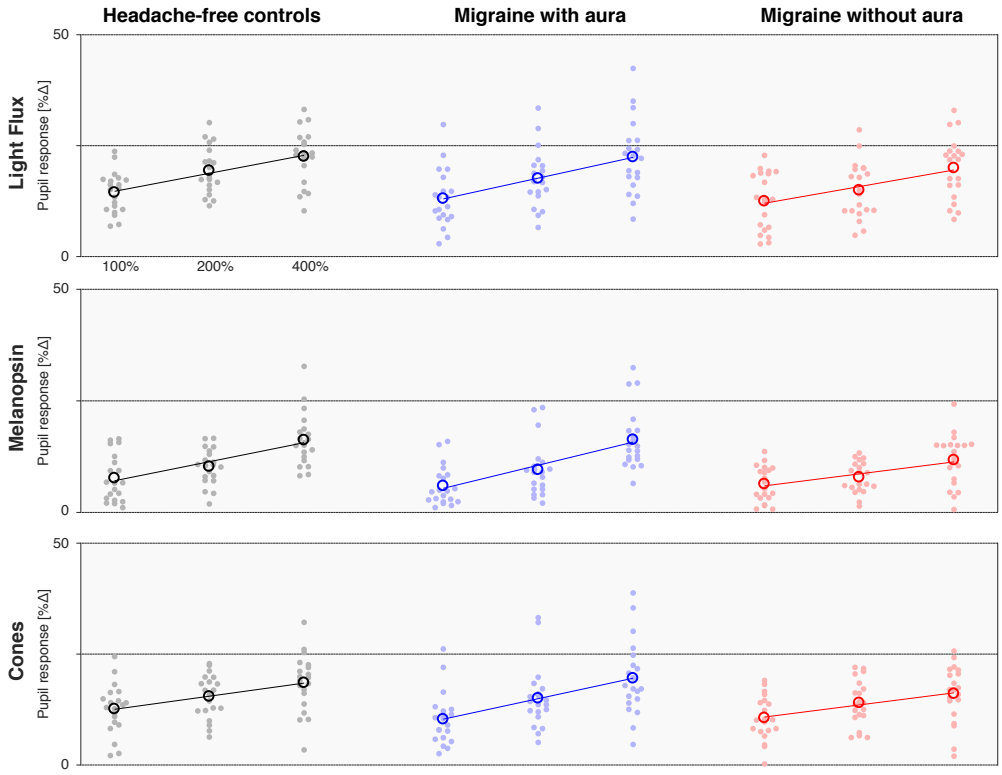

Supplementary Figure 1. Pupil response amplitudes by stimulus and group. Each row presents the mean percent change in pupil area (across the duration of the trial) elicited by stimuli that targeted a particular combination of photoreceptors, and each column contains the data from each individual group (n = 20 participant per group). The stimuli were presented at three different contrast levels (100, 200, and 400%), and these values (log-spaced) define the x-axis of each subplot. The mean (across trial) pupil response for a given stimulus and contrast is shown for each participant (filled circle), as is the mean response across participants (open circle). The best fit line to the mean pupil response across participants as a function of log contrast is shown in each subplot.

Supplementary Tables:

Stimulus	Contrast				Luminance	Chromaticity
	Melanopsin	***LMS***	***S***	***L–M***	**[cd/m2]**	**[x, y]**
Mean stimulus values across subjects						
Mel	397.06%	0.40%	-0.06%	-0.87%	322	0.58, 0.38
Cones	0.83%	397.72%	1.72%	1.02%	145	0.57, 0.36
LF	398.74%	399.41%	-2.09%	-0.08%	209	0.57, 0.36
Mean unsigned contrast error across subjects						
Mel	4.05%	0.51%	1.26%	0.87%	-	-
Cones	0.86%	2.32%	4.66%	1.05%	-	-
LF	1.42%	1.27%	3.33%	0.41%	-	-

Supplementary Table 1. **Stimulus Validation Measurements.** Before and after each experiment, we obtained 5 spectroradiographic measurements of each stimulus at its background and maximal (400% nominal) contrast level. From these measurements, we calculated the contrast on several receptor and post-receptoral mechanisms: melanopsin, the combined luminance channel (LMS), S-(L+M), and L-M. We also measured the luminance and chromaticity of the background spectrum for each stimulus. The upper portion of the table provides the mean of these validation measurements across sessions and subjects. The lower portion of the table presents the mean (across sessions and subjects) unsigned deviation of the validated stimuli from the nominal contrast levels.

Type	Link	Contents
Initial pre-registration	https://osf.io/5ry67/	- Defined initial plan for experiment, including subject recruitment, screening procedure, stimulus creation, experimental design, exclusion criteria, and primary analyses.
Addendum #1	https://osf.io/qtjyd/	- Modified subject exclusion criteria to exclude subjects with a history of ophthalmologic disease. - Modified subject exclusion criteria to exclude candidate migraine participants who had not experienced a headache within the previous month. Seven migraine subjects with no headache in the prior month were enrolled in the study prior to the adoption of this criterion and are included in the resulting data set. - Defined a specific target range for the luminance of the background stimulus spectrum. - Added *'Morningness-Eveningness Questionnaire'*. - Added a procedure to ask subjects in the week after a session if they have experienced a migraine since their participation in a session.
Addendum #2	https://osf.io/kf253/	- Defined a procedure to perform an examination of the pupil response data, masked to group assignment, to inform a revision of subject recruitment targets.
Addendum #3	https://osf.io/j3x24/	- Revised recruitment goal to 20 subjects within each group from the original target of 40.
Deviations		- We had proposed to report median values across subjects. Using the median value result in unstable bootstrap model fits due to the discontinuous nature of the discomfort ratings data. We therefore switched to the mean for all across-subject measures.

Supplementary Table 2. Summary of Pre-registrations, addenda, and protocol deviations.

Supplemental Methods

We used silent substitution to create stimuli designed to selectively target melanopsin, the cones, or both (Figure 1c). We presented 4 second pulses of these stimuli to participants and asked them to verbally report the degree of discomfort they experienced while simultaneous pupillometry was recorded (Figure 1d,e).

The study was approved by the Institutional Review Board of the University of Pennsylvania. All participants provided informed written consent, and all experiments adhered to the tenets of the Declaration of Helsinki.

Participants

A total of 60 participants between the ages of 25 and 40 were recruited from the greater Philadelphia area and University of Pennsylvania campus, in most cases using advertising on digital social media services. All candidate participants underwent screening using the Penn Online Evaluation of Migraine[1], which implements automated headache symptom classification using the International Classification of Headache Disorders (ICHD)-3-beta criteria. The POEM also incorporates a set of previously published questions regarding photophobia during and between headache. These responses were scored with a point for each yes response to questions 1 through 7 (referred to here as the Choi score)[2]. Potential participants also completed the Visual Discomfort Score (VDS) survey[3]. The VDS score was derived as the sum of scores from 23 questions regarding frequency of particular visual discomfort symptoms, each scored on a 0-3 scale from “never” to “almost always”. To be eligible for the study, potential participants were required to meet all inclusion criteria for one of three groups:

1) Migraine with visual aura (MwA): a) classification of migraine with visual aura by the POEM, b) Choi score of 6 or 7, c) a response of “yes” to the Choi query regarding the presence of photophobia during headache free periods, d) one or more headaches within the prior month.
2) Migraine without aura (MwoA): a) classification of migraine without aura by the POEM, b) Choi score of 6 or 7, c) a response of “yes” to the Choi query regarding the presence of photophobia during headache free periods, d) one or more headaches within the prior month.
3) Control: a) classification of mild non-migrainous headache or headache-free by the POEM, b) a response of “No” or “I don’t know” to a question regarding a family history of migraine, c) a response of “No” to a question regarding a history of childhood motion sickness, d) VDS score 7 or lower.

Exclusion criteria were a history of glaucoma, generalized epilepsy, a history of adverse reaction to dilating eye drops, a concussion in the last six months, ongoing symptoms from head trauma/concussion, best-corrected distance acuity below 20/40 assessed via Snellen eye chart, or abnormal color vision as assessed via Ishihara plates. Participants were not excluded based on

medication use, including migraine preventive medications, and were allowed to continue to take their current medications during data collection.

An inability to collect usable pupillometry from a participant was an additional exclusion criterion. Candidate participants were studied in the lab during a pupillometry screening session that mimicked a subset of trials from the main experiment. To pass this screening session, participants were required to provide acceptable pupillometry data on at least 9 of 12 trials. We screened 83 participants, and 2 were excluded on the basis of this screening criterion. Drawing from the 81 participants who met the pupillometry screening criterion, we ultimately collected archival data on 60 participants, with 20 participants from each group (MwA, MwoA, and controls). Of the remaining 21 participants, 15 either did not respond to subsequent attempts to enroll in the study or were screened after data collection had completed. An additional 6 participants participated in at least one session but failed to return for subsequent sessions.

Stimuli

We designed stimuli that target specific photoreceptor classes through the technique of silent substitution[4]. We targeted three main photoreceptor mechanisms: melanopsin, the cones, or both (Figure 1c). We use here the term "light flux" to describe the latter combined stimulus, although we note that our stimulus modulation is not simply a multiplicative scaling of the spectrum, which is what is usually implied by the term.

These stimuli were generated in the same manner as described in prior reports[5,6]. Briefly, we used a digital light synthesis engine (OneLight Spectra, Vancouver, BC, Canada) that produces stimulus spectra as mixtures of 56 independent primaries (~16 nm full width at half maximum) under digital control and can modulate between these spectra at 256 Hz. We tailored the photoreceptor spectral sensitivities for each individual observer, taking into account the participant's age, pupil size, and our field size of 27.5 degrees (Figure 1f). Cone fundamentals were based on the International Commission on Illumination (CIE) physiological cone fundamentals[7]. The CIE standard only specifies fundamentals up to field sizes of 10 degrees, so we obtain estimates for our 27.5 degree field by extrapolating the formula using the open-source Psychophysics Toolbox[8–10]. We created separate background and stimulation spectra that provided 1) a nominal 400% unipolar Weber contrast on melanopsin while silencing the cones for our melanopsin-directed background/stimulus pair (melanopsin direction), 2) 400% contrast on each L-, M-, and S-cone classes while silencing melanopsin for the cone-directed modulation/stimulus pair (cones direction), and 3) 400% contrast each on melanopsin and each L-, M-, and S-cone classes for the light flux modulation/stimulus pair (light flux direction) (Figure 1c). The background spectra for each stimulus type differed in background luminance, but had similar chromaticity (Supplementary Table 1) as calculated using the XYZ functions associated with the CIE 2006 10-degree cone

fundamentals (http://www.crvl.org)[7]. We also produced contrast levels of 100 and 200% for each stimulus direction by scaling the relevant stimulus spectrum. We did not explicitly silence rods or penumbral cones[6], although we believe that the luminance and temporal properties of our stimuli minimize the contribution of these photoreceptors.

Stimuli were presented through a custom-made eyepiece with a circular, uniform field of 27.5° diameter. The central 5° diameter of the field was obscured to block the effects of the foveal macular pigment which can cause variation in photoreceptor spectral sensitivity (Figure 1f).

We obtained 5 spectroradiometric measurements of the 400% stimuli and their backgrounds before and after each testing session. For each stimulus type, we determined contrast on the following post-receptoral mechanisms: LMS, L-M, S, and melanopsin. Supplementary Table 1 presents the average validation results across all sessions. The validation results for each session are included with the experimental data for download. We adjusted our apparatus over the duration of data collection to maintain the luminance of the background spectrum for the light flux stimulus between 160 and 254 cd/m^2.

We discarded data from a session if the post-experiment stimulus validation measurements did not meet our pre-registered criteria. Data were discarded if the median of the 5 post-experiment measurements was: 1) greater than 20% absolute contrast on any of the nominally silenced post-receptoral mechanisms; or 2) less than 350% contrast upon a targeted post-receptoral mechanism. In the event that data from a session were discarded, the session was repeated at a later date. Prior to starting a data collection session, pre-experiment stimulus validation measurements were required to meet these same criteria.

Experiment Structure

Each participant was studied during multiple data collection sessions, usually held on different days. In an attempt to minimize variation in circadian cycle across sessions, subsequent sessions were initiated within three hours of the time of day when the same participant started their first session.

Participants were exposed to similar “light history” prior to data collection. At the start of a session, participants entered the testing room and underwent pharmacologic dilation of their right eye with 0.5% proparacaine for anesthesia and then 1% tropicamide ophthalmic solution. Participants remained in the testing room for the next 20 minutes, receiving instructions and adjusting the position of the apparatus for comfort. Room lights were set so that the walls of the testing room had a measured luminance of ~150 cd/m2, equated to the background luminance of our light flux stimulus. After confirming the presence of pupil dilation, the room lights were turned off and a curtain closed behind the participant to block light from the screen of the computer that controlled the

apparatus. Apart from the light from the eyepiece, the participant remained in darkness for the remainder of the experiment. Participants viewed the stimuli through their pharmacologically dilated right eye and a 6 mm diameter artificial pupil to control retinal irradiance.

On each of many trials, the participant viewed a pulsed spectral modulation designed to target melanopsin, the cones, or both (Figure 1c). The transition from the background to the stimulation spectrum (melanopsin, cones, or light flux) and the subsequent return to the background were windowed with a 500 ms half-cosine. This step minimized the entopic percept of a Purkinje tree in the melanopsin-directed stimulus[6]. The total duration of the pulse was 4 seconds, after which the stimulus field returned to and remained at the background spectrum (Figure 1d). Twelve seconds after the pulse ended, participants were prompted by an auditory cue to verbally report their discomfort rating (described below). This verbal rating was recorded by a microphone during the 4 second response window, the end of which was marked by another auditory cue. There was a variable inter-trial-interval of 1.5 – 2.5 seconds (uniformly distributed) that reduced the predictability of the onset of the next trial.

Ten consecutive trials that targeted the same photoreceptor direction but varied in contrast were grouped together into an acquisition. The ordering of the contrast levels (100, 200, 400%) followed a counterbalanced sequence to avoid trial order effects[11]; the first trial was discarded so that all retained trials had controlled first-order stimulus history. A total of 6 acquisitions, 2 of each stimulus type, comprised a single session. Acquisitions were ordered such that consecutive acquisitions were not of the same stimulus class. Data collection for a participant was deemed sufficient when a subject had completed two sessions, and these sessions contained in total at least six acceptable trials—as judged by pupillometry—for each stimulus type. Only acceptable trials were included in pupillometry analysis, but all trials were included in analysis of discomfort ratings. We attempted to gather 4 sessions of data for each individual participant but retained all subjects with data collection that was deemed sufficient. Participants did not complete all 4 sessions for a variety of reasons, including failure of post-experiment stimulus validation, poor pupillometry requiring us to discard that session, or declining to return for subsequent sessions. Across all 60 participants, 45 completed 4 sessions (15 controls, 15 MwA, 15 MwoA), 11 completed 3 sessions (4 controls, 3 MwA, 4 MwoA), and 4 completed 2 sessions (1 control, 2 MwA, 1 MwoA).

Discomfort Ratings

At the end of each trial, participants were asked to rate the discomfort produced by the stimulus on a 0 – 10 scale. The experimenter read this prompt to the participant at the start of each session:

> *"Following each trial, please rate the degree of discomfort that you experienced from the light pulse on a scale of zero to ten. A score of zero*

means that the pulse was not at all uncomfortable. A score of five means that the light pulse was moderately uncomfortable. A score of ten means that the light pulse was extremely uncomfortable."

Following completion of the experiment, raters masked to group assignment manually transcribed these verbal discomfort ratings. Trials on which no rating was given, or on which the spoken rating was un-interpretable, were discarded.

Pupillometry

We recorded the consensual pupil response from the left eye of the participant (contralateral to the eye receiving the stimulus) using an infrared camera (Pupil Labs GmbH) mounted on a post ~25 mm from the eye. A video clip was recorded for each trial, starting 1.5-s prior to pulse onset and ending 12-s after pulse offset (Figure 1d,e). These videos were processed using custom software (https://github.com/gkaguirrelab/transparentTrack)[12] to fit an ellipse to the identified pupil boundary in each video frame, allowing us to extract pupil area over time.

This raw pupillometry data underwent several stages of pre-processing to remove and interpolate over frames in which the pupil had been poorly identified. The first stage involves blink censoring, which was performed by identifying frames in which the glint from the active infrared light source of the camera was absent. Several frames before and after each blink were also censored to remove blink-related artifacts, with these values adjusted on a per-participant basis. Next, frames in which the pupil was identified but poorly fit by the routine were censored. This step largely functioned to remove frames in which much of the pupil was obscured by the eyelid. Lastly, frames in which the identified pupil was implausibly large or small were removed. Linear interpolation was performed over censored frames. If more than 25% of frames in a given trial were censored that trial was discarded from analysis. Pupil responses were expressed as the percentage change in area relative to the 0.5-s prior to the stimulus onset.

Six participants had frequent, brief blinks that produced many missed frames of pupil tracking despite having video recording of the eye that was otherwise of good quality. The data from these participants were retained despite having more than 25% missing frames in a trial.

All manual adjustment of pupillometry, and indeed the development of the processing steps and criteria, was performed by investigators masked to the group membership of the participants.

Analysis

Data analysis was performed using custom MATLAB code (Mathworks). We used a one-way ANOVA to determine the effect of group upon the clinical and demographic measures. Significant effects were examined in post-hoc testing using the Tukey procedure.

We took the median of discomfort rating across trials within a participant, and the mean across participants within a group. Pupil response was quantified for each trial as the mean percent change in pupil area during the period of 0 to 16 seconds from stimulus onset, relative to the 0.5 seconds before stimulus onset. The mean response across trials within participant, and across participants within groups, was obtained.

We examined the discomfort and pupil data within a two stage, non-linear model (Figure 3a). The response to a stimulus (either discomfort rating or pupil constriction) is given by:

$$\text{Response} = m^* \log_{10}\left(\sqrt[\beta]{(\alpha^* C_{Mel})^\beta + C_{Cone}{}^\beta}\right) + b$$

where C_{Mel} and C_{Cone} are the contrasts produced upon the melanopsin and cone photoreceptors by a stimulus, and α, β, m, and b are the four parameters of the model.

The first two model parameters describe an initial, non-linear stage that combines the photoreceptor contrast inputs and provides an "ipRGC contrast" output. The melanopsin contrast (α) is weighted by the first parameter, and then the weighted melanopsin contrast and the cone contrast are then combined using the Minkowski distance metric, with the second parameter (β) being the exponent for the metric. The modeled ipRGC contrasts of the stimuli are then base-10 log transformed and passed through a two-parameter affine transformation (parameters, slope and intercept of the transformation). In reporting the parameters, we convert the intercept parameter to an "offset" value, which is the predicted response amplitude at an ipRGC contrast of 200%.

The model was fit to the mean (across participant) data for all stimuli, with separate models fits performed for each group, and for each data type (discomfort rating and pupil response). Model fitting was performed using the *fmincon* function in MATLAB to minimize the L2 norm between the modeled values and the data. This fitting procedure was repeated over 1000 bootstrap resamples (with replacement) of the participants to assess the variability of the model output. We observed that the β parameter deviated slightly from a normal distribution across bootstraps. Therefore, we obtained the median value for all parameters across bootstraps, and variability across bootstraps was expressed by dividing the inter-quartile range of the values across bootstraps by 1.35, yielding a measure commensurate with the standard deviation of the distribution and thus an estimate of the standard error of the mean of the central tendency of the parameters.

Pre-Registration and availability of data and analysis code
This study was the subject of an initial pre-registration document (https://osf.io/5ry67/) and subsequent addenda (project summary page: https://osf.io/qjxdf/). Supplementary Table 2 summarizes the pre-registration documents and our deviations from these protocols. The analysis code is available (https://github.com/gkaguirrelab/melSquintAnalysis), as will be the data following publication.

References

1. Kaiser EA, Igdalova A, Aguirre GK, Cucchiara B. A web-based, branching logic questionnaire for the automated classification of migraine. *Cephalalgia*. 2019. doi:10.1177/0333102419847749
2. Choi JY, Oh K, Kim BJ, Chung CS, Koh SB, Park KW. Usefulness of a photophobia questionnaire in patients with migraine. *Cephalalgia*. 2009. doi:10.1111/j.1468-2982.2008.01822.x
3. Conlon EG, Lovegrove WJ, Chekaluk E, Pattison PE. Measuring visual discomfort. *Vis cogn*. 1999. doi:10.1080/135062899394885
4. Estévez O, Spekreijse H. The “silent substitution” method in visual research. *Vision Res*. 1982;22(6):681-691. doi:10.1016/0042-6989(82)90104-3
5. Spitschan M, Bock AS, Ryan J, Frazzetta G, Brainard DH, Aguirre GK. The human visual cortex response to melanopsin-directed stimulation is accompanied by a distinct perceptual experience. *Proc Natl Acad Sci*. 2017;114(46):12291-12296. doi:10.1073/pnas.1711522114
6. Spitschan M, Aguirre GK, Brainard DH. Selective stimulation of penumbral cones reveals perception in the shadow of retinal blood vessels. *PLoS One*. 2015;10(4). doi:10.1371/journal.pone.0124328
7. CIE. Fundamental chromaticity diagram with physiological axes – Part 1. Technical Report 170-1 (Central Bureau of the Commission Internationale de l’Éclairage, Vienna). 2006.
8. Kleiner M, Brainard DH, Pelli DG, Broussard C, Wolf T, Niehorster D. What’s new in Psychtoolbox-3? *Perception*. 2007. doi:10.1068/v070821
9. Brainard DH. The Psychophysics Toolbox. *Spat Vis*. 1997. doi:10.1163/156856897X00357
10. Pelli DG. The VideoToolbox software for visual psychophysics: Transforming numbers into movies. *Spat Vis*. 1997. doi:10.1163/156856897X00366
11. Aguirre GK, Mattar MG, Magis-Weinberg L. De Bruijn cycles for neural decoding. *Neuroimage*. 2011. doi:10.1016/j.neuroimage.2011.02.005
12. Aguirre GK. A model of the entrance pupil of the human eye. *Sci Rep*. 2019. doi:10.1038/s41598-019-45827-3

Chapter 4 - Future Directions

Continued Analysis of Migraine Database

The cohort of 40 subjects diagnosed with migraine with and without aura, as well as the 20 headache-free control subjects offers further opportunity than what has already been explored. In addition to a cohort of migraine subjects available for potential future experiments, we already have collected data that is interesting enough to merit further investigation.

One such analysis is to examine another light-mediated response in these subjects that we already collected, reflexive eye closure as measured through EMG. As part of this study, we measured muscle activity of the orbicularis oculi, specifically squinting activity or blinks. Preliminary analysis shows that while the migraine with aura group shows increased EMG activity relative to headache-free controls, the migraine without aura group is not different from controls. We used pupillometry to quantify the amount of blinks within each group elicited by the light pulses, and this analysis shows a similar group level pattern, suggesting that the increased EMG activity in migraine with aura is at least partially related to increased blinking. We interpret this increased blinking activity as indicative of increased reflexive eye closure, which is essentially a reflex to protect the eye from potentially noxious stimuli. It is also interesting to compare this result to measures of cortical hyperresponsiveness, which often show an increased response amplitude to visual stimuli in migraine with aura, but no difference between migraine without aura and headache-free controls[1,2]. The dissociation between migraine groups is interesting, and suggests that the group difference is

more related to migraine-specific pathophysiology (or aura itself) rather than light sensitivity.

The pupillometry collected as part of this main study is also deserving of further study. Although our analysis suggests there is no difference in resting pupil size or constriction amplitude, there may be more subtle differences in migraine in the form of pupil response over time. We are also interested in examining the reproducibility of these pupil responses at the individual subject level in order to quantify individual differences.

Strengthening Localization Arguments

Part of the significance of the work presented here is the claim that light sensitivity in migraine does not result from specific pathology in the retina and instead the localization is more likely post-retinal. Although this idea represents significant progress in the study of light sensitivity, future experiments can better localize light sensitivity within the brain. Experiments using BOLD fMRI in particular seem well-suited to answer these questions.

The lab has previously shown the ability to measure cortical responses to melanopsin-directed stimulation. These experiments, however, were primarily focused on visual cortex. Moving forward, it would be interesting to examine the extent to which melanopsin-directed stimulation elicits responses in other brain regions linked to light sensitivity, including the three presumed mechanisms discussed in the *Introduction*. In particular, are there increased responses in thalamus or somatosensory cortex? Although imaging the brainstem is difficult, it

would be also interesting to determine if we can measure any altered responses there.

Increasing Melanopsin Contrast by Studying Colorblind Individuals

One of the inherent obstacles in our approach to studying melanopsin function in normally sighted individuals is that we are limited in the contrast we are able to place on melanopsin. Specifically, the need to balance the excitation across all three classes of cones, combined with restrictions imposed by our digital light synthesis engine gamut, only allow us to present 400% contrast melanopsin-directed stimulation. Although this stimulus intensity has been enough to empower this and related work, it represents a small fraction of the potential contrast humans are exposed to on a day-to-day basis. The ability to potentially achieve greater melanopsin contrast on our melanopsin-directed stimuli has a number of direct applications. For example, the BOLD response is inherently noisy, and increased melanopsin contrast could provide a larger signal and thereby facilitate future fMRI experiments.

Although 400% melanopsin contrast is the maximum we can create with our current device in normally sighted individuals, studying certain colorblind individuals offers an alternative. Specifically, we can create stimuli with greater melanopsin contrast for individuals with forms of colorblindness that result from a genetic lack of a single cone type. With our digital light synthesis engine, we can create stimuli with 1200% melanopsin contrast for individuals with deuteranopia, a form of colorblindness resulting from a genetic lack of the M-cone.

We have taken some preliminary steps to begin this line of investigation. As part of a first round of pilot testing, we were interested in addressing two main considerations. First, do individuals with deuteranopia behave similarly in how they respond to light relative to normally sighted individuals? Answering this question is necessary to ensure that some kind of mechanism to compensate for the lack of M-cone in these deuteranopic subjects does not alter light responses in these subjects. Second, with this functional similarity addressed, how do light responses scale with increased contrast? Here we want to ensure that increasing contrast from 400 to 1200% increases or alters the response in some way, and that system does not simply become saturated.

We have conducted pilot testing on 5 subjects with deuteranopia to begin to address these questions. We ran these deuteranopic subjects first in the same experiment as the main migraine study presented previously, and compared the responses in these deuteranopes to those normally sighted headache-free controls. Although underpowered, results from this initial testing suggested that deuteranopes do not behave differently from normally sighted trichromats. Next, we repeated the experiment, but increased the contrast levels, examining responses to 400%, 800%, and 1200% contrast stimulation. Pupillometry results generally showed that response amplitudes continued to increase past 400% contrast, but some degree of saturation was seen in some subjects in some stimulus conditions. These pilot results seem intriguing enough to continue this line of investigation, but the most immediate next step would be to increase the number of deuteranopic subjects studied.

Clinical Extensions

One of the most obvious extensions of this work is to examine melanopsin and ipRGC function in other relevant clinical contexts. Indeed, light sensitivity is found across numerous other clinical entities. Our lab has already started to study patients with light sensitivity due to traumatic brain injury. One feature that has been apparent in the small number of patients we have already studied is that they seem to be rather more light sensitive than the migraine population. Depending on the extent to which these subjects can tolerate our stimuli and experimental protocol, we may need to alter our typical approach in order to best design an experiment for these subjects.

Besides photophobia, sleep disorders appear to be another class of clinical entities likely to relate to variation in melanopsin and ipRGC function. Two disorders in particular have very strong melanopsin-specific hypotheses related to their pathophysiology. First is non-24 disorder, which is a condition in which people are completely unable to entrain their own endogenous circadian rhythm to the external world; that is they "free run"[3]. Most of these patients are blind, but some appear to have normal vision. One hypothesis then for the pathophysiology in these normally sighted patients is that they lack a functioning ipRGC-mediated retinohypothalamic tract. If this pathology is indicative of a global lack of ipRGC function, we might anticipate that these subjects have deficits in pupil constriction as well, particularly to melanopsin-directed stimulation. Second, people with delayed sleep phase syndrome fall asleep and wakeup late[4]. One hypothesis for

the underlying pathophysiology is that these individuals are hypersensitive to the phase shifting or sleep delaying effects of light[5]. An open question then is to what extent is the retina hypersensitive in these subjects, including for example as manifest in the pupil response.

Lighting design

As light can be disruptive or even debilitating, there is great interest in lighting design to alleviate these issues. Although these types of therapeutic applications are beyond the scope of the present work, some of our conclusions may be significant by extension. One of the most common applications of basic melanopsin physiology is software that changes screen lighting to reduce blue light content to improve sleep. Popular commercial examples include *f.lux* (https://justgetflux.com/) and Apple's *Night Shift* (https://support.apple.com/en-us/HT207513). One of the core issues with this approach is its focus on melanopsin. Our work with discomfort ratings show that even if discomfort is mediated by ipRGCs, phototransduction by both melanopsin and the cones can contribute. Recent evidence shows that similar cone input through ipRGCs for entrainment of the circadian system is also functionally relevant[6].

There is indeed opportunity for improvement of screens of electronic devices, lenses, and room lighting by taking advantage of our growing understanding of the reflexive functions of vision. Maximizing benefit, however, requires further basic science insight into the photoreceptor mechanisms for the

reflexive function of vision in question as well as validation of the efficacy of the intended manipulation.

References

1. Datta R, Aguirre GK, Hu S, Detre J a, Cucchiara B. Interictal cortical hyperresponsiveness in migraine is directly related to the presence of aura. *Cephalalgia*. 2013;33(6):365-374. doi:10.1177/0333102412474503
2. Kincses ZT, Veréb D, Faragó P, et al. Are Migraine With and Without Aura Really Different Entities? *Front Neurol*. 2019. doi:10.3389/fneur.2019.00982
3. Uchiyama M, Lockley SW. Non-24-hour sleep-wake rhythm disorder in sighted and blind patients. *Sleep Med Clin*. 2015. doi:10.1016/j.jsmc.2015.07.006
4. Nesbitt AD. Delayed sleep-wake phase disorder. *J Thorac Dis*. 2018. doi:10.21037/jtd.2018.01.11
5. Watson LA, Phillips AJK, Hosken IT, et al. Increased sensitivity of the circadian system to light in delayed sleep–wake phase disorder. *J Physiol*. 2018. doi:10.1113/JP275917
6. Mouland JW, Martial F, Watson A, Lucas RJ, Brown TM. Cones Support Alignment to an Inconsistent World by Suppressing Mouse Circadian Responses to the Blue Colors Associated with Twilight. *Curr Biol*. 2019. doi:10.1016/j.cub.2019.10.028